

AD 667983



USAAVLABS TECHNICAL REPORT 66-64

**COMPARISON OF LONGITUDINAL STABILITY
CHARACTERISTICS OF THREE TILT-WING
VTOL AIRCRAFT DESIGNS**

By

R. A. Cornutt
M. C. Curtiss, Jr.

January 1968

**U. S. ARMY AVIATION MATERIEL LABORATORIES
FORT EUSTIS, VIRGINIA**

**CONTRACT DA 44-177-AMC-8(T)
PRINCETON UNIVERSITY
PRINCETON, NEW JERSEY**

*This document has been approved
for public release and sale; its
distribution is unlimited.*



Reproduced by the
CLEARINGHOUSE
for Federal Scientific & Technical
Information Springfield Va. 22151

**DDC
RECEIVED
APR 15 1968
REGULATED**

102

ADDITIONAL FOR	
UNCLASSIFIED	WHITE SECTION <input checked="" type="checkbox"/>
UNANNOUNCED	BUFF SECTION <input type="checkbox"/>
JUSTIFICATION	
BY	
DISTRIBUTION AVAILABILITY CODES	
DISC.	AVAIL. OR SPECIAL

Disclaimers

The findings in this report are not to be construed as an official Department of the Army position unless so designated by other authorized documents.

When Government drawings, specifications, or other data are used for any purpose other than in connection with a definitely related Government procurement operation, the United States Government thereby incurs no responsibility nor any obligation whatsoever; and the fact that the Government may have formulated, furnished, or in any way supplied the said drawings, specifications, or other data is not to be regarded by implication or otherwise as in any manner licensing the holder or any other person or corporation, or conveying any rights or permission, to manufacture, use, or sell any patented invention that may in any way be related thereto.

Trade names cited in this report do not constitute an official endorsement or approval of the use of such commercial hardware or software.

Disposition Instructions

Destroy this report when no longer needed. Do not return it to originator.

UNCLASSIFIED

AD 667 983

COMPARISON OF LONGITUDINAL STABILITY CHARACTERISTICS
OF THREE TILT-WING VTOL AIRCRAFT DESIGNS

R. A. Curnutt, et al

Princeton University
Princeton, New Jersey

January 1968

Processed for . . .

**DEFENSE DOCUMENTATION CENTER
DEFENSE SUPPLY AGENCY**



U. S. DEPARTMENT OF COMMERCE / NATIONAL BUREAU OF STANDARDS / INSTITUTE FOR APPLIED TECHNOLOGY



DEPARTMENT OF THE ARMY
U. S. ARMY AVIATION MATERIEL LABORATORIES
FORT EUSTIS, VIRGINIA 23604

This report has been reviewed by this command and is considered to be technically sound. This work, which was performed under Contract DA 44-177-AMC-8(T), was undertaken to compare the longitudinal stability characteristics of three tilt-wing VTOL aircraft from data obtained from wind tunnel tests, flight tests, and the Princeton Dynamic Model Track tests. It is published for the exchange of information and the stimulation of ideas.

Task 1P125901A14233
Contract DA 44-177-AMC-8(T)
USAAVLABS Technical Report 66-64
January 1968

COMPARISON OF LONGITUDINAL STABILITY
CHARACTERISTICS OF THREE TILT-WING
VTOL AIRCRAFT DESIGNS

Report 749

by

R. A. Curnutt
H. C. Curtiss, Jr.

Prepared by

Department of Aerospace and Mechanical Sciences
Princeton University
Princeton, New Jersey

for

U. S. ARMY AVIATION MATERIEL LABORATORIES
FORT EUSTIS, VIRGINIA

This document has been approved
for public release and sale; its
distribution is unlimited.

SUMMARY

Experimental values of the longitudinal stability derivatives of three tilt-wing VTOL aircraft configurations as obtained from tests of several models are presented. Results from the NASA full-scale wind tunnel at Langley Field, the Princeton track, the LTV Aerospace Corporation wind tunnel and flight test are included. An analysis is included which utilizes root-locus and analog computer studies to compare the characteristic roots and transient response of the aircraft as the longitudinal derivatives are varied within the range exhibited by these data. Trim conditions at wing incidences from 20 to 90 degrees are considered.

The three configurations included in the analysis were found to exhibit quite similar stability characteristics in the low-speed regime. Good correlation was found to exist between NASA wind tunnel data and Princeton Dynamic Model Track data for the VZ-2 aircraft.

Consideration is given to the importance of various derivatives in determining the response characteristics. A large number of analog computer traces are included, showing variations in response characteristics caused by changes in individual derivatives.

FOREWORD

This research was performed by the Department of Aerospace and Mechanical Sciences, Princeton University, under the sponsorship of the United States Army Aviation Materiel Laboratories Contract DA 44-177-AMC-8(T), with financial support from the United States Navy, Bureau of Weapons, and the Air Force Flight Dynamics Laboratory. The research was monitored by Mr. Richard L. Scharpf of the United States Army Aviation Materiel Laboratories.

The research was conducted by R. A. Curnutt and Assistant Professor H. C. Curtiss, Jr., of Princeton University. The authors wish to express their appreciation to Sikorsky Aircraft Division of the United Aircraft Corporation for granting permission to use data of their VTOL aircraft design.

CONTENTS

	<u>Page</u>
SUMMARY	iii
FOREWORD	v
LIST OF FIGURES.viii
LIST OF SYMBOLS.	xi
INTRODUCTION.	1
STATIC DERIVATIVE COMPARISON	3
ROOT-LOCUS ANALYSIS OF DERIVATIVES	20
ANALOG COMPUTER STUDY OF AIRCRAFT DERIVATIVES AND DYNAMIC RESPONSE.	25
DISCUSSION OF RESULTS OF COMPUTER AND ROOT-LOCUS STUDIES	33
CONCLUSIONS	36
RECOMMENDATIONS.	37
REFERENCES	85
DISTRIBUTION.	87

LIST OF FIGURES

<u>Figure</u>		<u>Page</u>
1	Axis System and Notation	4
2	Wing Incidence Versus Trim Speed, Including Average Line and Flight Test Data	15
3	Z_{α} Versus Trim Speed, Including Derivative Ranges	16
4	X_{α} Versus Trim Speed, Including Derivative Ranges	16
5	M_{α} Versus Trim Speed, Including Derivative Ranges	17
6	Z_u Versus Trim Speed, Including Derivative Ranges	18
7	X_u Versus Trim Speed, Including Derivative Ranges	18
8	M_u Versus Trim Speed, Including Derivative Ranges	19
9	$M_{\dot{\theta}}$ Versus Trim Speed, Including Derivative Ranges.	19
10	Computer Circuit to Generate Input Pulse	26
11	Typical Characteristic Roots	38
12	Response to Step and Pulse Inputs	39
13	Sketch of VZ-2 Research Aircraft.	40
14	Photograph of 2-Propeller VZ-2 Model	41
15	Sketch of 2-Propeller Transport Model	42
16	Photograph of 2-Propeller Transport Model.	43
17	Sketch of 4-Propeller VTOL Transport	44
18	Photograph of 4-Propeller VTOL Transport Model, Showing Princeton Track Facility.	45
19	Superimposed Plan Views of Each VTOL Model	46
20	Typical Test Data From Princeton Track Facility.	47
21	Root Locus Sketch, Varying M_{α} for $i_w \approx 40^\circ$	48
22	Root Locus Sketch, Varying X_{α} for $i_w \approx 40^\circ$	49

23	Root Locus Sketch, Varying M_u for $i_w \approx 40^\circ$	50
24	Root Locus Sketch, Varying M_α for $i_w \approx 60^\circ$	51
25	Root Locus Sketch, Varying M_u for $i_w \approx 60^\circ$	52
26	Root Locus Sketch, Varying M_u for $i_w \approx 90^\circ$	53
27	Analog Computer Diagram	54
28	Superposed Analog Computer Responses to a Pulse Control Input; $i_w = 90^\circ$ to 40°	55
29	Superposed Analog Computer Responses to a Pulse Control Input; $i_w = 50^\circ$ to 20°	56
30	Superposed Analog Responses for Individually Varied Derivatives; $i_w = 20^\circ$, $V_o = 160$ ft/sec	57
	(A) Varying M_u	57
	(B) Varying M_α	58
31	Superposed Analog Responses for Individually Varied Derivatives; $i_w = 40^\circ$, $V_o = 100$ ft/sec	59
	(A) Varying X_u	59
	(B) Varying X_α	60
	(C) Varying Z_u	61
	(D) Varying Z_α	62
	(E) Varying M_u	63
	(F) Varying M_α	64
32	Superposed Analog Responses for Individually Varied Derivatives; $i_w = 50^\circ$, $V_o = 75$ ft/sec	65
	(A) Varying M_u	65
	(B) Varying M_α	66
	(C) Varying M_θ	67
33	Superposed Analog Responses for Individually Varied Derivatives; $i_w = 55^\circ$, $V_o = 65$ ft/sec	68
	(A) Varying M_u	68
	(B) Varying M_α	69

Figure

	<u>Page</u>
34	Superposed Analog Responses for Individually Varied Derivatives; $i_w = 60^\circ$, $V_o = 55$ ft/sec 70
	(A) Varying X_u 70
	(B) Varying X_α 71
	(C) Varying Z_u 72
	(D) Varying Z_α 73
	(E) Varying M_u 74
	(F) Varying M_α 75
	(G) Varying M_θ' 76
35	Superposed Analog Responses for Individually Varied Derivatives; $i_w = 90^\circ$, $V_o = 0$ 77
	(A) Varying X_u 77
	(B) Varying M_u 78
	(C) Varying M_θ' 79
36	Analog Responses with Individual Derivatives Exhibiting Both Average and Zero Values; $i_w = 20^\circ$, $V_o = 160$ ft/sec 80
	(A) $X_\alpha = 0$ 80
	(B) $Z_u = 0$ 81
	(C) $Z_\alpha = 0$ 82
37	Analog Responses for Average and Zero Values of X_α ; $i_w = 40^\circ$, $V_o = 100$ ft/sec 83
38	Analog Responses for Average and Zero Values of Z_u ; $i_w = 60^\circ$, $V_o = 55$ ft/sec 84

LIST OF SYMBOLS

- A propeller disc area, square feet
- \bar{c} wing chord, feet
- C_T , thrust coefficient based on slipstream velocity, $\frac{T}{q_s A}$
- C_L lift coefficient, $\frac{L}{qS}$
- D drag, pounds
- F force, pounds
- F_L lift, pounds
- g acceleration due to gravity, 32.2 feet per second per second
- i_w wing incidence, degrees; zero when horizontal ($\theta_{fus} = 0$)
- i_t horizontal tail incidence; positive, trailing edge down, degrees
- I_y moment of inertia in pitch (about Y axis), slug-feet squared
- J $\sqrt{-1}$
- k_y radius of gyration in pitch, feet
- L lift, pounds
- m mass, slugs
- M pitching moment, foot-pounds; positive nose up
- q freestream dynamic pressure, $\frac{1}{2} \rho V^2$, pounds per square foot
- q $\equiv \dot{\theta}$; pitch rate in radians per second; positive nose up
- q_s slipstream dynamic pressure, $q + \frac{T}{A}$, pounds per square foot
- R propeller radius, feet
- rpm propeller rotational speed, revolutions per minute
- s Laplace operator; root of characteristic equation; $s = \sigma + j\omega$, per second

S wing area, square feet
t time, seconds
T thrust, pounds
 $T_{1/2}$ time to half amplitude, seconds
 T_2 time to double amplitude, seconds
u horizontal velocity, feet per second
V free stream velocity, feet per second (Note: V is always horizontal in static tests.)
w vertical velocity, feet per second; positive down
W weight, pounds
X "horizontal" force, aligned with wind; positive forward, pounds
Z "vertical" force, perpendicular to wind; positive down, pounds

DERIVATIVES

$M_u = \frac{1}{I_y} \frac{\partial M}{\partial u}$; change in pitching moment with velocity; referred to as "velocity stability" in this report, per foot second

$M_\alpha = \frac{1}{I_y} \frac{\partial M}{\partial \alpha}$; angle of attack stability, per second squared

$M_{\dot{\theta}} = \frac{1}{I_y} \frac{\partial M}{\partial \dot{\theta}}$; $\equiv M_q$; pitch damping, per second

$M_{\dot{\theta}'} = M_{\dot{\theta}} + M_{\dot{\alpha}}$, per second

$M_{\delta_s} = \frac{1}{I_y} \frac{\partial M}{\partial \delta_s}$; control sensitivity, $\frac{\text{rad/sec}^2}{\text{inch}}$

$M_{\delta_s} = - 0.05 \frac{\text{rad/sec}^2}{\text{inch}}$ for this report

$$X_u = \frac{1}{m} \frac{\partial X}{\partial u}; \text{ drag damping, per second}$$

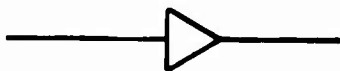
$$X_\alpha = \frac{1}{m} \frac{\partial X}{\partial \alpha}; \text{ change in "horizontal" force with angle of attack, feet per second squared}$$

$$Z_u = \frac{1}{m} \frac{\partial Z}{\partial u}; \text{ lift due to velocity, per second}$$

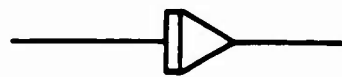
$$Z_\alpha = \frac{1}{m} \frac{\partial Z}{\partial \alpha}; \text{ vertical damping, feet per second squared}$$



Potentiometer



Summer (inverter)



Integrator



Switch

GREEK SYMBOLS

α fuselage angle of attack; positive nose up, radians unless otherwise noted (perturbation quantity)

β propeller mean blade angle, radians

γ flight path angle; positive nose up, degrees or radians

δ_s moment control (stick) displacement; positive forward, inches

δ_f flap deflection; positive down, degrees

θ fuselage pitch angle; positive nose up, radians unless otherwise noted (perturbation quantity)

σ real part of "s" , 1/second

- Ω propeller rotational speed, radians per second
- ω damped natural frequency, imaginary part of "s", radians per second
- $\Delta()$ indicates incremental or perturbation quantity
- λ scale factor = $\frac{\text{full-scale linear dimension}}{\text{model linear dimension}}$
- ρ air density, slugs per cubic foot
- μ horizontal advance ratio = $\frac{V}{\Omega R}$, ratio of forward velocity to propeller tip speed
- τ time constant of δ_s , pulse input, seconds

SUBSCRIPTS

- o initial, or trim, conditions; i.e., $V_o = V_{\text{trim}}$
- t tail
- w wing

INTRODUCTION

For many years the performance and stability and control characteristics of new aircraft designs have been predicted through the use of experiments with models. To enhance the usefulness and value of model data, a continuing evaluation of these data from three points of view is desirable. These are:

- a. Correlation of model and full-scale data. This comparison is particularly useful in determining the nature and importance of the scale effects.
- b. Correlation of data from similar models in various facilities. This comparison is valuable in estimating the sensitivity of the data to details of model design and construction, to the characteristics of the particular facility, and to test procedures, as well as to scale effect.
- c. Correlation of data from similar designs and the comparison of these data with theory. As a result of this approach, theoretical methods are developed that can be used with confidence to predict the significant phenomena of future designs.

Continuous efforts of this kind in the area of conventional aircraft have resulted in a firm basis on which to predict the characteristics of new designs and to evaluate model tests with some confidence.

Care must be taken, however, in extrapolating this fixed-wing background to radically different configurations, where the exact nature of the scale effects may be subtle and where the complexities of the flow fields preclude "exact" theoretical analyses.

As new configurations arise, the relative importance of the various factors that contribute to the stability derivatives of a vehicle may be considerably altered. For example, the stability characteristics of a tilt-wing VTOL at low speeds are largely dominated by the nature of the propeller forces and moments and the forces produced by the wing-slipstream interaction, effects that are usually of secondary importance on a conventional aircraft. Therefore, pursuit of the above three areas of correlation is desirable and necessary to gain confidence in future model tests and theoretical predictions of the stability characteristics of tilt-wing VTOL aircraft.

The above statements can be generalized to include all VTOL aircraft, where the predominate effects on the stability characteristics that require detailed consideration may be referred to as power effects as in Reference 9, Chapter VIII. The phrase "power effects" then refers to any direct effects of the thrust producing device (the propeller forces and moments, for example) as well as indirect effects (the propeller slipstream).

This study was directed toward the above objectives with respect to the longitudinal stability characteristics of tilt-wing aircraft. Comparison of model data from different facilities, as well as full-scale data where available, is included. Three different configurations are compared to determine the general trends of the longitudinal stability characteristics of these VTOL aircraft at low speeds. Because of similarities in the experimental data, it is possible to discuss the longitudinal stability characteristics of a "typical" tilt-wing VTOL at low speeds in quite general terms.

The purpose of this study, then, is first to compare the longitudinal stability derivatives of three VTOL aircraft as obtained from several sources, and then, using these experimental derivatives, to analyze the dynamic response of a "typical" VTOL aircraft in the transition regime.

The data presented in this report are taken from different facilities. Included is the NASA full-scale wind tunnel at Langley Field with a 30-by-60-foot test section (References 1, 2 and 4) and the LTV Aerospace Corporation wind tunnel, 15-by-17-foot test section (Reference 12), flight test, and the Princeton Dynamic Model Track (Reference 16). The Princeton track consists of a servo-controlled carriage riding on a track enclosed in a 30-by-30-foot building, with accurate speed control from 0 to 40 feet per second. The data taken here consist only of force and moment measurements, although the dynamic model track may also be used for semi-free dynamic response tests, as well as the static measurements presented here.

STATIC DERIVATIVE COMPARISON

AIRCRAFT AND SOURCES OF DATA

Of the several tilt-wing VTOL designs of the past 5 or 6 years, three have been tested on the Princeton University Dynamic Model Track, and these are the aircraft studied in this report. They include models of the two-propeller VZ-2 research aircraft, a two-propeller VTOL transport, and a four-propeller tilt-wing transport.

Data for the VZ-2 configuration consist of 1/4-scale model tests in the Langley full-scale tunnel (References 1 and 2), full-scale tests in the Langley full-scale tunnel (Reference 4), flight test (Reference 3), and tests of a dynamically similar 1/5.2-scale model on the Princeton Dynamic Model Track (Reference 8).

The two-propeller transport is represented by a 1/10-scale powered model, and all data are taken from a Princeton report (Reference 7). Test results for the four-propeller aircraft are obtained from a to-be-published Princeton University report (Reference 15) and from some trim-velocity data from the LTV Aerospace Corporation; a NASA report of 1/9-scale model tests is also used (Reference 6).

Photographs and sketches of some of the models appear in Figures 13 through 18, along with a sketch of all three aircraft superimposed to show the geometric relationships with all of the aircraft scaled to the same gross weight (Figure 19). Equivalent full-scale characteristics are listed in Table VII.

DISCUSSION OF DATA

The object in using these various sources of data was to obtain the static longitudinal stability derivatives of the various aircraft for comparison. These derivatives include the rates of change of vertical (Z) and horizontal (X) force and pitching moment with angle of attack and forward velocity. All results are obtained for "trim" conditions: zero fuselage angle of attack and zero acceleration (horizontal force equals zero).

The stability derivatives are presented in dimensional form for an equivalent 40,000-pound aircraft. In this method of presentation, the pitching moment derivatives are divided by the moment of inertia and the force derivatives are divided by the mass. Stability derivatives for geometrically similar aircraft of different sizes may be obtained through the use of the scale factors given in Table I.

The relationship between the nondimensional $C_{m\alpha}$ and its dimensional counterpart is given as (Reference 9)

$$M_{\alpha} \equiv \frac{1}{I_y} \frac{\partial M}{\partial \alpha} = \frac{g}{\bar{c} C_L (k_y/\bar{c})^2} C_{m_{\alpha}}$$

Although tests were conducted on only three aircraft designs, eight models (including full-scale) were considered, and three facilities were represented. Tests ranged from model track tests to full-scale flight tests, and configurations varied widely. There were 19 wing incidences, 8 flap settings, and 13 horizontal tail incidences.

The presentation and comparison of the data involve both wing angle and trim velocity. However, for each aircraft there is, of course, a unique relationship between trim velocity and wing incidence as shown in Figure 2. Previous investigations (Reference 17, Appendix III) have indicated that comparison based on trim velocity should bring out the similarities among the three aircraft more clearly than one based on wing incidence angle. Therefore, all stability derivatives are presented as functions of trim speed. The corresponding wing incidence angles are given in Figure 2.

All data are presented in the wind-axis system, shown in Figure 1. Both in the wind tunnel and in the dynamic model track, forces were measured perpendicular and parallel to the horizontal free stream velocity. For this reason, the forces will occasionally be referred to as "horizontal" or "vertical" forces, although this is only precisely true when the aircraft is in straight and level flight ($\gamma = 0$). The forces could also be referred to as conventional lift and drag, but the inclusion of thrust components makes the use of X and Z preferable. In the NASA reports, $-Z = F_L$.

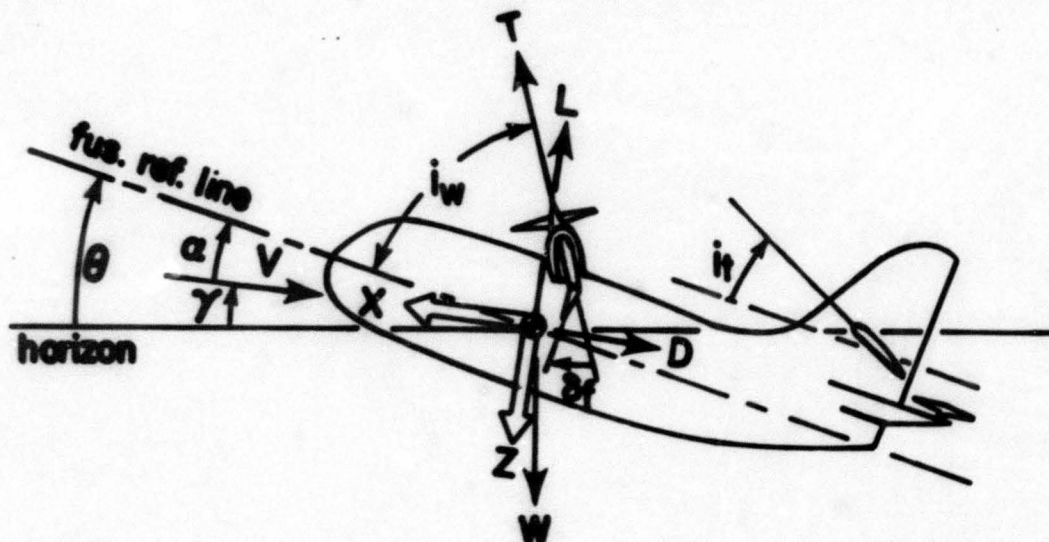


FIGURE 1. AXIS SYSTEM AND NOTATION

EVALUATION OF STABILITY DERIVATIVES FROM DATA

In the Introduction it was noted that the stability characteristics of tilt-wing VTOL aircraft at low speeds are dependent upon the forces and moments developed by the propellers as well as the interaction of the propeller slipstream with the wing. The presence of these effects, which may be placed under the general heading of power effects, gives rise to one important feature that should be considered in experiments conducted to determine stability derivatives. This is the fact that the force and moment variations with velocity cannot be readily calculated, as would be the case for an aircraft with no significant power or compressibility effects. Therefore, specific experiments should be conducted to determine these derivatives.

For example, consider the calculation of the lift variation with velocity. By definition,

$$L = \frac{1}{2} \rho S V^2 C_L . \quad (1)$$

If the power and compressibility effects are negligible, then the lift coefficient is a function of angle of attack only,

$$C_L = C_L(\alpha) ,$$

and the lift variation with velocity is

$$\frac{\partial L}{\partial V} = \rho S V C_L . \quad (2)$$

Knowing the trim value of the lift coefficient, this derivative may be readily calculated. If, however, a propeller-driven aircraft is considered, and power effects are important, then the lift coefficient will be a function of propeller advance ratio, μ , and blade angle, β :

$$C_L = C_L(\alpha, \beta, \mu) .$$

The lift variation with velocity will be

$$\frac{\partial L}{\partial V} = \rho S V C_L + \frac{1}{2} \rho S V^2 \frac{\partial C_L}{\partial \mu} \frac{\partial \mu}{\partial V} . \quad (3)$$

Therefore, experiments should be conducted at constant angle of attack,

with variable advance ratio to determine the additional term $\frac{\partial C_L}{\partial \mu}$. The

simplest way to conduct experiments to determine the velocity derivatives is to vary only one parameter, either the propeller rotational speed or the tunnel speed. The results will be independent of which parameter is varied unless propeller blade flexibility effects are important, in which case

only variation of tunnel speed will give the proper result.

If the tunnel speed is varied, then the derivative is determined directly. If propeller rotational speed is varied, then from the definition of lift coefficient,

$$\frac{\partial L}{\partial \Omega} = \frac{1}{2} \rho S V^2 \frac{\partial C_L}{\partial \mu} \frac{\partial \mu}{\partial \Omega} \quad (4)$$

where, from the definition of μ ,

$$\mu = \frac{V}{\Omega R}$$

$$\frac{\partial \mu}{\partial \Omega} = - \frac{V}{\Omega^2 R} \quad (5)$$

The derivative $\frac{\partial C_L}{\partial \mu}$ can then be determined and $\frac{\partial L}{\partial V}$ may be calculated from (3), where

$$\frac{\partial \mu}{\partial V} = \frac{1}{\Omega R} \quad (6)$$

The experiments described in References 1 and 3 were not conducted in either of these two ways, and so a slightly different technique must be used to obtain the velocity derivatives. There is insufficient data in References 2 and 4 to determine the velocity derivatives.

In References 1 and 3, data are presented for accelerated and decelerated flight conditions. To investigate the effect of acceleration and deceleration on the angle of attack derivatives, the propeller rotational speed and wind tunnel speed were varied to maintain a constant lift force at zero angle of attack. This information may be used in the following fashion to calculate the stability derivatives. By the condition of the experiment,

$$\frac{dL}{dV} = 0$$

and by definition,

$$\frac{dL}{dV} = \rho S V C_L + \frac{1}{2} \rho S V^2 \frac{\partial C_L}{\partial \mu} \frac{d\mu}{dV} = 0 \quad (7)$$

Now $\frac{d\mu}{dV}$ is known from the experiment and physically represents the change in the advance ratio with tunnel velocity necessary to maintain the lift constant. Now $\frac{\partial C_L}{\partial \mu}$ may be calculated from the above expression:

$$\frac{\partial C_L}{\partial \mu} = - \frac{2C_L}{V} \frac{1}{\frac{d\mu}{dV}} . \quad (8)$$

And therefore from equation (3), we may calculate $\frac{\partial L}{\partial V}$ as

$$\frac{\partial L}{\partial V} = \rho S V C_L \left(1 - \frac{\frac{\partial \mu}{\partial V}}{\frac{d\mu}{dV}} \right) \quad (9)$$

where the partial derivative is calculated from the definition of μ , equation (6), and therefore

$$\frac{\partial L}{\partial V} = \rho S \gamma C_L \left(1 - \frac{1}{\Omega R} \frac{d\mu}{dV} \right) . \quad (10)$$

Now, in a similar fashion we may use the experimental results for $\frac{dD}{dV}$ and $\frac{dM}{dV}$, i.e., the drag and moment variations with velocity with both propeller

rotational speed and tunnel speed varying, to calculate $\frac{\partial D}{\partial V}$ and $\frac{\partial M}{\partial V}$. Then

$$\left. \frac{dD}{dV} \right|_{\alpha=0} = \rho S V C_D + \frac{1}{2} \rho S V^2 \frac{\partial C_D}{\partial \mu} \frac{d\mu}{dV} , \quad (11)$$

and, having solved for $\frac{\partial C_D}{\partial \mu}$, we find

$$\frac{\partial D}{\partial V} = \rho S V C_D + \frac{1}{2} \rho S V^2 \frac{\partial C_D}{\partial \mu} \frac{\partial \mu}{\partial V} \quad (12)$$

with a similar solution for $\frac{\partial M}{\partial V}$. It should be noted that this interpretation is valid only if propeller blade flexibility is unimportant.

SCALING

For purposes of comparison, all data and results given in this report were adjusted to represent full-scale aircraft with a gross weight of 40,000 pounds. Only points of primary interest related to scaling will be discussed here; a more detailed discussion of dynamically similar models is found in Reference 16.

Data for the VZ-2 aircraft were available both from model and full-scale tests, so two scale factors are involved. For scaling the full-scale aircraft at a gross weight of 3200 pounds to a weight corresponding to the actual full-scale for the VTOL transports, the data were adjusted according to Table I, but the scale factor, λ , was equal to the cube root of the ratio of weights, or

$$\lambda = \sqrt[3]{\frac{400}{32}} \quad (13)$$

All numbers in this report can be scaled to represent any desired gross weight by simply determining λ as in equation (13) and scaling according to Table I. Precisely speaking, the relationships given in Table I apply to a series of different size aircraft built from the same plans.

There is one other point to consider in the area of scaling. When the model tests are performed, it is necessary to vary the thrust settings as the transition progresses. On the full-scale aircraft, this is normally accomplished by changing propeller pitch, as the engine rpm is usually governed. For small models, however, it is both difficult and impractical to control thrust accurately with variable propeller pitch alone. Hence, in Reference 1, rpm was varied to regulate the thrust setting, while β remained fixed. In the Princeton tests described in Reference 8, propeller blade angle and model velocity were adjusted as the wing incidence was reduced from hovering. This procedure requires a number of runs to iterate to the proper combination of model velocity and blade angle for level flight trim, with the horizontal force equal to zero and the vertical force equal to the scale weight of the model. To simplify the testing procedure in Reference 15, the blade angle was set at the hovering value, and the forward speed at which the horizontal force was zero was determined experimentally. This generally resulted in too large a value of vertical force. The data obtained from this type of experiment may be precisely interpreted in terms of the full-scale aircraft at some altitude above sea level determined by the ratio of measured vertical force to scale weight.

Use of the trim data from Reference 1 and the interpretation of the data of Reference 15 at sea level conditions depend on the assumption that blade angle and advance ratio are interchangeable; either may be varied so long as the proper ratio of disc loading to free stream dynamic pressure is maintained. This means that, since in both cases blade angle was fixed, propeller torque is not accurately simulated, and the rotation of the slipstream will not be the same on the scaled-up model as on the full-scale aircraft. While these effects may be negligible, this assumption has not been verified, and an investigation into this particular area is recommended. Presently, it is thought that as long as the blade angle is reasonably close to the correct value, this assumption is satisfactory and results in simplification of the static experiments.

PRESENTATION OF DERIVATIVES

Figures 2 through 9, which follow, present the longitudinal stability derivatives and wing incidence versus trim velocity. It is important to realize that many wing incidences are represented, as well as different aircraft and various sources of data, so that some special scheme is necessary to identify the points. As was previously mentioned, the wing incidence determines trim speed, so that, in the following presentations of derivatives, wing tilt angle has been omitted entirely. The key to be used is given in Table II.

As a cross-reference, Table III gives the flap setting and horizontal tail incidences for each of the static derivative points of Figures 2 through 9. The points are listed by data source.

It is significant to note that a few of the derivative points were obtained from data which exhibited nonlinearities, although most were approximately linear for a reasonable range about the trim point. The two or three curves which were nonlinear over the entire range of α or u were not included. It is considered that the general nature of the experimental data justified the linearized analysis in most cases. Care should be taken, however, in interpreting the linearized results in flight conditions where important derivatives (such as M_α) are zero or near zero.

Further analysis must be made before any conclusions can be drawn from the graphs as presented; however, a few observations can be made. Note first that the "angle of attack" loses its significance in hover, where it is instantaneously 0 or $\pm 90^\circ$. Thus, the angle-of-attack derivative curves as presented are not meaningful at zero velocity. Little or no data are available on the vertical velocity derivatives in hovering, so angle of attack was chosen as a variable. A rough estimate of the vertical velocity derivatives in hover may be obtained from the variation of the angle-of-attack derivatives with forward speed near zero forward speed.

The X_α , Z_α , X_u , and M_u curves seem to have well defined shapes, but the values of M_α and Z_u are slightly more scattered. It should be noted that the velocity stability (M_u) tends to change sign at the trim speed

associated with approximately 60° wing incidence, quite possibly due to small nonlinearities in the data.

After determining the relative importance of scatter in the data, these graphs will be considered more carefully.

TABLE I
SCALE FACTORS

Linear Dimension	λ
Area	λ^2
Mass, Force	λ^3
Moment	λ^4
Moment of Inertia	λ^5
Linear Velocity	$\lambda^{1/2}$
Angular Velocity	$\lambda^{-1/2}$
Time	$\lambda^{1/2}$
Disc Loading, Dynamic Pressure	λ
X_α, Z_α	1
X_u, Z_u	$\lambda^{-1/2}$
M_α	λ^{-1}
M_u	$\lambda^{-1.5}$
M_θ	$\lambda^{-1/2}$

Note: Multiply model properties by scale factor to obtain full-scale properties.

TABLE II
KEY TO SYMBOLS FOR FIGURES 2 THROUGH 9

Airplane	Data Source*	Symbol
VZ-2	NASA 1	●
	Princeton 8	○
	Princeton**	hover ●
	NASA 4	◐
	NASA 2	rigid propeller ⊙
2-Propeller Transport	Princeton 7	□
4-Propeller Transport	Princeton 15	◇
	Reference 12	◊
	Flight Test 18	◈
Tandem-Rotor Helicopter	Princeton 10	▲
Single-Rotor Helicopter	Princeton 13	◑

*Numbers correspond to references.
**Unpublished.

TABLE III

CONFIGURATIONS FOR DATA POINTS OF FIGURES 2 THROUGH 9

Aircraft	Reference	V_{trim} (ft/sec)	i_w (deg)	δ_f (deg)	i_t (deg)
VZ-2	NASA 1, 2	22	80	none	off**
		77	60	"	"
		111	40	"	"
		176	20	"	"
		200	4	"	0°
	Princeton 8	37	70	none	off
		66	57	"	"
		94	44	"	"
	NASA 4	93	50	none	0°
		110	45	"	"
		121	40	"	"
		133	35	"	"
		154	30	"	"
		175	25	"	"
	2-Propeller Transport	Princeton 7	0	88.5	0
0			80	30	56
25,27			70	30	44
53,67*			60	30	25
94,99*			50	30	0
4-Propeller Transport	Princeton 15	0	90	0	45
		32	70	15	50
		55	60	32.5	30
		80	40	55	0

* $\theta_{fus} = -2^\circ$ for second V_{trim} listed.** $i_t = 10^\circ$ for M_u, M_α .

TABLE III - Contd.

Aircraft	Reference	V_{trim} (ft/sec)	i_w (deg)	δ_f (deg)	i_t (deg)	C_{T_s}
4-Propeller Transport	LTV 12	0	90	0	off	1.0
		42	60	40	"	0.95
		49	40	60	"	0.93
		64	30	60	"	0.85
		100	20	60	7°	0.6
	LTV Flight Test	34	65	0	32	
		51	50	30	30.5	
		73	40	30	26	
		90	30	30	19	
		118	20	30	11.5	
		208	0	30	0	

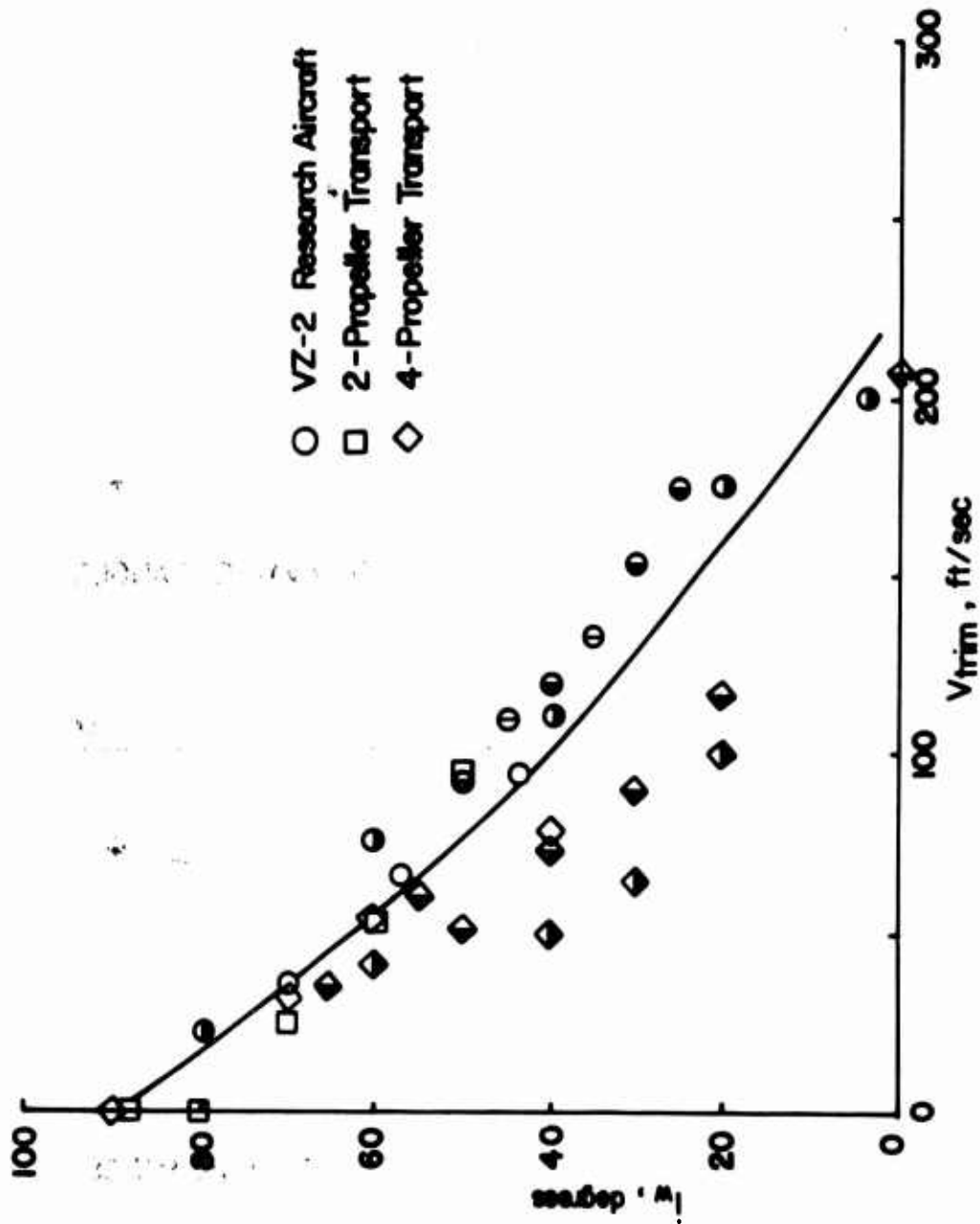


FIGURE 2. WING INCIDENCE VERSUS TRIM SPEED, INCLUDING AVERAGE LINE AND FLIGHT TEST DATA

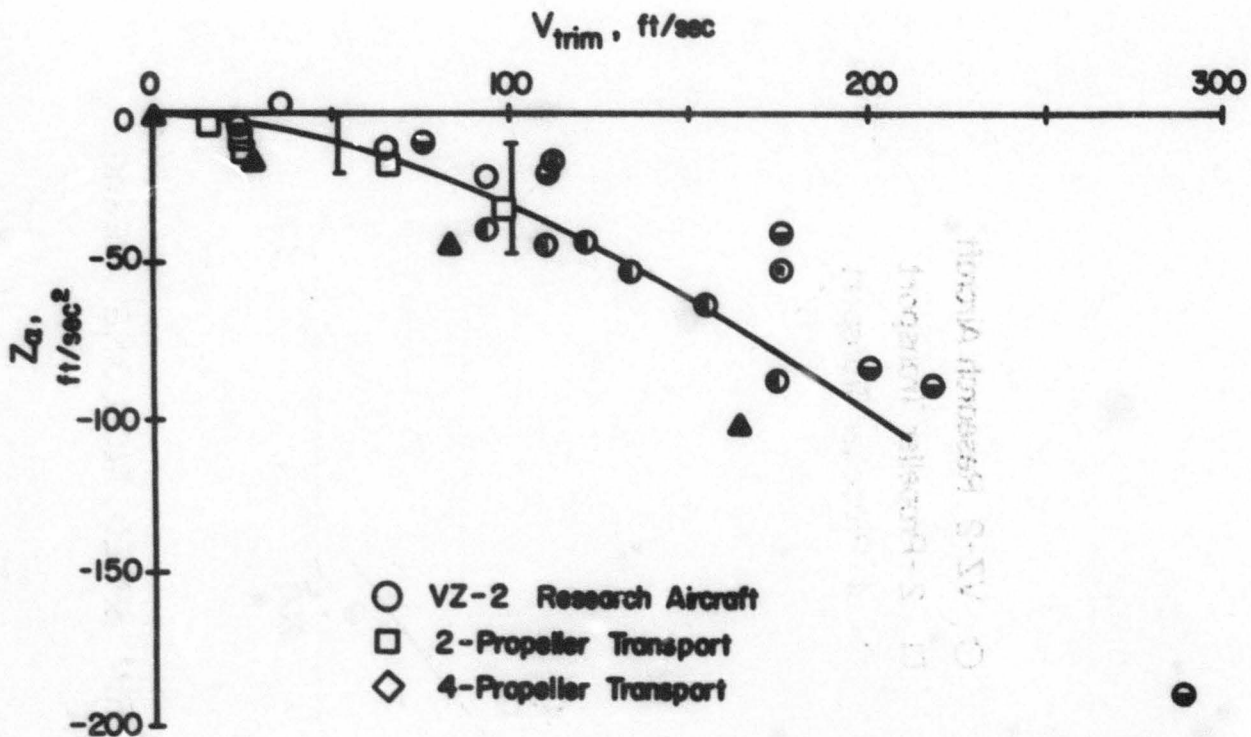


FIGURE 3. Z_{α} VERSUS TRIM SPEED, INCLUDING DERIVATIVE RANGES

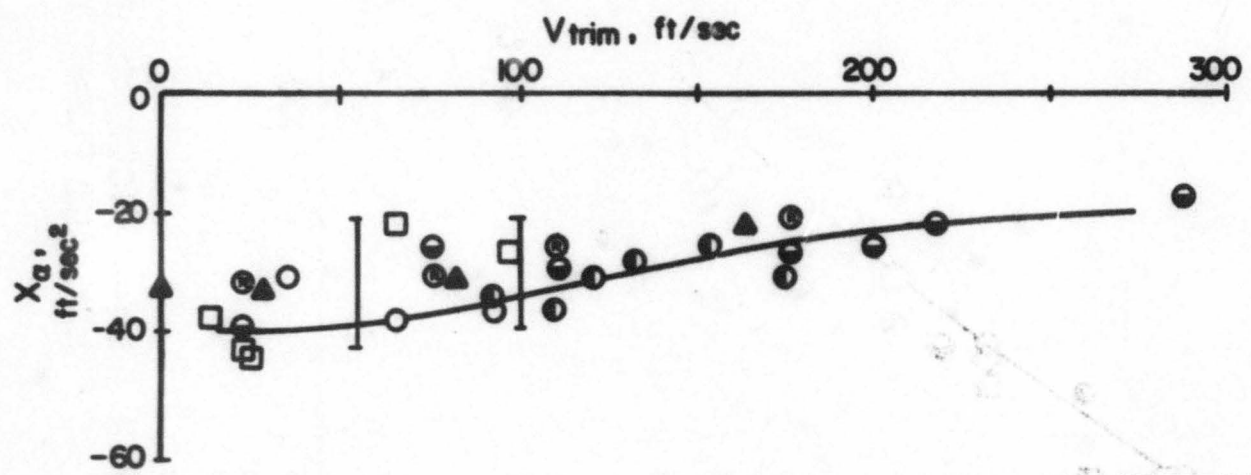


FIGURE 4. X_{α} VERSUS TRIM SPEED, INCLUDING DERIVATIVE RANGES

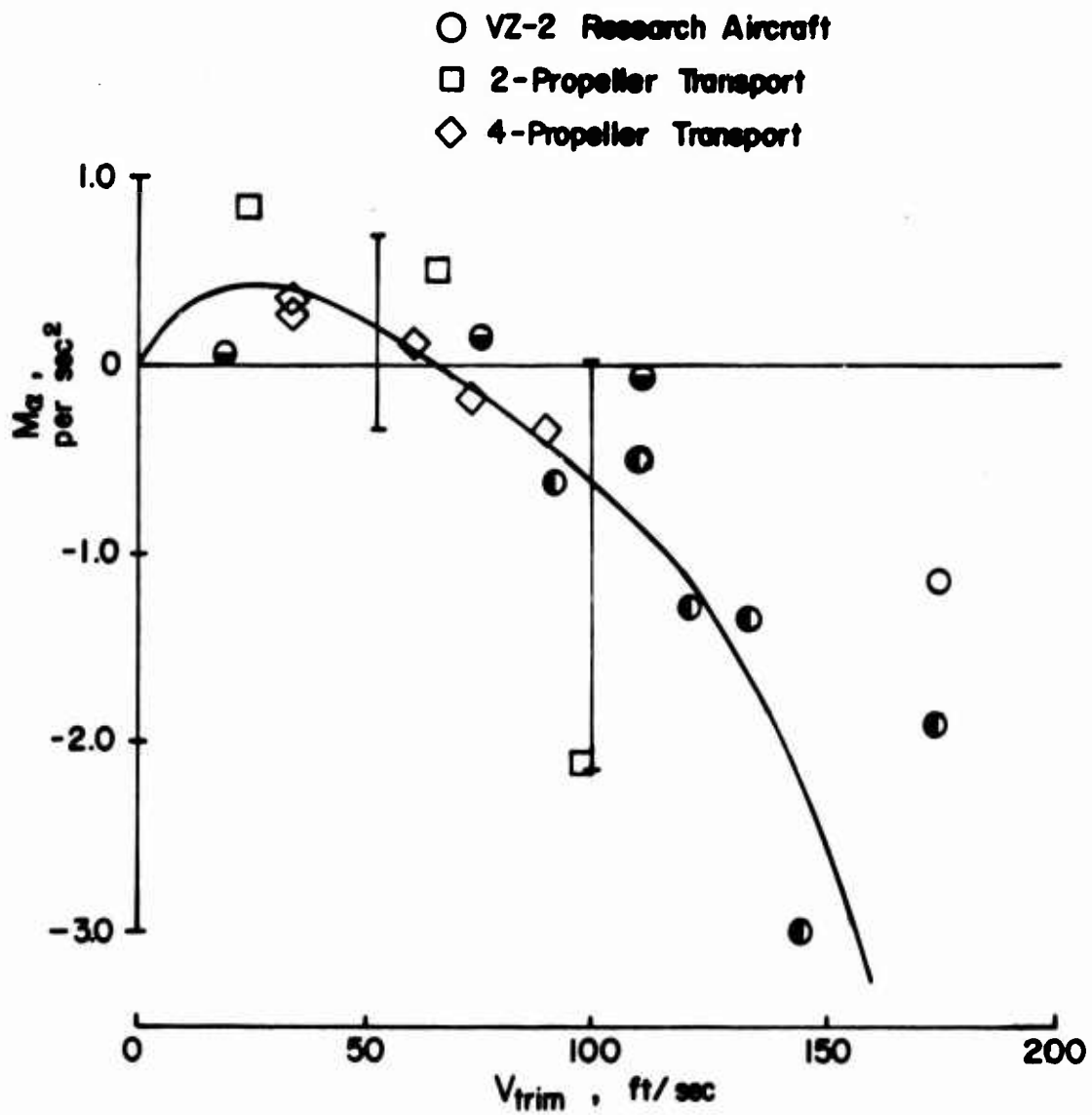


FIGURE 5. M_a VERSUS TRIM SPEED, INCLUDING DERIVATIVE RANGES

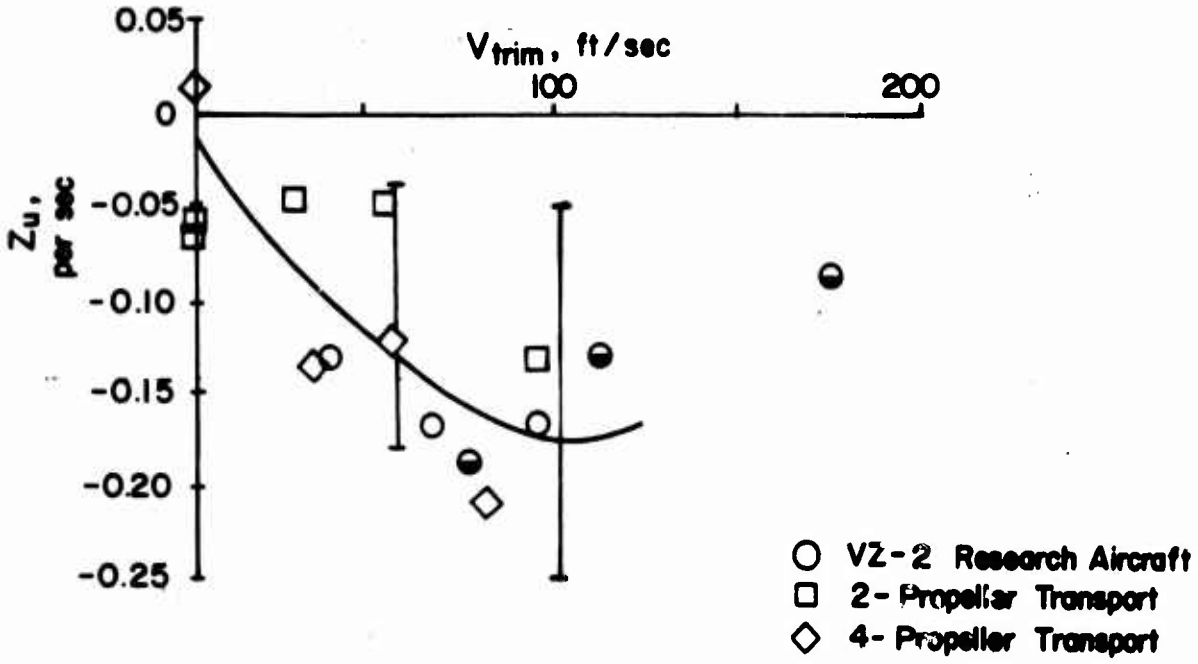


FIGURE 6. Z_u VERSUS TRIM SPEED, INCLUDING DERIVATIVE RANGES

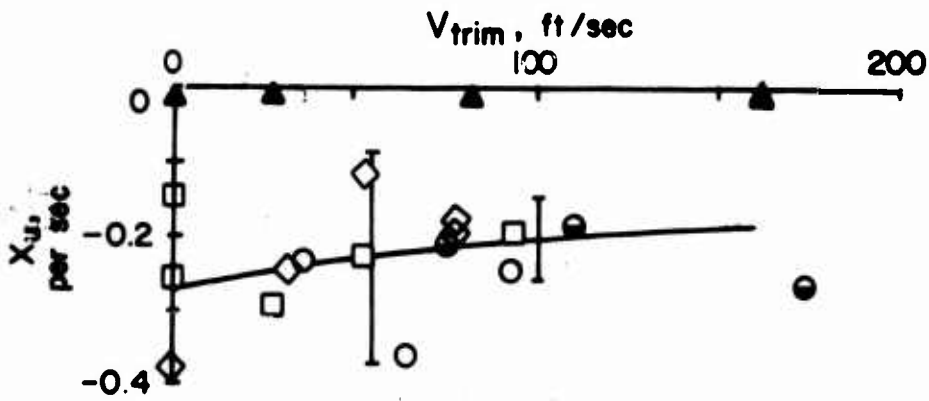


FIGURE 7. X_u VERSUS TRIM SPEED, INCLUDING DERIVATIVE RANGES

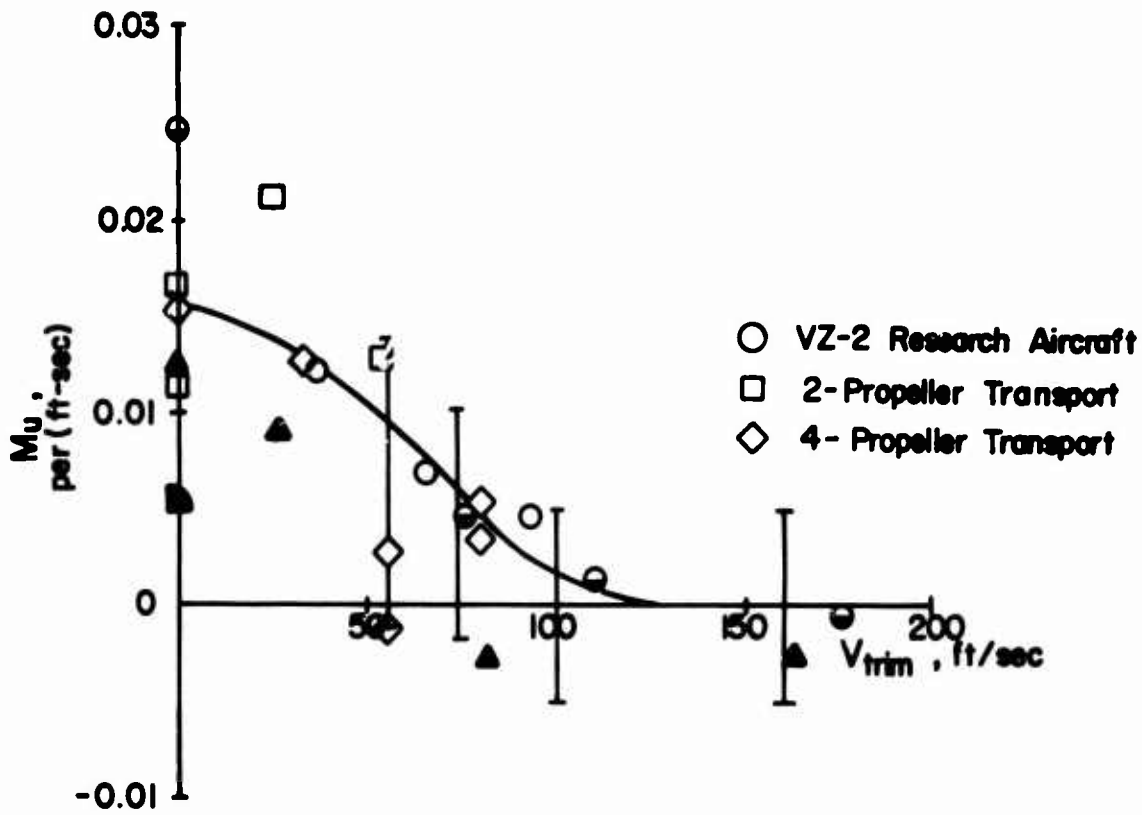


FIGURE 8. M_{u_u}' VERSUS TRIM SPEED, INCLUDING DERIVATIVE RANGES



FIGURE 9. $M_{g'_\phi}$ VERSUS TRIM SPEED, INCLUDING DERIVATIVE RANGES

ROOT-LOCUS ANALYSIS OF DERIVATIVES

INTRODUCTION AND EQUATIONS OF MOTION

The analysis consists of two parts: a root-locus study of the characteristic roots of a typical VTOL, and an analog computer analysis of the transient response of the aircraft. The results of this study should give an estimate of the accuracy to which the stability derivatives of a tilt-wing VTOL should be measured. To firmly establish the importance of the variations of the derivatives, the handling qualities, i.e., the task of piloting the aircraft, must be considered. In this regard, it should be noted that a number of the stability derivatives have a dual importance since they determine the sensitivity of the aircraft to gust disturbances as well as the dynamic response characteristics. Further discussion of this relationship in hovering may be found in Reference 5. Detailed consideration of this aspect of the problem is outside the scope of this report.

The root-locus analysis is based on conventional longitudinal, linearized, small-perturbation equations, as given by Seckel in Reference 9. A moment control was chosen for the input, which is reasonable for a constant-altitude transition. In the equations, $M_{\dot{\theta}}$ was used as M_{θ} , and $M_{\dot{\alpha}}$ was neglected, since M_{θ} and M_{α} were not available separately.

For hovering, a two-degree-of-freedom approximation was employed in which the angle of attack variable was removed and the vertical mode of motion suppressed. This vertical mode is generally an uncoupled convergence that has little effect on the other modes, making the approximation useful for stability analyses. The wind-axis equations of motion, in Laplace transform notation, are

$$(X_u - s) \Delta u + (X_\alpha + g) \Delta \alpha - g \Delta \theta = 0$$

$$\frac{Z_{A1}}{V_0} \Delta u + \left(\frac{Z_\alpha}{V_0} - s \right) \Delta \alpha + s \Delta \theta = 0$$

$$- M_u \Delta u - M_\alpha \Delta \alpha + (s - M_{\dot{\theta}}) s \Delta \theta = M_{\delta_s} \Delta \delta_s$$

and the characteristic determinant is

$$\begin{vmatrix} X_u - s & X_\alpha + g & -g \\ \frac{Z_u}{V_0} & \frac{Z_\alpha}{V_0} - s & s \\ -M_u & -M_\alpha & s(s - M_\theta) \end{vmatrix} = 0 .$$

METHOD OF ANALYSIS

Averaging Concept

The method of approach was to draw a "graphical average" line through the points for each derivative and then to consider points obtained from this line as typical of a tilt-wing VTOL aircraft. This method allows a more general analysis, since the individual aircraft have been replaced by an average one, and variations in period, damping, etc., will be more meaningful. The plots of derivatives (Figures 3 through 9) with the "envelope" of points, as well as the ranges of variation, are presented. Table IV lists these ranges in a more concise form.

Note that some of the figures contain derivative values representative of a tandem-rotor helicopter and that the M_u curve includes a point for a single-rotor helicopter as well. It is hoped that these points, each of which is scaled to represent a 40,000-pound aircraft, will be interesting and helpful for purposes of comparison with the tilt-wing data.

It must be realized that there are many combinations of values for the coefficients in the equations of motion, and that the average values presented here do not represent an aircraft with optimal stability characteristics. An analysis of the effects of the individual coefficients on the stability characteristics is desirable, however, and the average values represent useful initial conditions.

Characteristic Roots

The ensuing discussion is in terms of wing incidence angles rather than trim velocities. The trim velocity/wing incidence curve of Figure 2 is used to obtain the representative wing incidence settings.

Average or typical values of derivatives from Table IV are introduced into the equations of motion, and three sets of characteristic roots are calculated, representing wing incidences of 40° , 60° , and 90° (Figure 11). As was previously mentioned, the vertical degree of freedom is not included

TABLE IV
DERIVATIVE RANGES FOR THREE WING INCIDENCES

Derivative	$i_w = 40^\circ$		$V_0 = 100\text{fps}$		$i_w = 60^\circ$		$V_0 = 55\text{fps}$		$i_w = 90^\circ$		$V_0 = 0$
		Avg		Avg		Avg		Avg		Avg	
X_u per sec	- 0.1	- 0.2	- 0.3		- 0.1	- 0.22	- 0.36		- 0.15	- 0.3	- 0.4
X_α ft/sec ⁴	-20	-31.5	-40		-20	-25.8	-42		*	*	*
$\frac{Z_u}{V_0}$ per ft	- 0.0005	- 0.0021	- 0.0025		- 0.0007	- 0.0025	- 0.0033		*	*	*
$\frac{Z_\alpha}{V_0}$ per sec	- 0.1	- 0.315	- 0.5		0	- 0.21	- 0.36		*	*	*
M_u per ft-sec	0.005	0	- 0.005		0.014	0.01	- 0.001		0.025	0.016	0.01
M_α per sec ²	0.2	- 1.15	- 2.2		0.7	0.172	- 0.25		*	*	*
M_θ per sec	- 0.4	- 0.59	- 0.9		0	- 0.08	- 0.2		0.1	- 0.12	- 0.3

*Not included in approximation.

for the hover case. The roots for the 40° incidence are a short-period oscillation with a period of about 6.2 seconds, and a lightly damped oscillation with a period of about 26 seconds. The 60° case exhibits a very heavily damped oscillation with a period of about 45 seconds, and an unstable oscillation with a period of about 8.4 seconds, with a time to double amplitude of about 70 seconds. The hovering roots represent a convergence and an unstable oscillation with a period of 9.5 seconds, with $T_2 = 2.6$ seconds.

Root-Locus Equations

A series of root-locus diagrams is constructed, corresponding to equations similar to the following one which represents a change in M_α :

$$\frac{\Delta M_\alpha \left[s^2 - X_u s - g \frac{Z_u}{V_0} \right]}{\text{[Characteristic Equation]}} = 1 .$$

ΔM_α represents the variation from the average value of M_α used to obtain the characteristic roots, and is also the gain along the locus of roots. Using this technique, it is possible to study the character of the aircraft roots as the individual derivatives are varied, and at the same time provide a guide for a subsequent analog computer analysis.

RESULTS OF ROOT-LOCUS ANALYSIS

The results of the root-locus study indicate the predominate effect of the pitching moment derivatives in determining the dynamic response characteristics of these tilt-wing VTOL aircraft. Root-locus sketches showing the effect of more important derivative variations are presented in Figures 21 through 26.

For the 40° wing incidence, only M_α had a significant effect on the root locations. This sketch is shown along with X_α and M_u for the 40° case in Figures 21 through 23. The variation of M_α had a large effect on the aircraft characteristic modes of motion; consequently, a considerable difference between a scaled-up VZ-2 and the two-propeller transport might be expected since these vehicles represent the two extreme values of M_α at this wing incidence. It is also important to note that these differences in M_α were obtained from model tests, and may be caused by unusual horizontal tail incidences.

For the 60° set of loci, alterations in Z_u , Z_α , X_u , and M_α , produced small changes in the dynamics, whereas alterations in M_α and M_u

resulted in significant variations (Figures 24 and 25). The largest negative value of $M_{\dot{\alpha}}$ was sufficient to make the dynamic motion of the aircraft stable. The maximum positive value of $M_{\dot{\alpha}}$ resulted in an oscillatory instability, while the maximum negative value gave rise to a pure divergence. The variation of the characteristic roots due to the range of the force derivatives at $i_w = 60^\circ$ were all similar in magnitude to the trend shown for $X_{\dot{\alpha}}$ at $i_w = 40^\circ$ in Figure 22.

The hovering roots were affected little by changes in $X_{\dot{\alpha}}$, and the period of oscillation was controlled by $M_{\dot{\alpha}}$; $M_{\dot{\beta}}$ principally affected rate of growth of the unstable oscillation. In general, the dynamics of all three aircraft were quite similar in hover.

ANALOG COMPUTER STUDY OF AIRCRAFT DERIVATIVES AND DYNAMIC RESPONSE

INTRODUCTION

The results of the root-locus analysis indicated that certain derivatives, when varied within the ranges exhibited by the aircraft concerned, caused very little change in the root locations; hence, period and damping remained nearly the same. Others, primarily pitching moment derivatives, caused considerable changes in root locations. In order to obtain further insight into the nature of the motions of the aircraft, the response of the various configurations to pulse inputs was studied using an analog computer. In some cases the root-locus plots may indicate substantial changes in root location when there are only small changes in the first few seconds of the response. The dynamic response of the aircraft must be studied before any conclusions can be drawn about differences or similarities among aircraft, or, for that matter, about desired accuracies in model testing.

To accomplish this study of transient responses, an analog computer program was undertaken, using a PACE TR-48 Analog Computer and a Sanborn four-channel recorder. The equations of motion which were set up on the computer are as follows:

$$\dot{u} = X_u \Delta u + X_\alpha \Delta \alpha + g \Delta \alpha - g \Delta \theta$$

$$\dot{\alpha} = \frac{Z_u}{V_0} \Delta u + \frac{Z_\alpha}{V_0} \Delta \alpha + \Delta \dot{\theta}$$

$$\ddot{\theta} = M_u \Delta u + M_\alpha \Delta \alpha + M_{\dot{\theta}} \Delta \dot{\theta} + M_{\delta_s} \Delta \delta_s$$

The derivatives were individually introduced through potentiometer settings and were varied for the different runs. The computer diagram is given in Figure 27.

SELECTION OF INPUTS

The choice of inputs for the runs was based on several considerations. As was mentioned, only a moment disturbance was assumed so that the input corresponds to an increment in longitudinal stick deflection, $\Delta \delta_s$. The character of the response to a stick motion is not dependent on the input; that is, the period and damping of the motion are not functions of the control deflection, owing to the assumption of linearity. Figure 12 shows a comparison between a step response and a pulse response for a typical case. The transient motion that results from a step input is excessive for an aircraft with a low angle of attack stability, and is probably not a

practical input in flight tests of these aircraft. Consequently, a pulse input was selected. To obtain a readily repeatable pulse input, a first-order network as shown in Figure 10 was used.

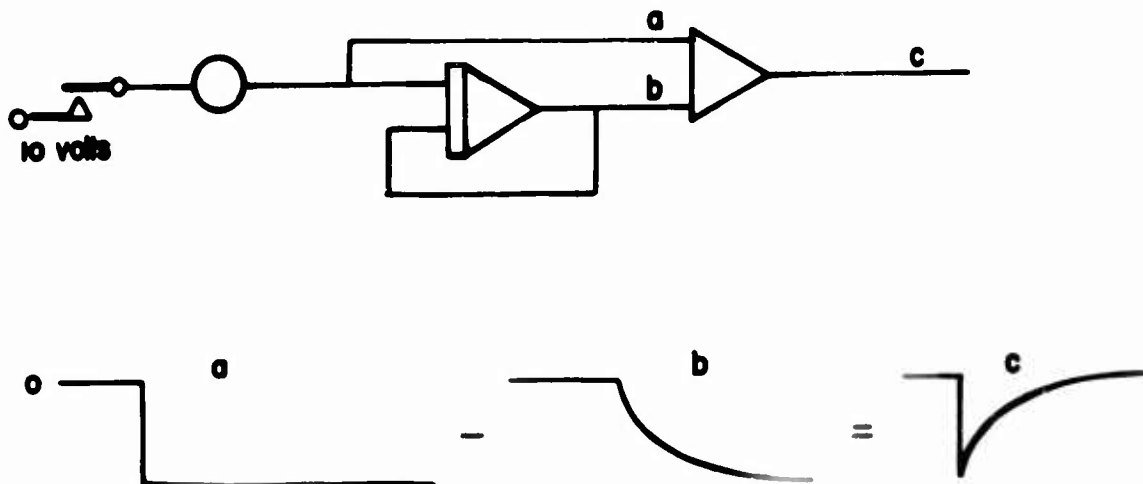


FIGURE 10. COMPUTER CIRCUIT TO GENERATE INPUT PULSE

A 1.0-second time constant was used at wing incidences below 50° and a 0.1-second time constant above 50° . The control sensitivity, M_{δ_S} , was equal to $-0.05 \frac{\text{rad/sec}^2}{\text{inch}}$ (Reference 5).

RESULTS OF ANALOG ANALYSIS

Discussion of Runs

Nearly two hundred runs were made for wing incidences ranging from 20° to 90° and trim velocities from zero to 160 feet per second. Responses were obtained for the basic sets of derivatives at nine wing incidences; for certain representative incidences, derivatives were varied within their respective ranges, with some being set equal to zero.

The majority of runs were for comparison of the responses as the individual derivative was varied within its range obtained from the data. This was accomplished by first making a run with all derivatives set at their average values; the derivative in question was then set for its maximum and minimum values, etc., until a set of traces was obtained for each derivative. Superimposed traces are presented in Figures 28 through 38.

While no effort was made to conduct a detailed comparison, the response curves obtained from the computer study were found to be very similar to measured transient response data, as shown in References 3 and 6.

To make a rough judgment of the importance of variations in the transient response in the task of piloting the aircraft, it is assumed that any changes in the response that occur after 10 seconds would be of minor importance to the pilot. It should be noted, however, that some derivatives, such as M_u , while not causing significant changes in the initial response of the aircraft, will result in considerable variations in the gust sensitivity of the aircraft which would be of significance in piloting the aircraft (Reference 5).

While flying qualities are not part of this study, the real significance of the variations in the derivatives is in relation to the task of piloting the aircraft.

Comparison of Responses for Various Wing Incidences

Let us first consider the various responses exhibited by the simulated aircraft for several transition states. In Figure 28, the responses are shown for wing angles of 90° through 40° , all for the same input. Below 40° , the responses to this pulse input are very small, by comparison. These responses, including $i_w = 50^\circ$, are shown in Figure 29, with expanded vertical scales. Note that an unstable oscillation exists for incidences above about 50° , or below a velocity of about 75 feet per second (45 knots). Variations in the dynamics are very minor for the first 5 seconds after the input.

Responses for Individual Derivative Variations

Figures 30 through 38 represent the results of varying individual derivatives on the computer. The graphs themselves are superimposed analog computer traces, where in each case the dashed line represents the response when the particular derivative assumed its average, or typical, value. Many of the curves are interesting from the standpoint that they exhibit no significant variations as the derivatives are changed within their respective ranges. These, however, do not warrant individual discussions, so they have been compiled and listed in Table V.

Some of the figures present "borderline" cases, such as shown in Figure 34(B). This represents changes in X_{α} for $i_w = 60^\circ$, and $V_0 = 55$ feet per second. Within the first 10 seconds, there are about 3° of variation in pitch angle for the different derivative values, although the initial response commanded by the stick is the same. The velocity difference constitutes no more than a 5-percent change from trim, and maximum pitch rate is not more than 2° per second. While these variations are thought to be insignificant, they are to be recognized since decreasing the value of drag due to angle of attack is a destabilizing effect.

In Figure 31(F), the important effect of angle of attack stability is exemplified: $M_{\alpha} = 0$ represents a slightly convergent mode, and any positive or statically unstable value leads to divergence which becomes increasingly rapid as M_{α} increases positively.

It may be noted at this point that the significant variations in responses have been due almost entirely to fluctuations in moment derivatives, while force derivative variations have had little effect. Therefore, only the moment derivatives were varied for 20° , 50° , and 55° wing incidences.

Figure 32(A) is interesting in that a relatively short-period, divergent oscillation appears when the speed stability is increased sufficiently.

Both Figures 32(B) and 33(B) indicate the effects of M_{α} on the stability of the aircraft; although a relatively large negative value is essential for stability, the divergence rate is slow for the range of M_{α} investigated.

Figure 34(E) shows the variation in response for the ranges of M_{α} at $V_0 = 55$ feet per second ($i_w = 60^{\circ}$). There is a considerable difference in the response after about 6 seconds; in fact, at 10 seconds, there is a 20° variation in pitch angle for the values of M_{α} considered. A 20-percent reduction from the trim speed is encountered after 10 seconds for $M_{\alpha} = -0.001$.

The variation in M_{α} for $i_w = 60^{\circ}$ is expressed by Figure 34(F), in which large positive M_{α} (statically unstable) leads to a rather rapid divergence in u and θ . It is essential to note that the two data points which contribute to the upper (positive) values of M_{α} for $i_w = 50^{\circ}$ through 80° are both for the two-propeller transport model. These values are apparently due to the fact that the horizontal tail incidence was high: 25° for $i_w = 60^{\circ}$, and 44° for $i_w = 70^{\circ}$. In fact, in Figure 5, the data point at $V_0 = 65$ feet per second is for this configuration with $i_w = 60^{\circ}$ and $i_t = 25^{\circ}$. The data point at $V_0 = 98$ feet per second is for $i_w = 50^{\circ}$, but $i_t = 0^{\circ}$. As can be seen, a variation in M_{α} of about 2.6 separates the points.

At a trim velocity of 98 feet per second, this difference is of the same magnitude as the horizontal tail contribution to the angle of attack stability. This contribution may be estimated from Reference 9, page 60 as

$$(\Delta M_{\alpha})_T = - \frac{l_T S_T C_{L_{\alpha_T}} q \eta_T \left(1 - \frac{d\epsilon}{d\alpha} \right)}{I_y}$$

where

l_T	tail length, 28 feet
q	free stream dynamic pressure, 11.5 p.s.f.
S_T	tail area, 210 square feet
$C_{l_{\alpha_T}}$	lift curve slope of horizontal tail, 3.9 per radian (aspect ratio = 4)
I_y	123,000 slug-feet squared
η_T	tail efficiency factor
$\frac{d\epsilon}{d\alpha}$	rate of change of downwash with angle of attack

There is a lack of experimental data for these configurations that makes it difficult to estimate the last two factors. It would be expected that the tail efficiency would be greater than one due to the effects of the slipstream that would tend to compensate for $\frac{d\epsilon}{d\alpha}$. Therefore, to obtain a rough estimate of the above term, it is assumed that

$$\eta_T \left(1 - \frac{d\epsilon}{d\alpha} \right) = 1 .$$

Substituting these values,

$$(\Delta M_{\alpha})_T = - 2.2 \text{ per second squared.}$$

If the horizontal tail were stalled, the lift curve slope would be approximately zero and would provide no contribution to the angle of attack stability.

This would indicate that the tail incidences used in some of the two-propeller transport tests are destabilizing and would not be recommended for use on the actual aircraft. (Information of this type is an objective of the Princeton Dynamic Model Track tests and should not detract from the model comparisons.)

The effects of varying pitch damping are evident in Figure 34(G), where a 5° variation in θ is found between the different values of M_θ , for $i_w = 60^\circ$. Figure 35(C) shows more pronounced changes, mainly due to the possibility of a positive value of M_θ in hover.

Distortion of the response curve due to changes in M_u clearly shows a variation in period in Figure 35(B). As was expected from the root-locus diagram (Figure 26) for this hovering case, the damping ratio remains essentially unchanged as M_u is increased; however, the time to double amplitude is decreased.

Discussion of Derivative Approximations

A rough summary of the analog computer results may be obtained by considering what changes in the response are incurred if certain of the derivatives are simply set equal to zero.

Remember that this analysis is based on a set of linearized equations, and any approximations which appear to be good under this assumption might prove to be very unsatisfactory if the derivatives, in fact, exhibit nonlinearities. Approximations to motions which are of large amplitude or long period would, in this case, be most unsatisfactory. Note also that only u , θ , and $\dot{\theta}$ have been considered for these approximations, so that the effect of setting Z_{α} equal to zero on the angle of attack and normal acceleration responses, for example, has not been included.

Figures 36(A) through 36(C) for $i_w = 20^\circ$ and $M_u = 0$ show the cases of X_{α} , Z_u , and Z_{α} equal to zero. A reasonable approximation to the u , θ , and $\dot{\theta}$ is obtained with each of these derivatives equal to zero.

For the 40° case ($V_0 = 100$ feet per second), the only reasonable approximation was for $X_{\alpha} = 0$ (Figure 37), although there is some change in the Δu response. For $i_w = 60^\circ$ (Figure 38), the approximation for $Z_u = 0$ proved to be quite good. The results of this phase of the study are presented in Table VI, and are meant to be no more than guidelines to simplifying assumptions. The variables listed are those which were closely approximated when the respective derivative equaled zero.

TABLE V

SUMMARY OF ANALOG COMPUTER RESPONSE DATA

	90°	60°	55°	50°	40°	20°
i_w	0 ft/sec	55	65	75	100	160
X_u	*	*			*	
X_α	-	$\theta, \dot{\theta}$			*	
Z_u	-	*			*	
Z_α	-	*			*	
M_u	$u, \theta, \dot{\theta}$	$u, \theta, \dot{\theta}$	$u, \theta, \dot{\theta}$	$u, \theta, \dot{\theta}$	*	*
M_α	-	$u, \theta, \dot{\theta}$	$u, \theta, \dot{\theta}$	$u, \theta, \dot{\theta}$	$u, \theta, \dot{\theta}$	*
$M_{\dot{\theta}}$	$\theta, \dot{\theta}$	*		$u, \theta, \dot{\theta}$		

Derivatives marked with a hyphen in the 90° column were not included in the hover equations.

Blank indicates that a run was not made.

* indicates that no significant change in response was observed in 10 seconds.

Variables listed were significantly affected by varying that particular derivative.

TABLE VI

SUMMARY OF APPROXIMATION RESULTS

Derivative equal to zero	$i_w = 90^\circ$	$i_w = 60^\circ$	$i_w = 40^\circ$	$i_w = 20^\circ$
X_u	-	θ	-	$\dot{\theta}$
X_α	$*X_w = 0$	-	$\theta, \dot{\theta}$	$u, \theta, \dot{\theta}$
Z_u	$*Z_u = 0$	$u, \theta, \dot{\theta}$	$\dot{\theta}$	$\theta, \dot{\theta}$
Z_α	$*Z_w = 0$	Marginal	-	Marginal
M_u	-	-	$u, \theta, \dot{\theta}$	$u, \theta, \dot{\theta}$
M_α	$*M_w = 0$	-	-	-

(Variables listed are well approximated with derivative = 0)

*Two-degrees-of-freedom approximation assumption.

DISCUSSION OF RESULTS OF COMPUTER AND ROOT-LOCUS STUDIES

IMPORTANCE OF SCATTER IN DATA

The object of this study has been to evaluate and compare the longitudinal stability derivatives of models of three tilt-wing VTOL aircraft. In order to establish the degree of similarity between these VTOL types, as well as test facilities, a comprehensive analysis of the derivatives was undertaken. This analysis was necessitated by the appearance of scatter in some of the derivative data, notably for Z_u , M_u , and M_α (Figures 6, 8, and 5, respectively).

The results of the analysis indicate that the effect of any variations of the force derivatives was minor on the dynamic response. Variations in the moment derivatives, however, were more significant and proved to be the important ones. The effects of M_α , while important, have been given only limited consideration because the limited availability of data made a thorough study of its effects unwarranted.

The following sections cover the subject of scatter in the data from the source and model standpoints.

DATA FROM DIFFERENT SOURCES

As is evident from Figures 3 through 9, there is excellent correlation between NASA and Princeton data on the VZ-2 aircraft. This is especially significant since different size models as well as different testing procedures were used.

COMPARISON OF DERIVATIVES AMONG VTOL TYPES

Presentation of the stability derivatives of these tilt-wing aircraft as a function of forward speed results in a reasonably orderly variation of the derivatives through the transition regime.

The majority of the data for the force derivatives Z_α , X_u , and X_α follow the average lines and thus appear to be insensitive to configuration differences or variations in the wing incidence/forward speed relationship. The insensitivity in X_α arises from the fact that the major contribution to this derivative is due to the tilting of the thrust vector of the vehicle. X_α is equal to -32.2 ft/sec^2 for all configurations in the limiting case of hover.

The angle of attack stability of all the vehicles follows a general trend, being unstable at low speeds and changing sign and becoming stable as forward speed is increased. The primary source of this favorable trend is the stabilizing contribution of the horizontal tail increasing with increasing free stream dynamic pressure. Variations in the data indicate

that the horizontal tail is stalled on one configuration as discussed earlier.

The derivatives Z_u and M_u show more variation among the configurations. It would be expected that these derivatives are more sensitive to details of the individual configurations and the wing incidence/forward speed relationship. Both of these terms would depend upon flap setting and tail incidence as well as propeller incidence, whereas the angle of attack derivatives would not be particularly sensitive to these quantities as long as the surfaces are not stalled. Note also that the speed stability M_u is a function of the manner in which the aircraft is trimmed; that is, it depends on the proportion of trimming moment supplied by the tail rotor or other trimming device compared to that provided by the horizontal tail.

Thus, for various reasons, including the probable existence of nonlinearities, the velocity stability derivative variations among the models are difficult to explain in the region where the derivative is small. The variations of M_u exhibited in these tests, however, had little effect on the initial response of the simulated aircraft, even though instabilities eventually resulted from values of M_u which were either too large or too small. For these reasons, it is believed that no appreciable differences in velocity stability exist among these tilt-wing VTOL aircraft, although more sensitive measurements in the tests for determining M_u would be beneficial to a more thorough analysis.

These remarks refer only to the effects of M_u on the transient response. It should be noted that this derivative also has an important role in determining the gust sensitivity of the vehicle at low speeds (Reference 5), and in this respect the variations noted here may take on additional significance.

TABLE VII
COMPARISON OF FULL-SCALE VTOL CHARACTERISTICS

	VZ-2*	4-Prop. Transport	2-Prop. Transport
Gross Weight (lb)	40,000	40,000	40,000
I_y (slug-ft ²)	164,000	123,000	123,000
Disc Loading (lb/ft ²)	52.6	53.3	44.2
Wing Span (ft)	58	67.5	56
Wing Area (ft ²)	636	535	470
Propeller Type	flapping	rigid	rigid
Propeller Diameter (ft)	22	15.5	24
Fuselage Length (ft)	61.2	50	50

*Full-scale VZ-2 scaled to 40,000-pound gross weight.

CONCLUSIONS

Several conclusions have been made as a result of this study. However, it is important to recognize the limitations of the analysis: it was first assumed that the motions of the aircraft could be represented by linearized equations, and a subsequent averaging process was utilized to obtain coefficients for these equations.

Based on these assumptions, the following conclusions have evolved:

1. Longitudinal force derivatives exhibited by the three types of tilt-wing VTOL aircraft considered are quite comparable. Variations in the derivatives from average values do not exert significant effects on the dynamic response characteristics of these aircraft.
2. The most critical derivatives are the pitching moment derivatives. The pitching moment variation with angle of attack is unstable at low speeds and stable at high speeds. The pitching moment variation with horizontal velocity is large and positive at low speeds and decreases towards zero as forward speed increases.
3. No important approximations can be suggested for further analysis owing, in part, to the presence of nonlinearities in the derivatives as they become quite small. It may be noted that M_u , while very important at the lower speeds, becomes much less significant at velocities above about 100 feet per second.

RECOMMENDATIONS

1. Further analysis should be conducted to determine the significance of nonlinearities in the static data from which the longitudinal derivatives are obtained. This study should include consideration of the dynamic motions in flight conditions where the linearized derivatives (in particular, $M_{\dot{q}}$ and $M_{\dot{u}}$) are zero or near zero.
2. A thorough study should be made of the flow about the horizontal tail in order to determine the dynamic pressure and downwash angles at the tail at very low speeds.
3. It is strongly recommended that stability and control tests of powered models be conducted in such a manner that the velocity derivatives can easily be obtained from wind tunnel and flight data.
4. A series of experiments should be conducted to determine the validity of the assumption that blade angle and advance ratio are interchangeable in model thrust settings. Measurements of forces and moments should be made and compared in experiments related to stability and control for various combinations of β and u , and the question of preservation of slipstream rotation should be carefully considered.

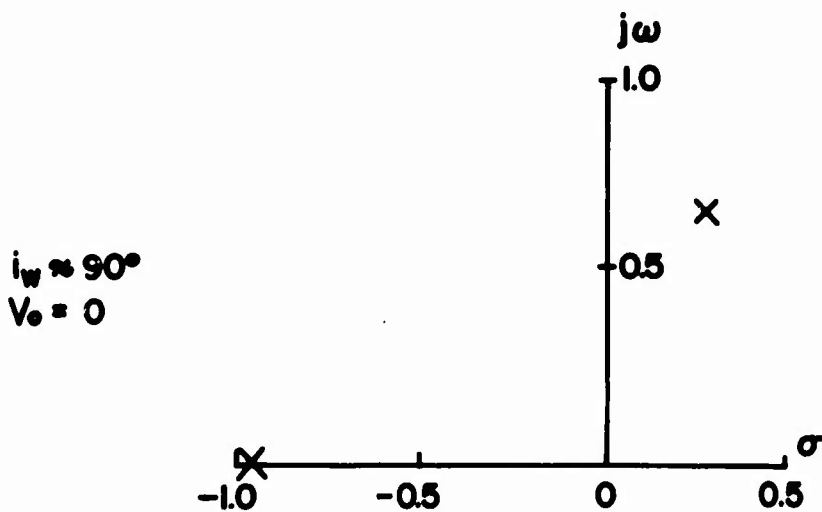
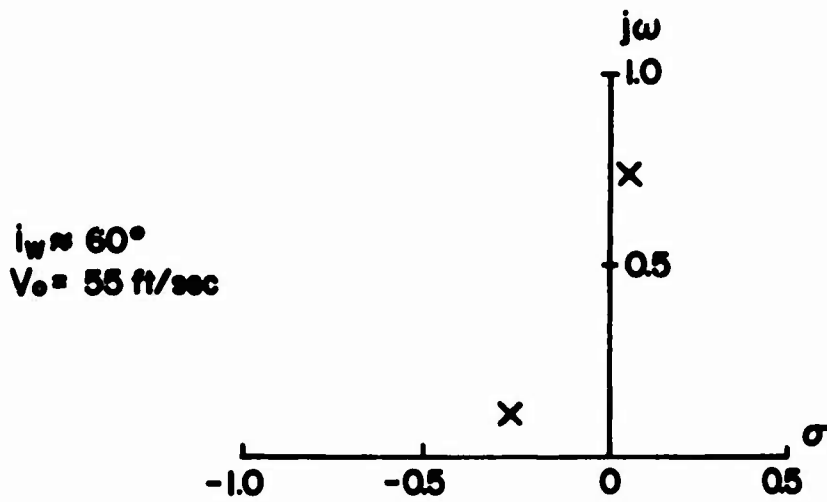
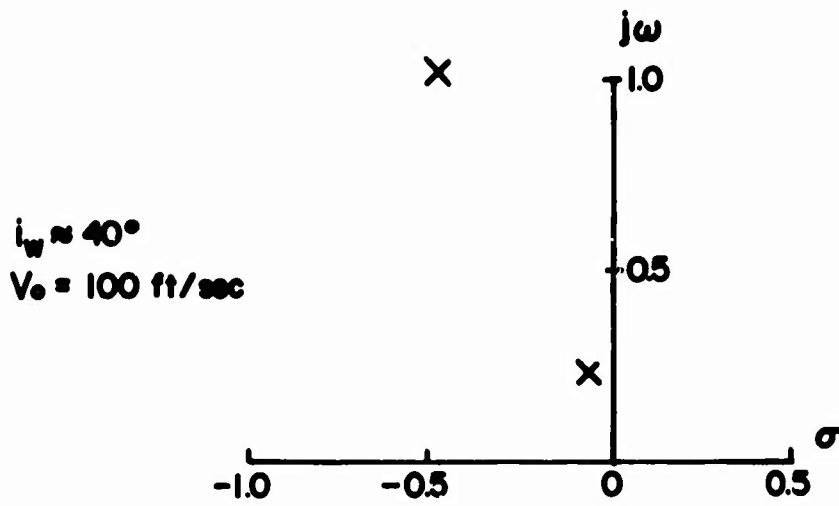


FIGURE II. TYPICAL CHARACTERISTIC ROOTS

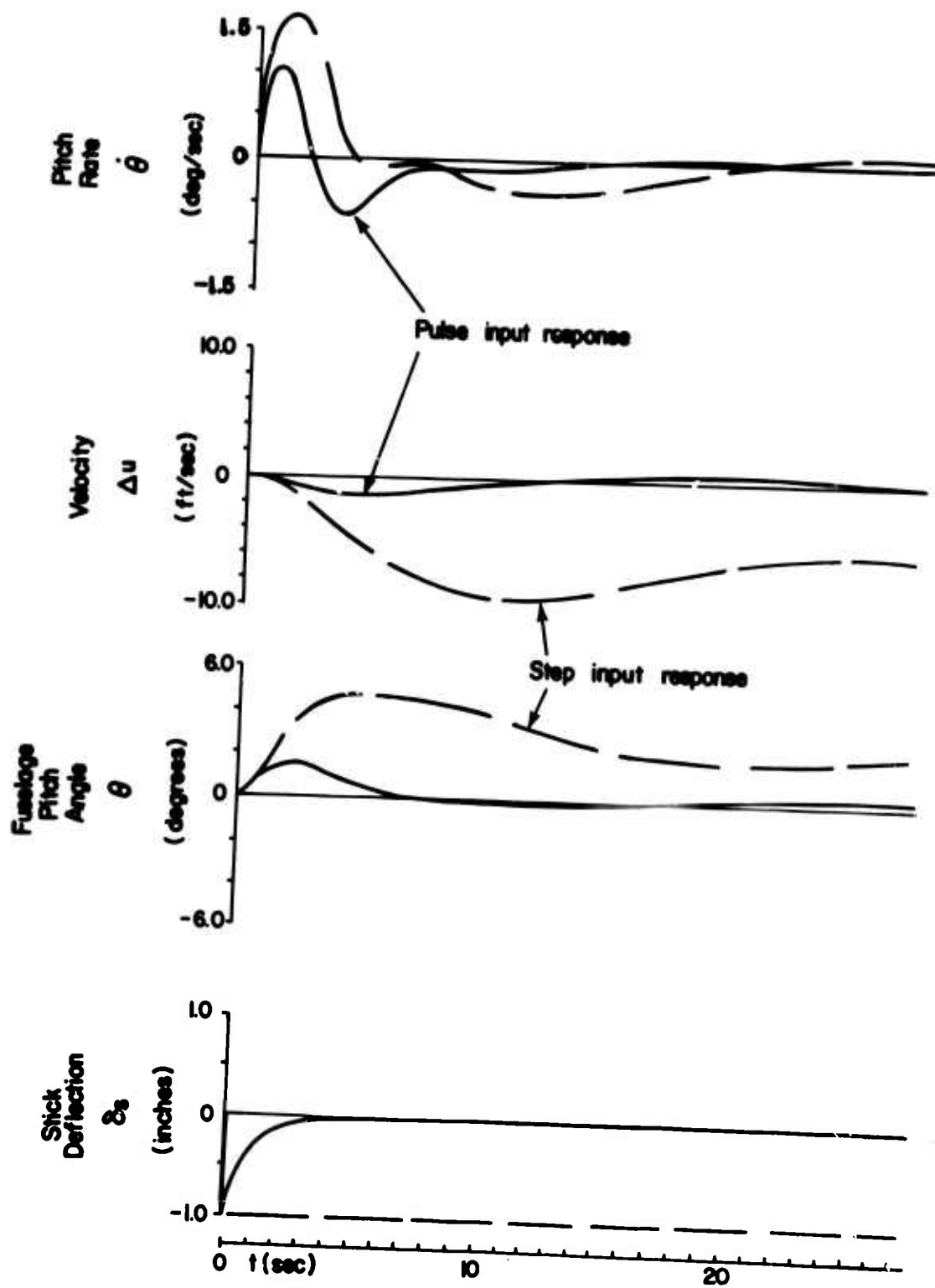


FIGURE 12. RESPONSE TO STEP AND PULSE INPUTS

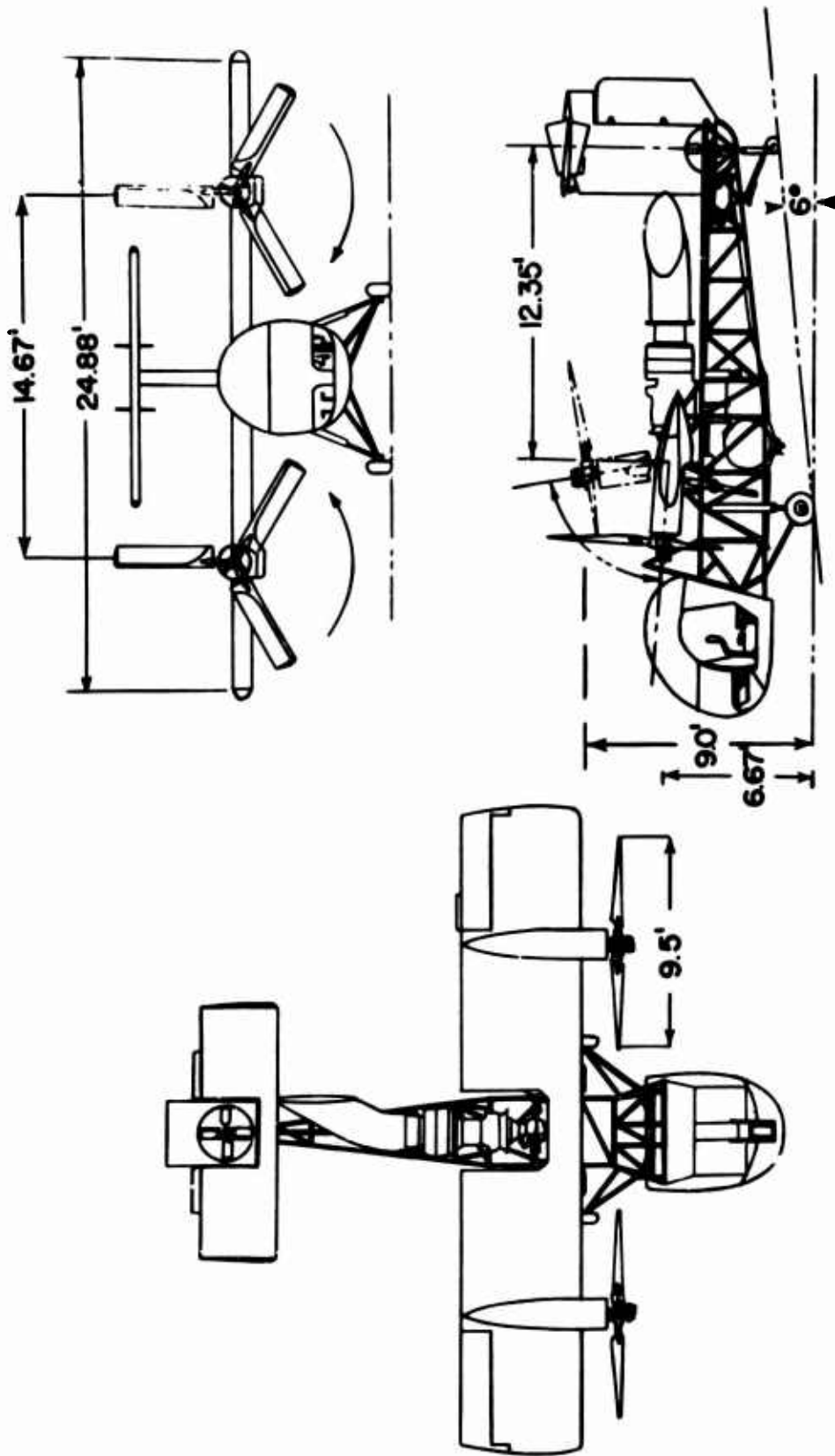


FIGURE 13. SKETCH OF VZ-2 RESEARCH AIRCRAFT

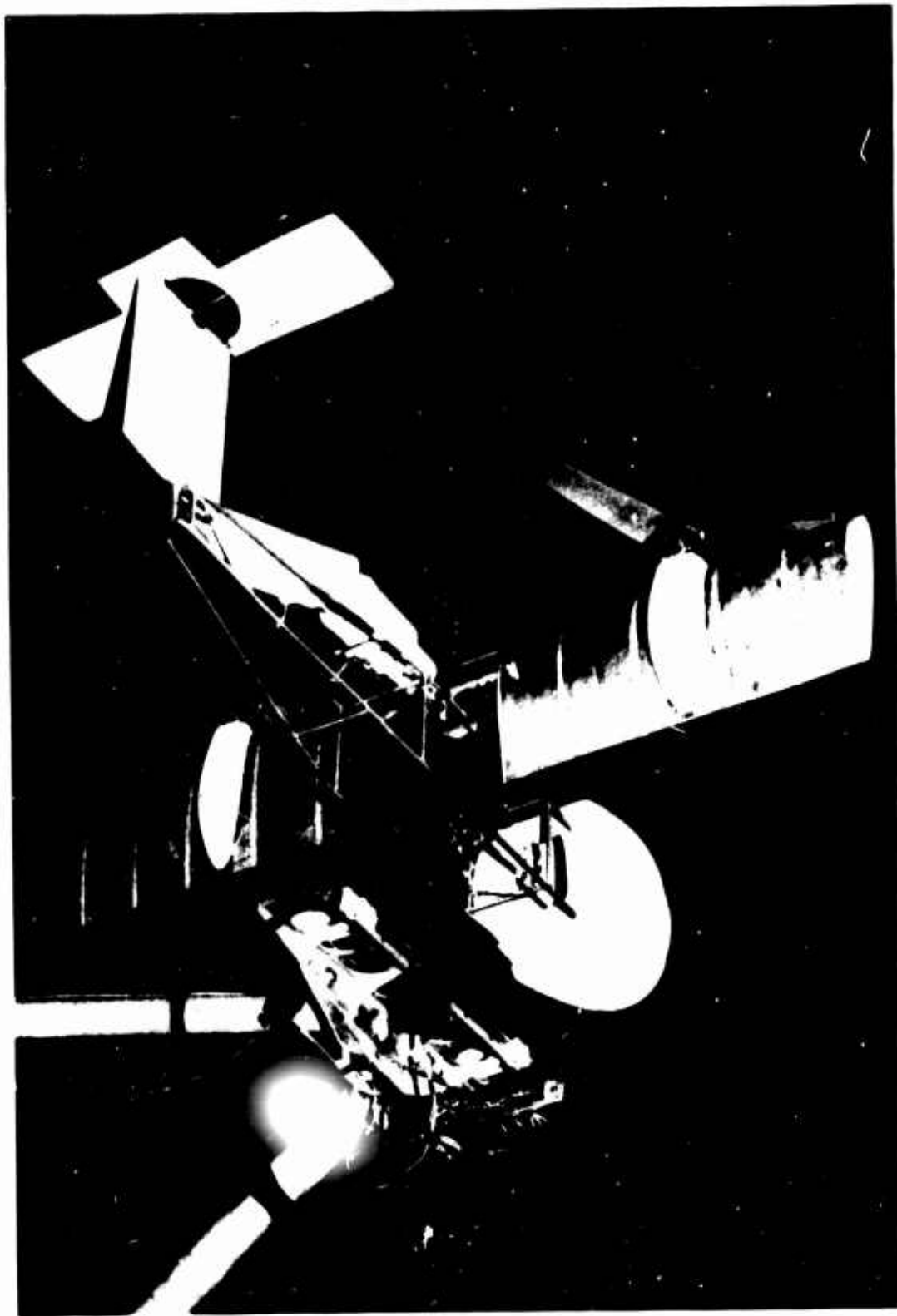


FIGURE 14. PHOTOGRAPH OF 2-PROPELLER VZ-2 MODEL

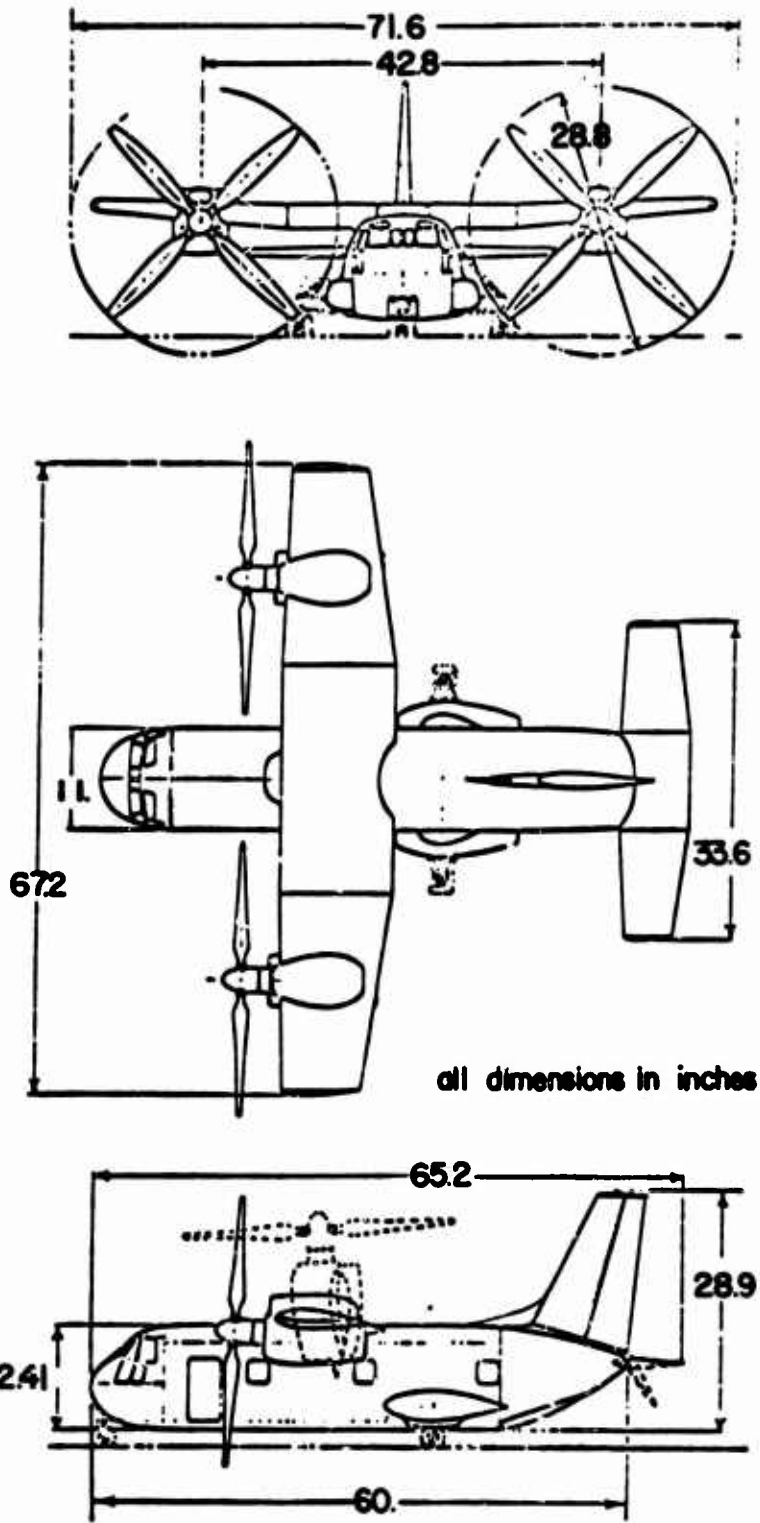


FIGURE 15. SKETCH OF 2-PROPELLER TRANSPORT MODEL

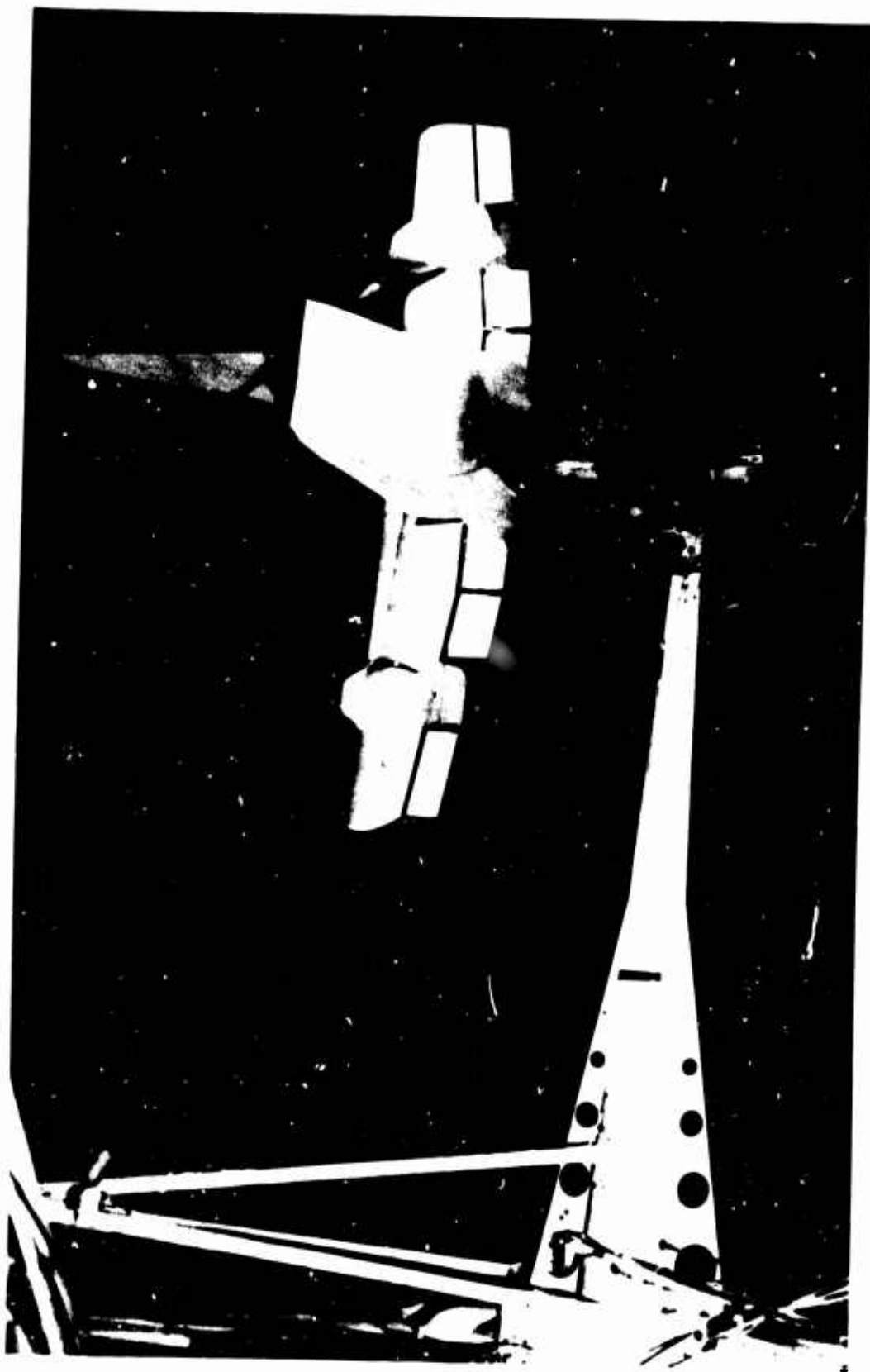


FIGURE 16. PHOTOGRAPH OF 2-PROPELLER TRANSPORT MODEL

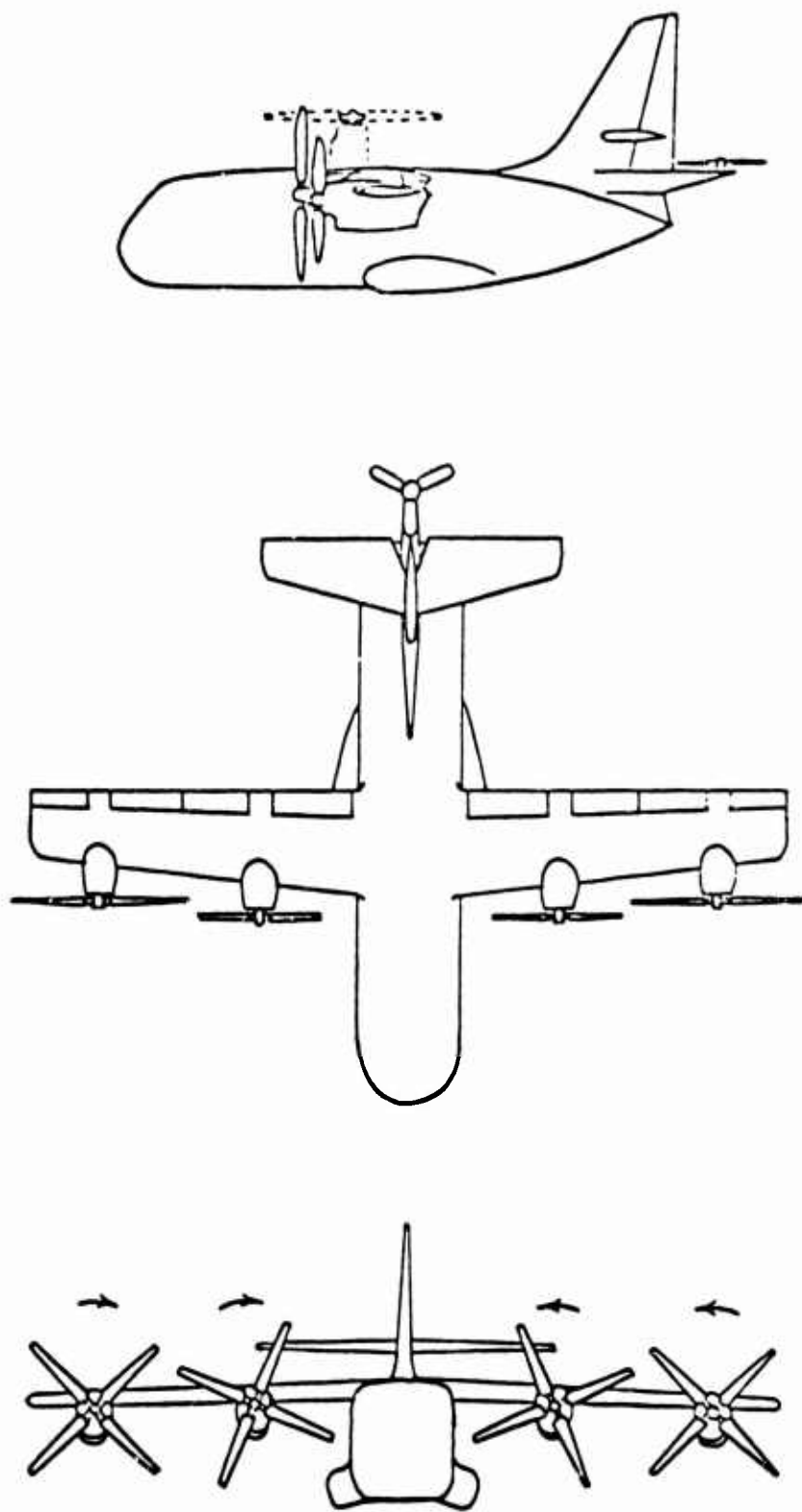


FIGURE 17. SKETCH OF 4-PROPELLER VTOL TRANSPORT



FIGURE 18. PHOTOGRAPH OF 4-PROPELLER VTOL TRANSPORT MODEL, SHOWING PRINCETON TRACK FACILITY

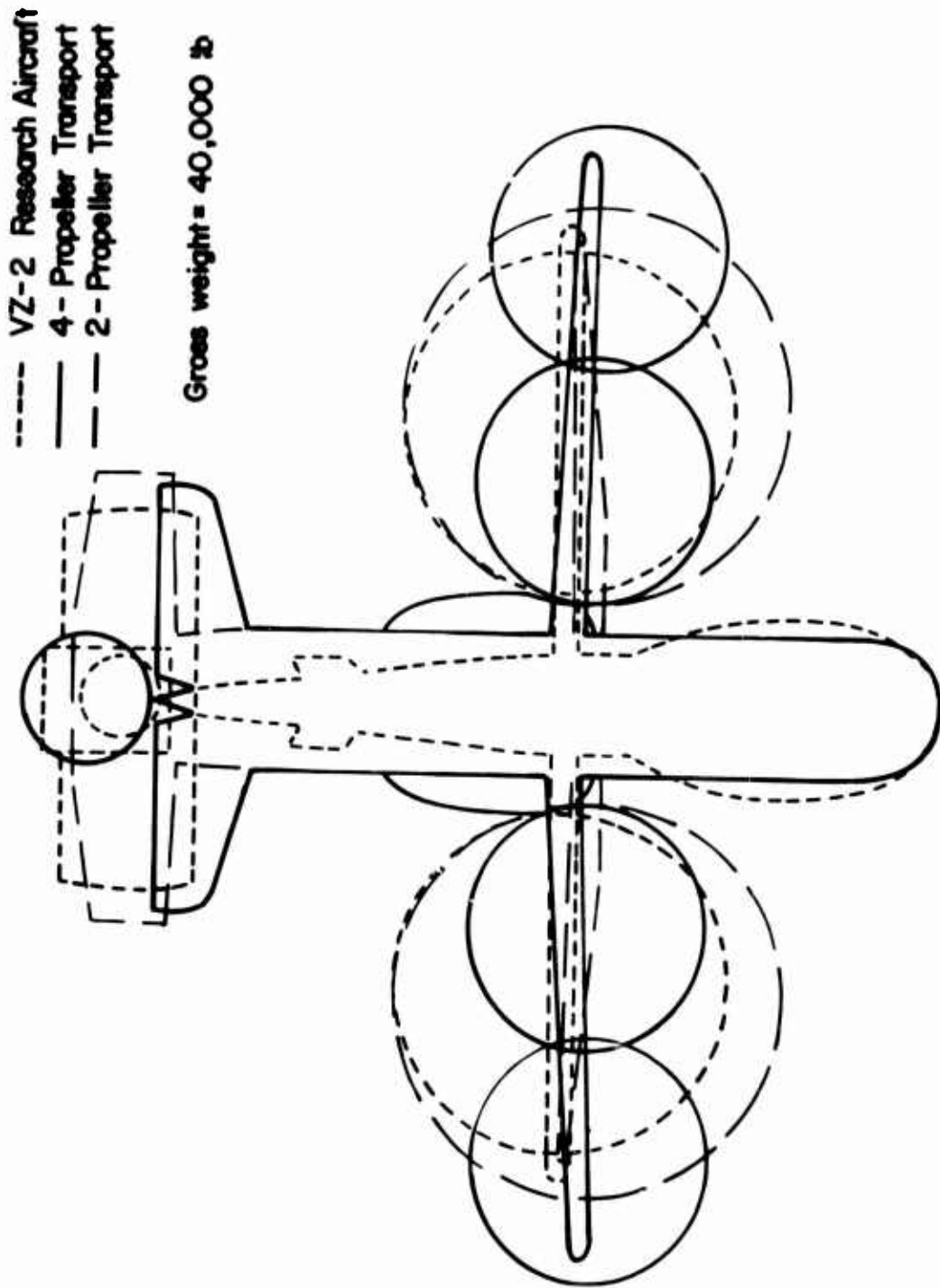


FIGURE 19. SUPERIMPOSED PLAN VIEWS OF EACH VTOL MODEL

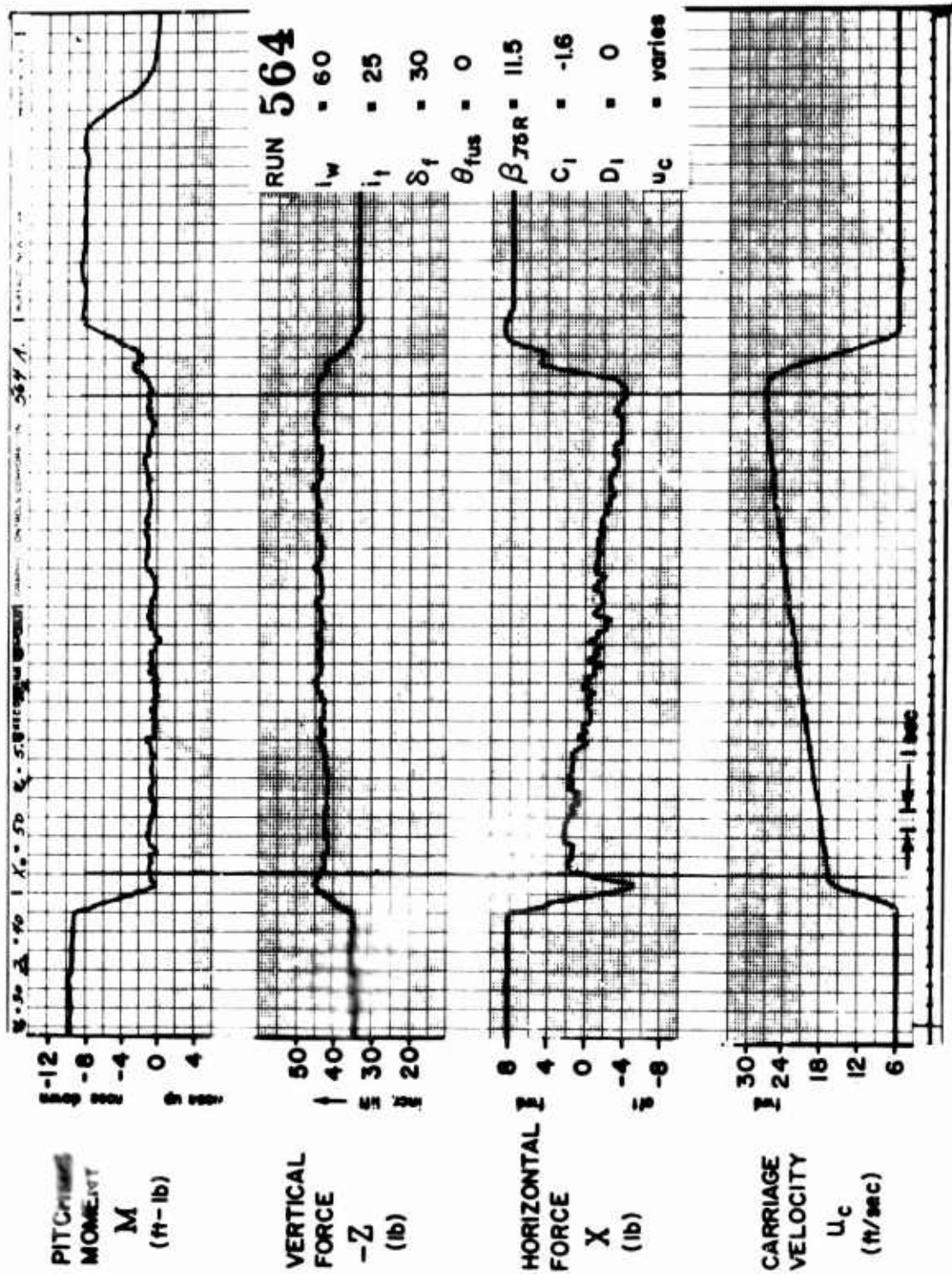


FIGURE 20. TYPICAL TEST DATA FROM PRINCETON TRACK FACILITY

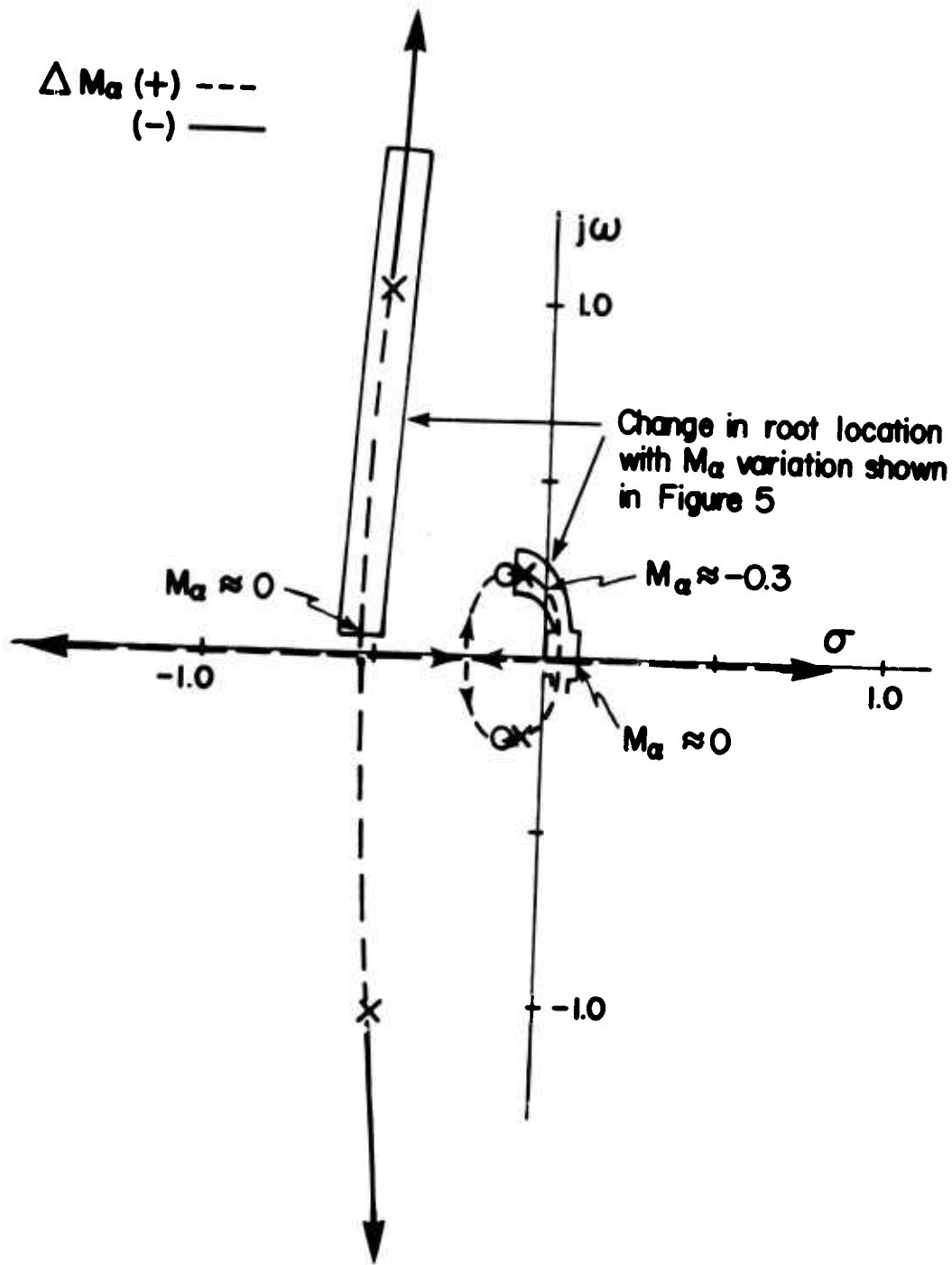


FIGURE 21. ROOT LOCUS SKETCH, VARYING M_a FOR $i_w \approx 40^\circ$

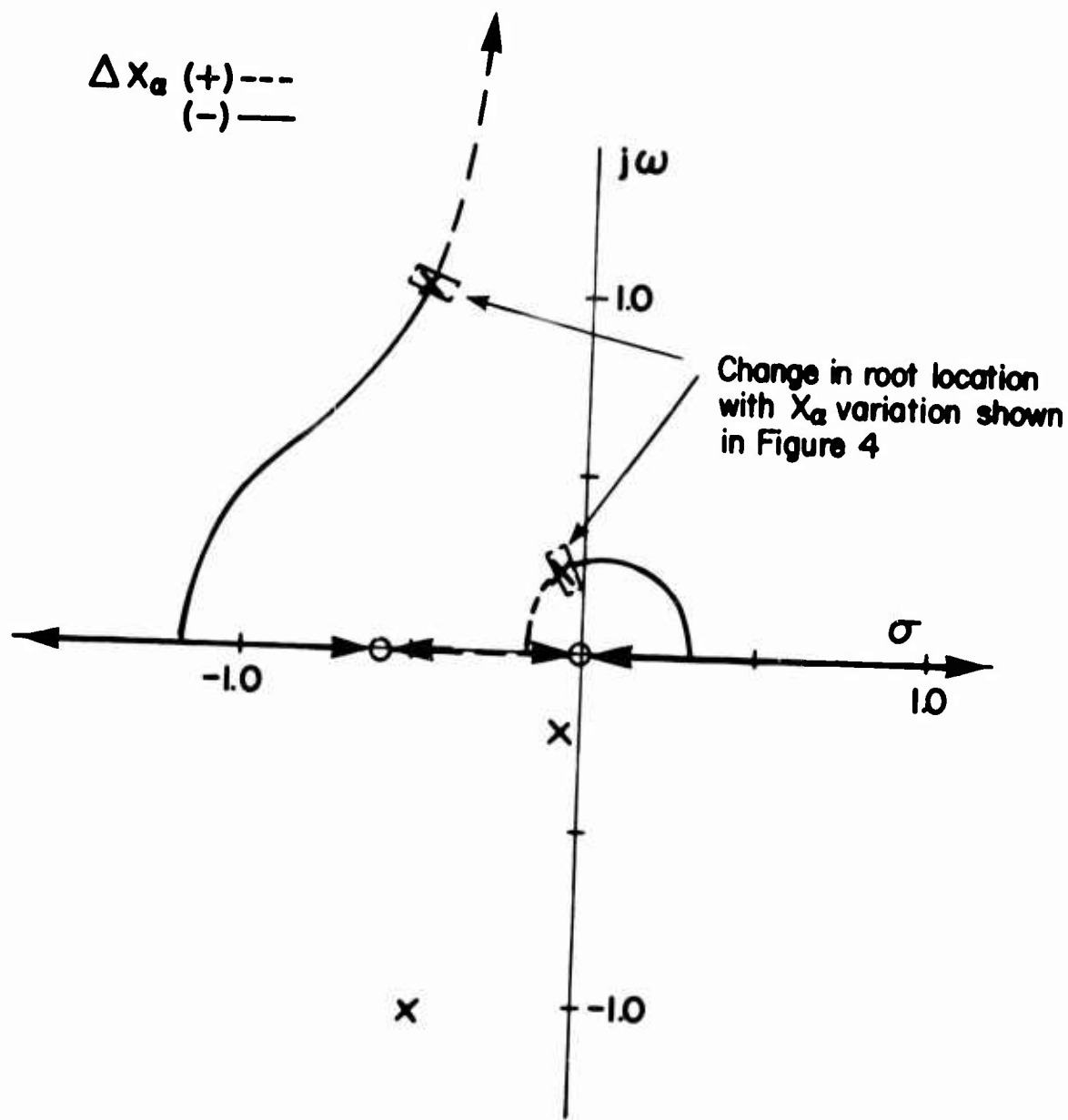


FIGURE 22. ROOT LOCUS SKETCH, VARYING X_a
 FOR $i_w \approx 40^\circ$

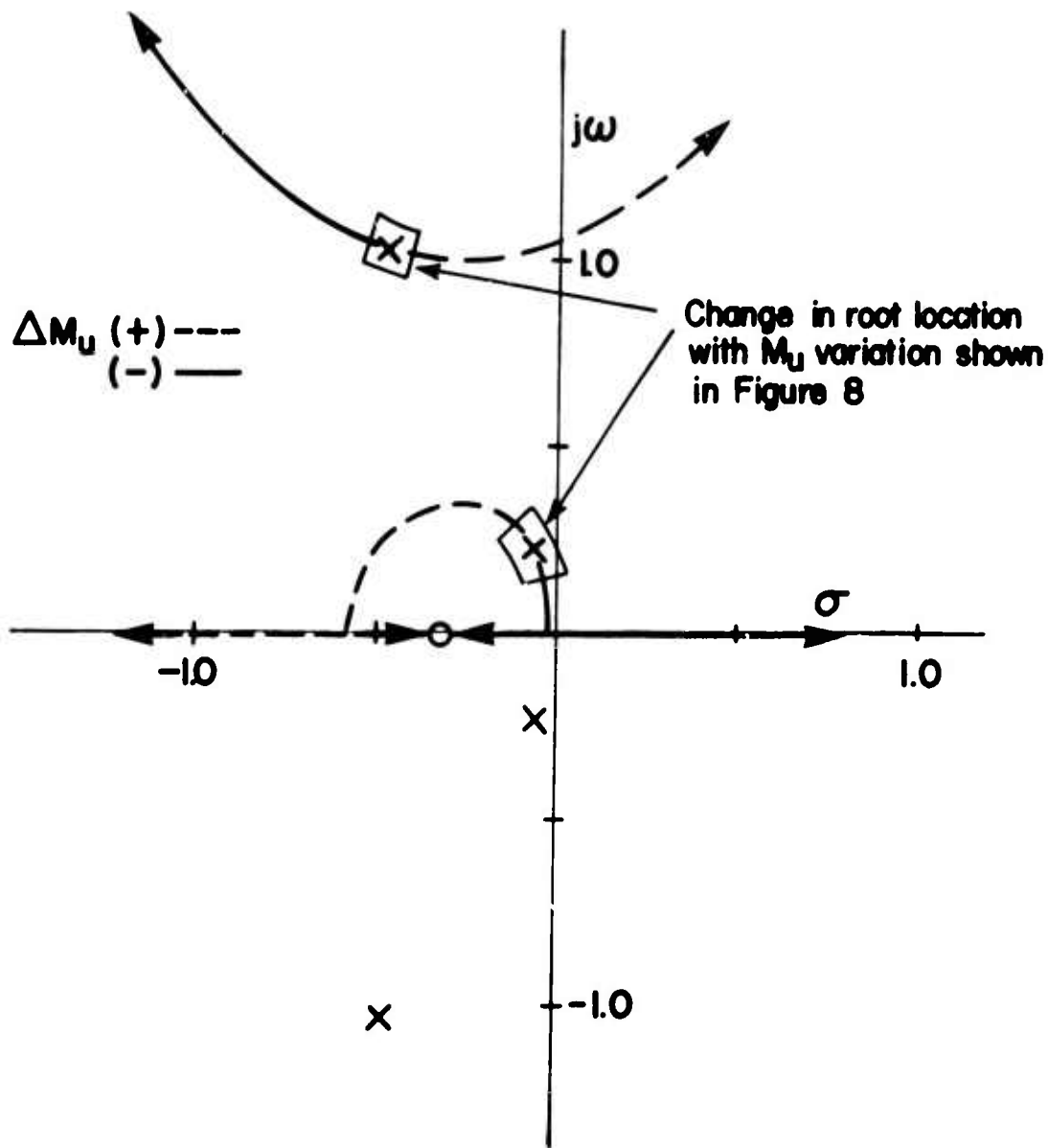


FIGURE 23. ROOT LOCUS SKETCH, VARYING M_u
 FOR $i_w \approx 40^\circ$

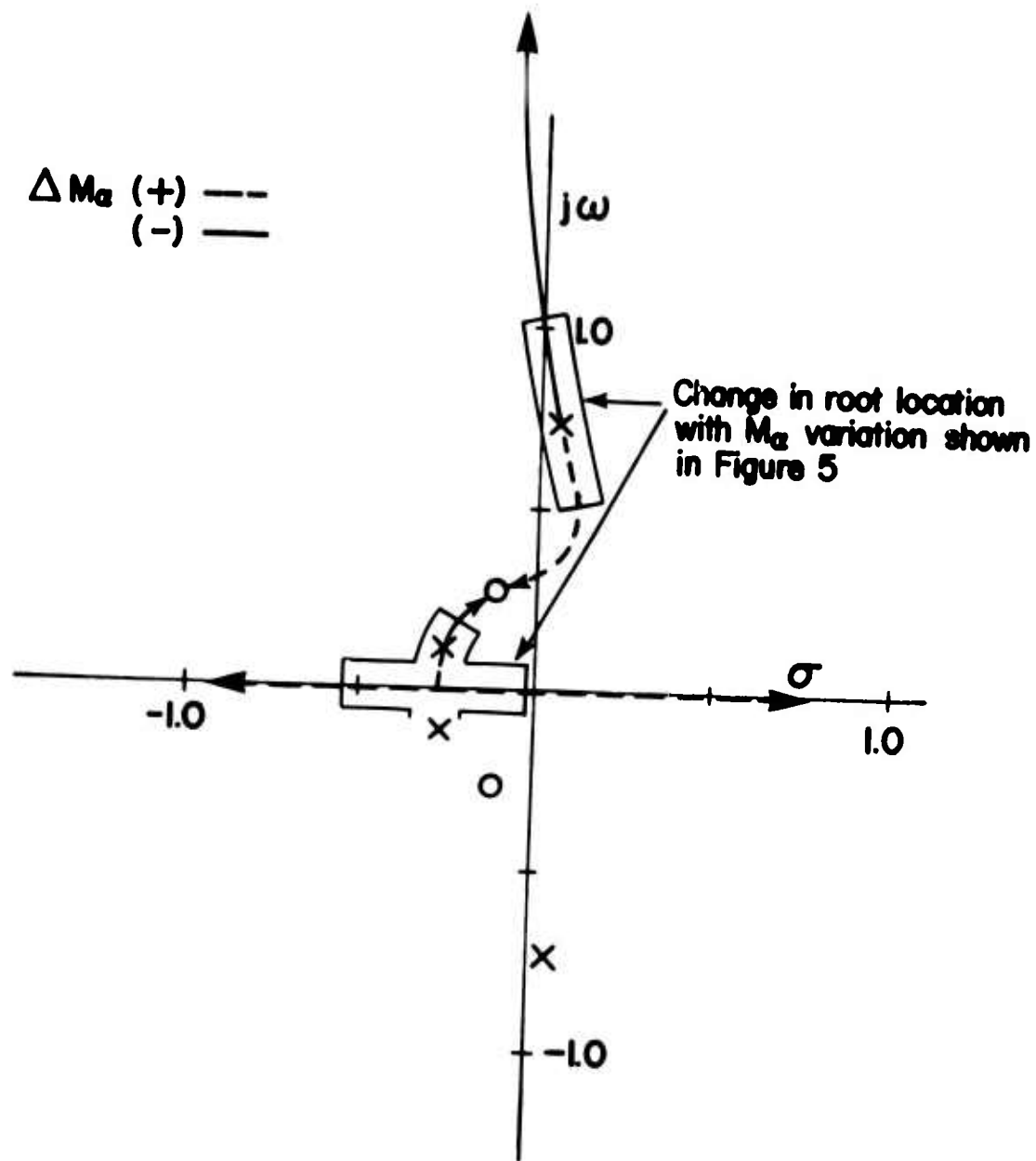


FIGURE 24. ROOT LOCUS SKETCH, VARYING M_a FOR $i_w \approx 60^\circ$

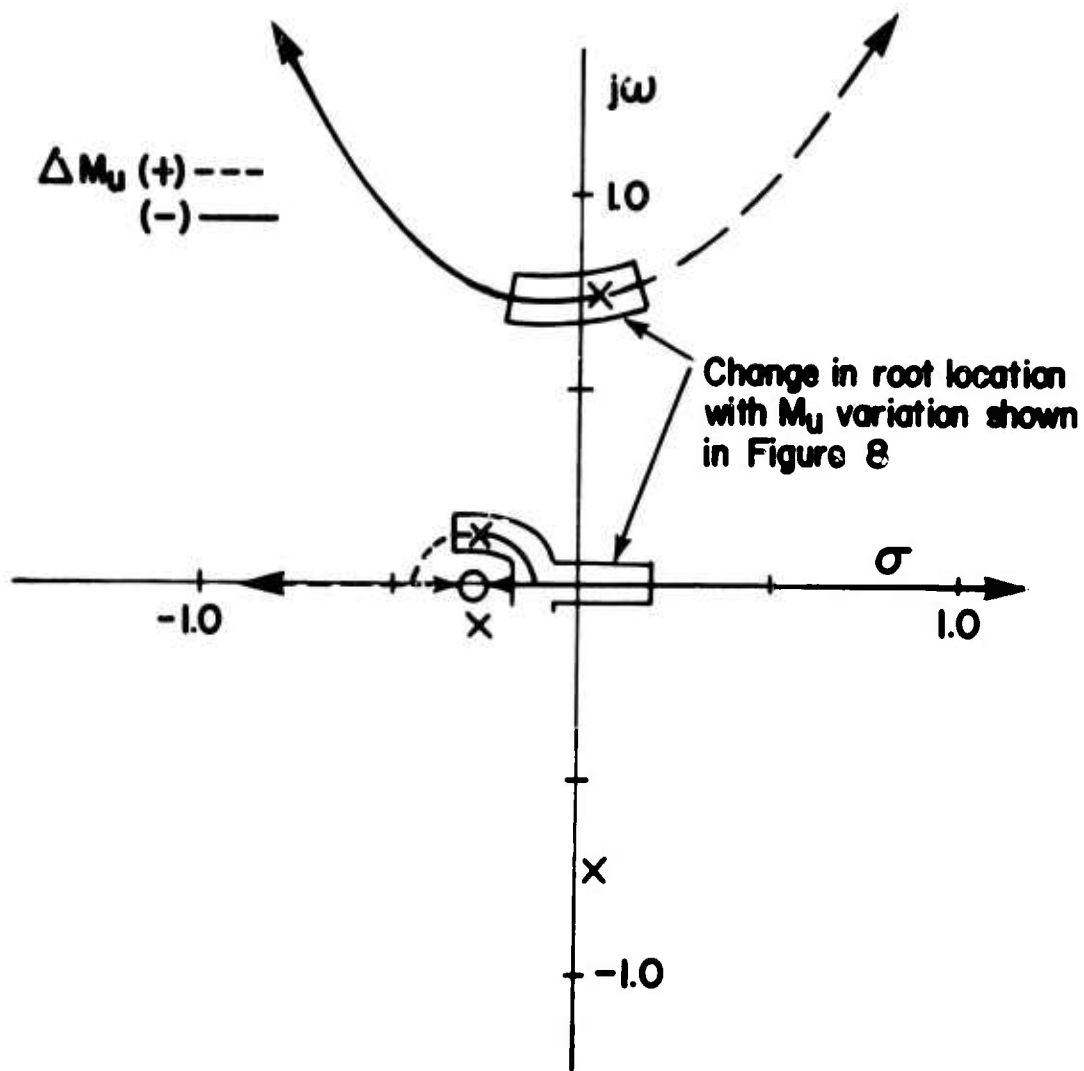


FIGURE 25. ROOT LOCUS SKETCH, VARYING M_u
FOR $i_w \approx 60^\circ$

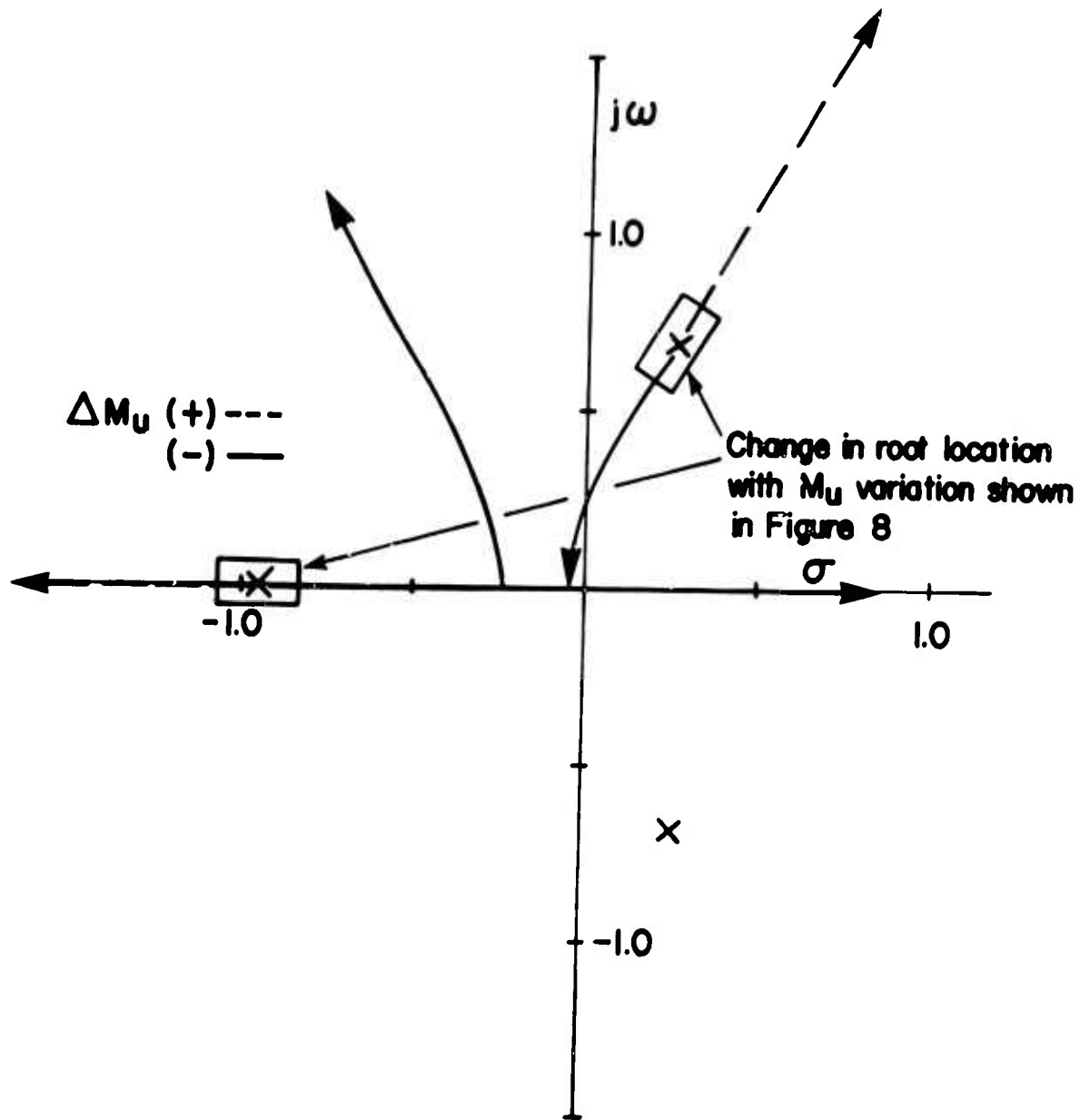


FIGURE 26. ROOT LOCUS SKETCH, VARYING M_U FOR $i_w \approx 90^\circ$

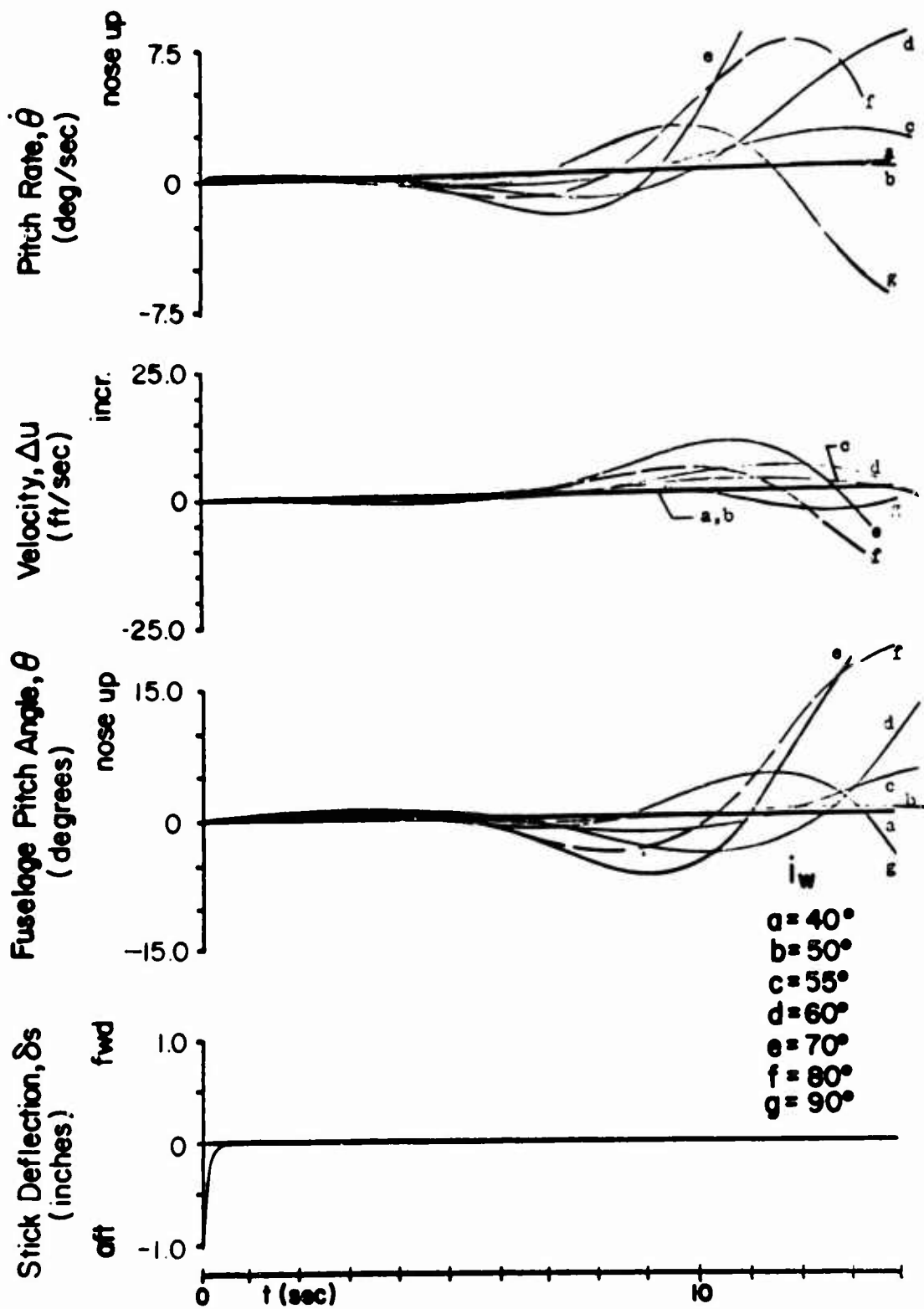


FIGURE 28. SUPERPOSED ANALOG COMPUTER RESPONSES TO A PULSE CONTROL INPUT; $i_w = 90^\circ$ TO 40°

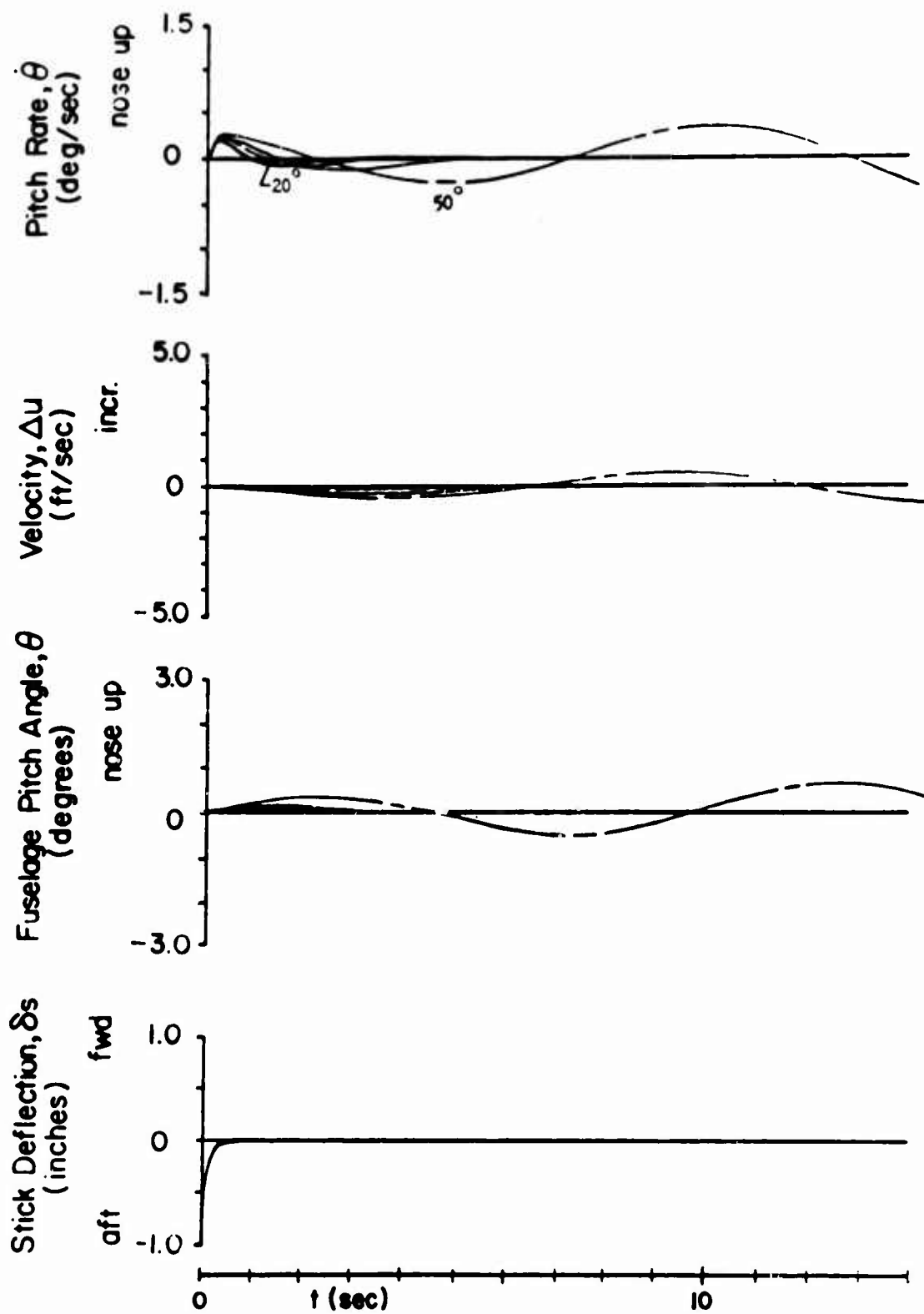


FIGURE 29. SUPERPOSED ANALOG COMPUTER RESPONSES TO A PULSE CONTROL INPUT; $i_w = 50^\circ$ TO 20°

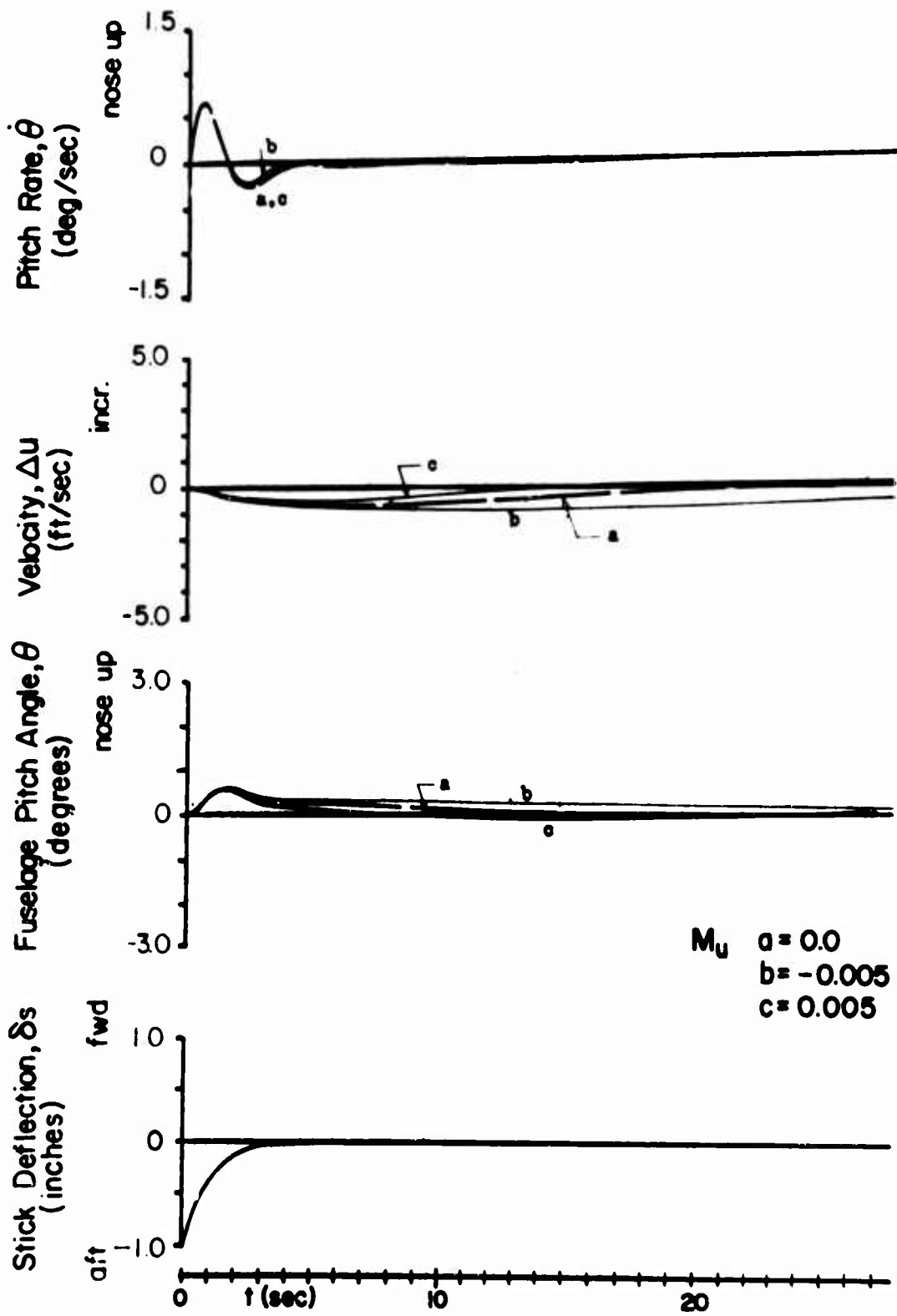


FIGURE 30. SUPERPOSED ANALOG RESPONSES FOR INDIVIDUALLY VARIED DERIVATIVES; $i_w = 20^\circ$, $V_o = 160$ FT/SEC (A) VARYING M_u

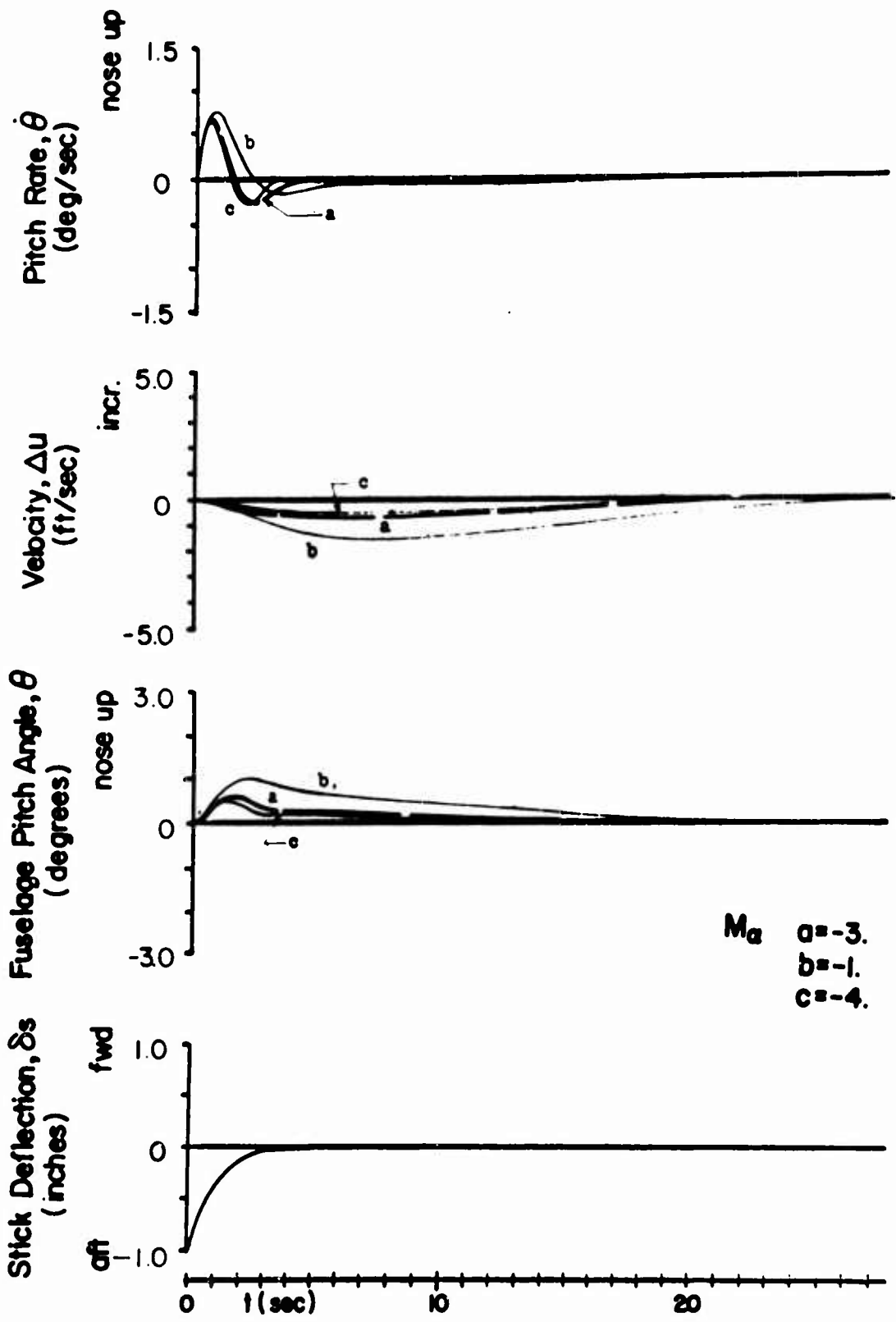


FIGURE 30 (B). VARYING M_a

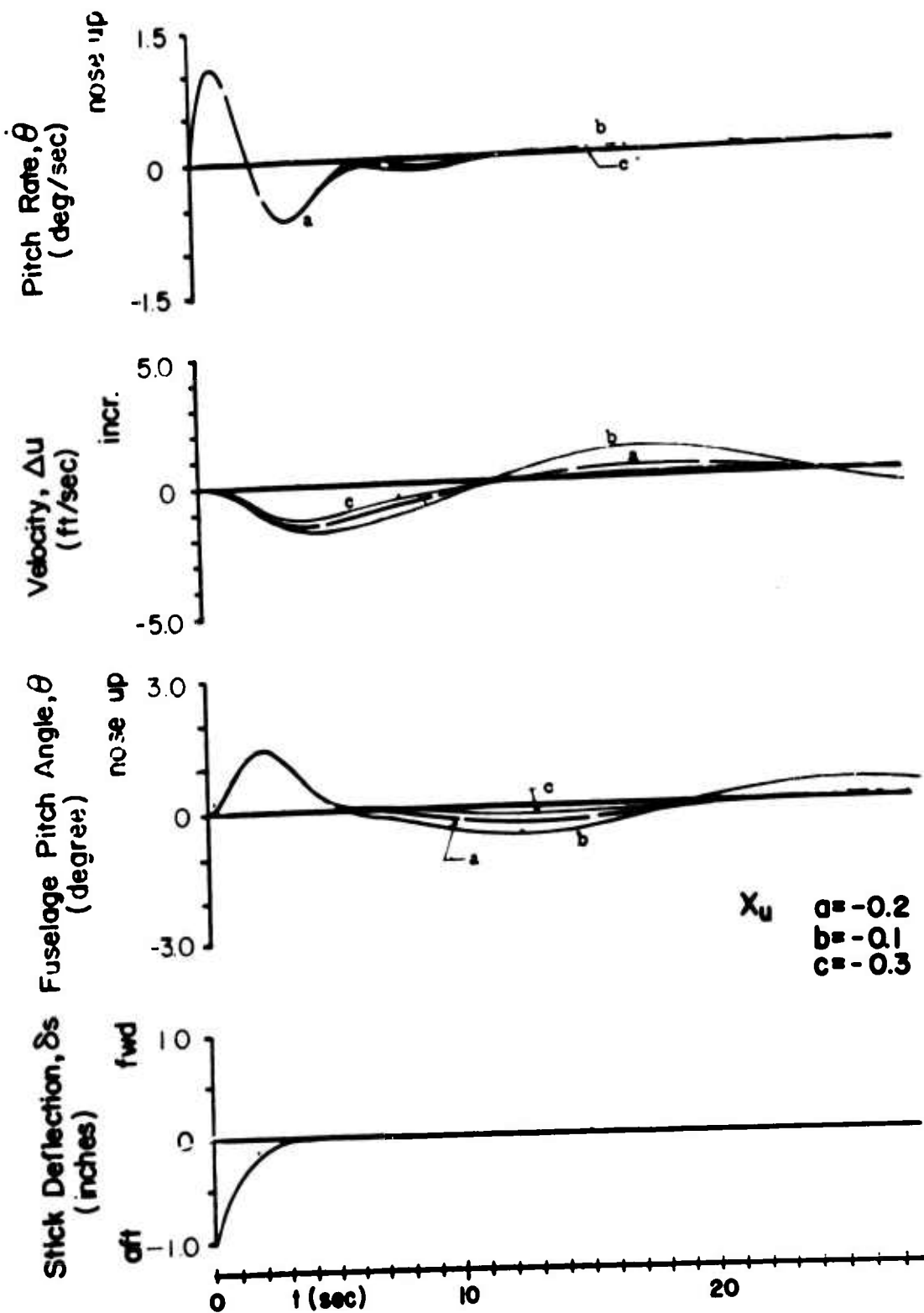


FIGURE 31. SUPERPOSED ANALOG RESPONSES FOR INDIVIDUALLY VARIED DERIVATIVES; $i_w = 40^\circ$, $V_0 = 100$ FT/SEC (A) VARYING X_u

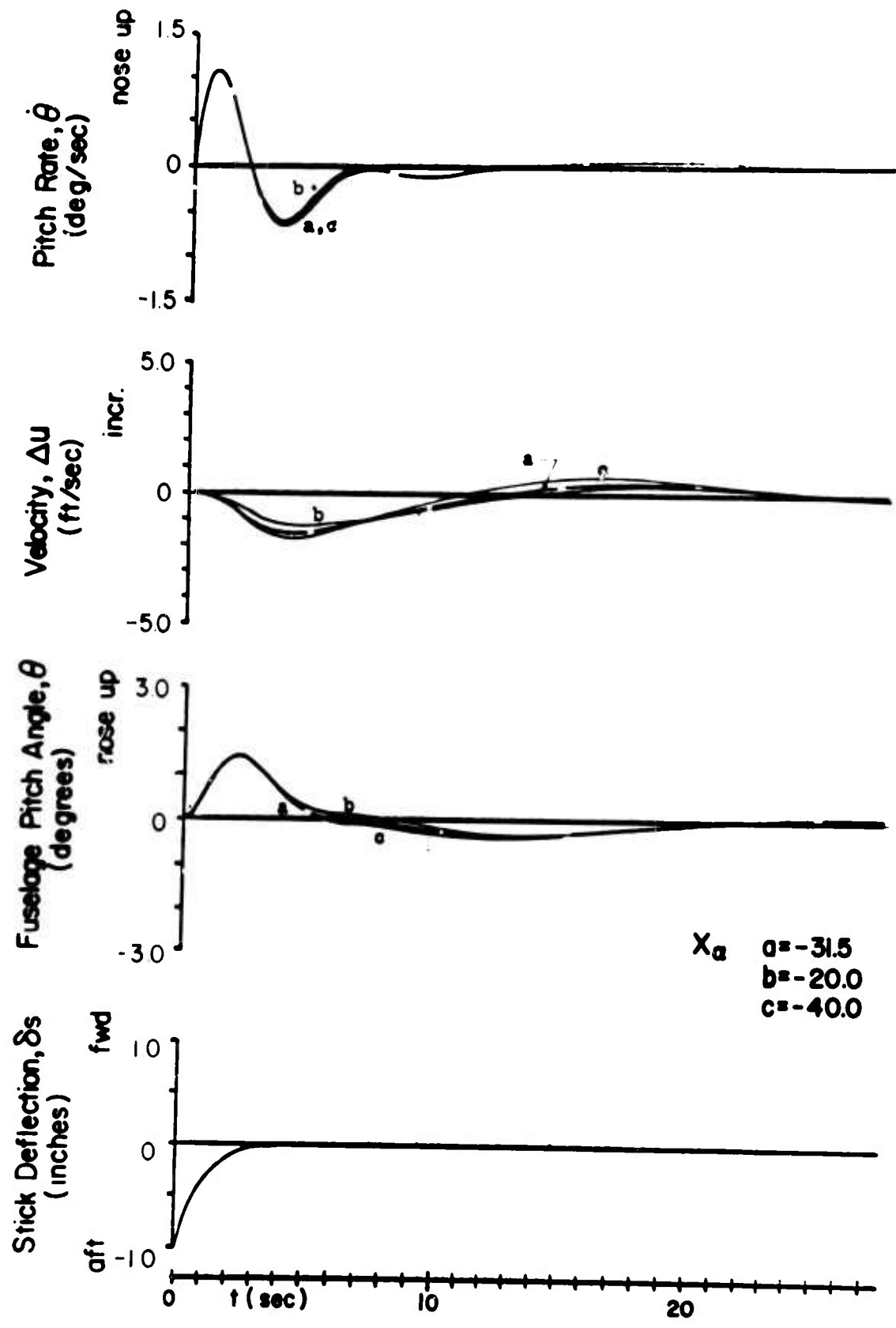


FIGURE 31 (B). VARYING X_α

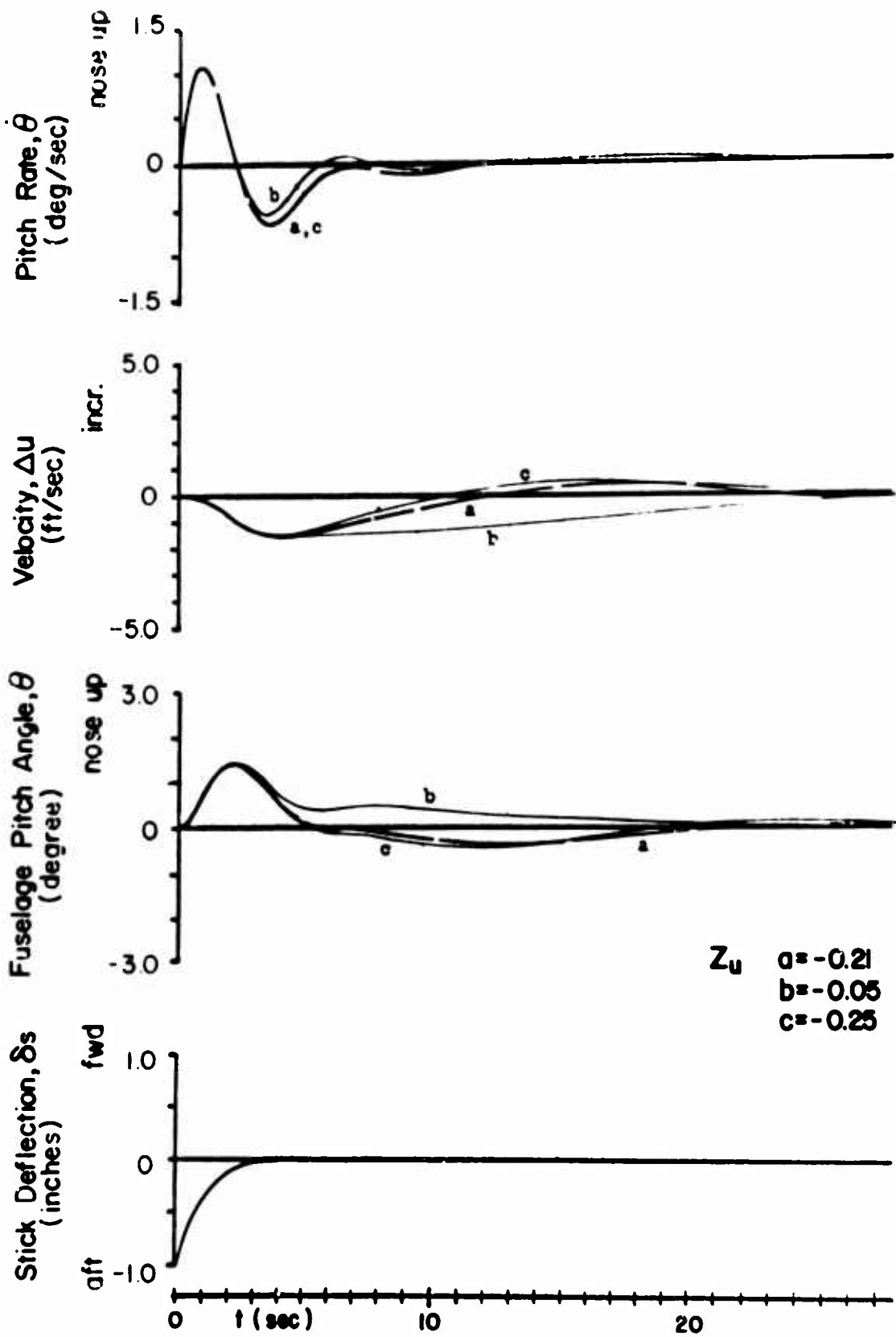


FIGURE 31 (C). VARYING Z_u

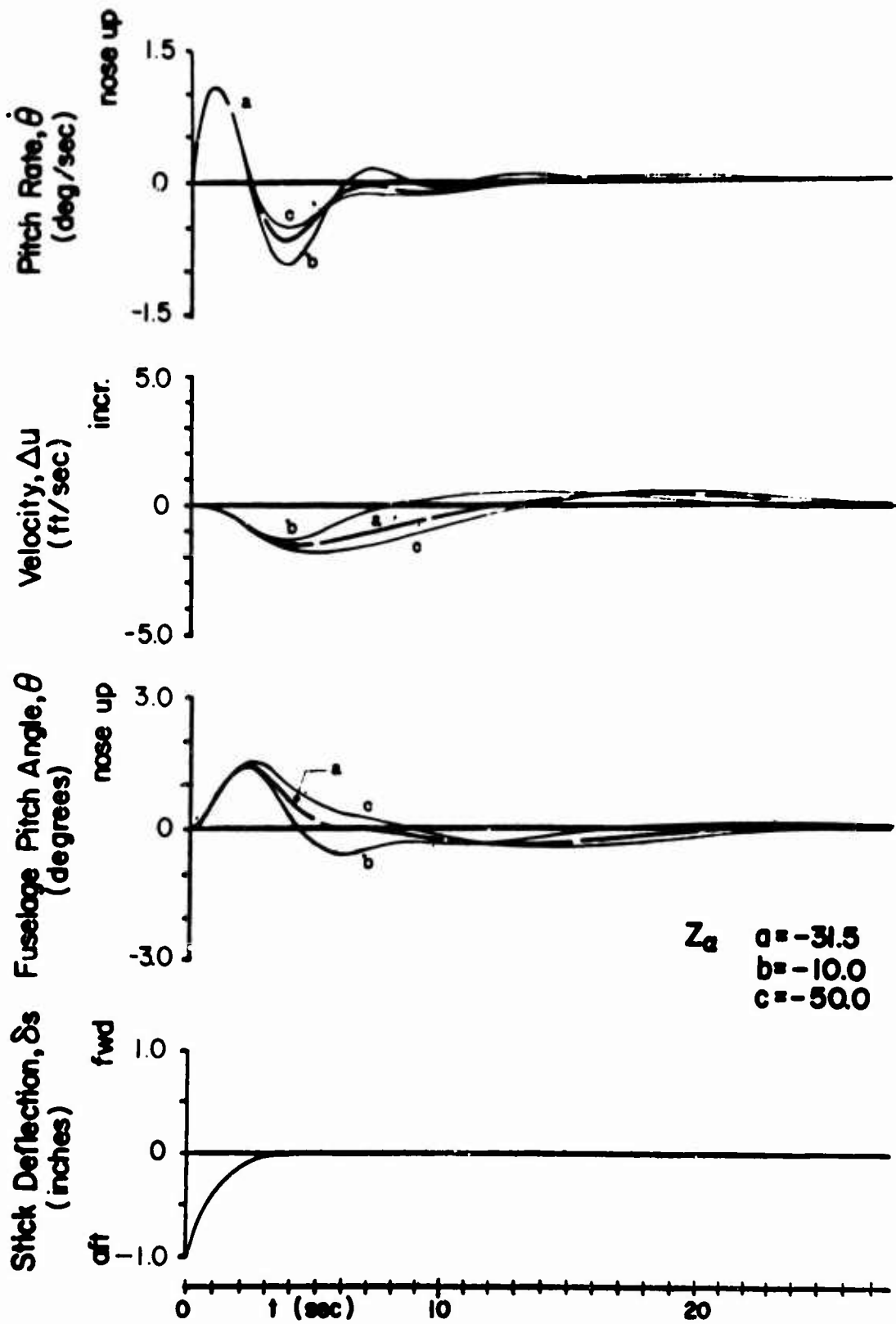


FIGURE 31 (D). VARYING Z_a

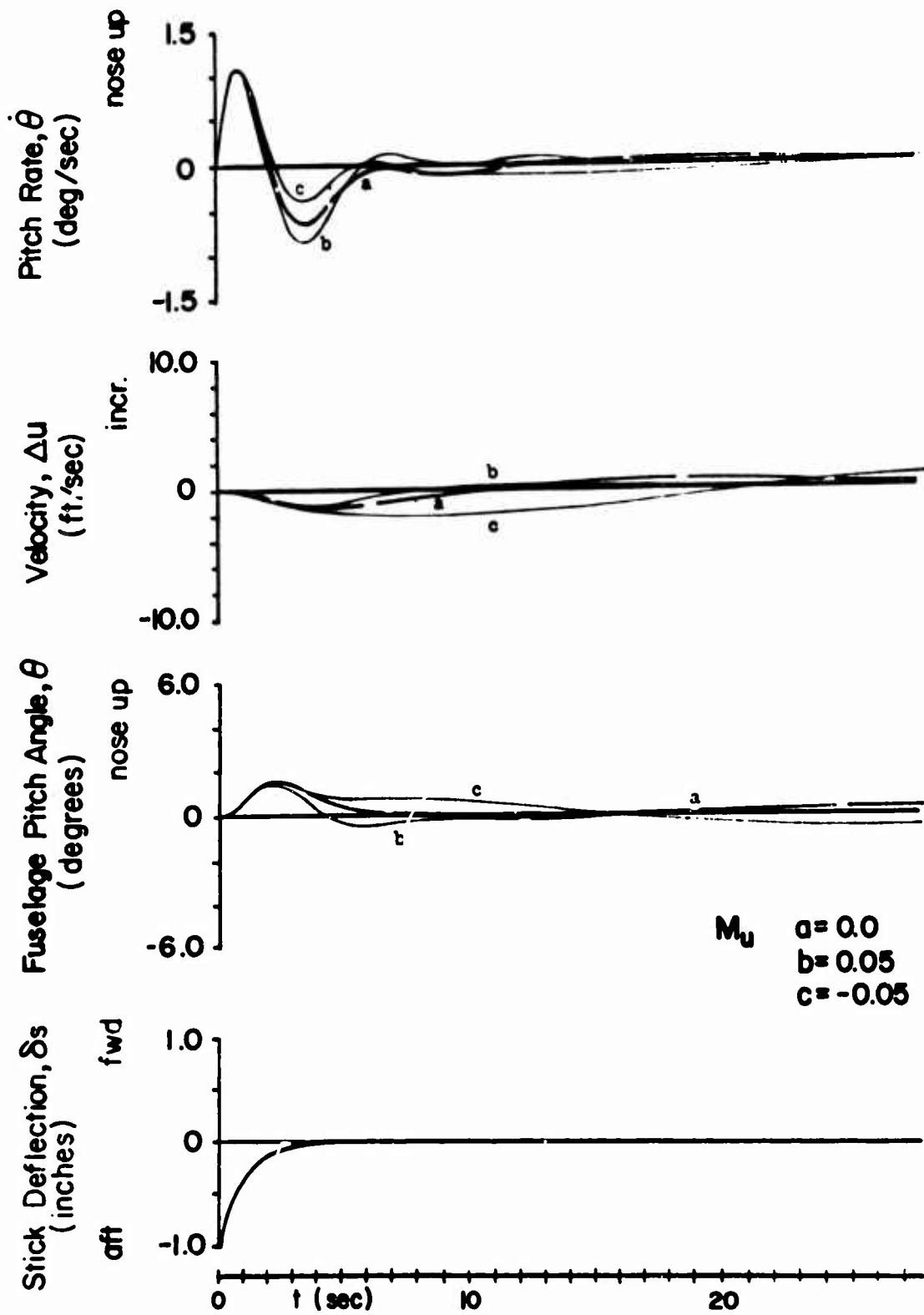


FIGURE 31 (E). VARYING M_u

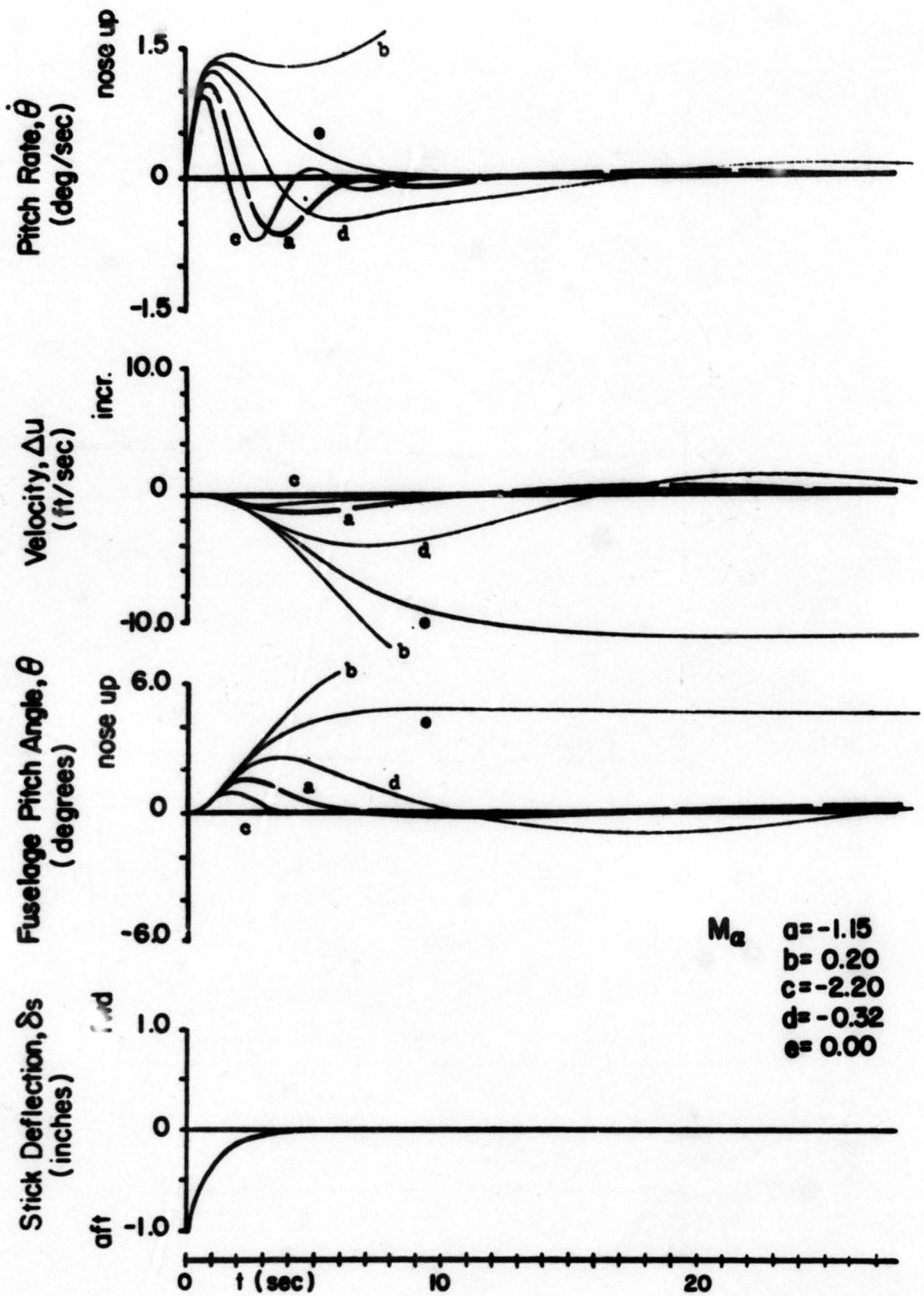


FIGURE 31 (F). VARYING M_a

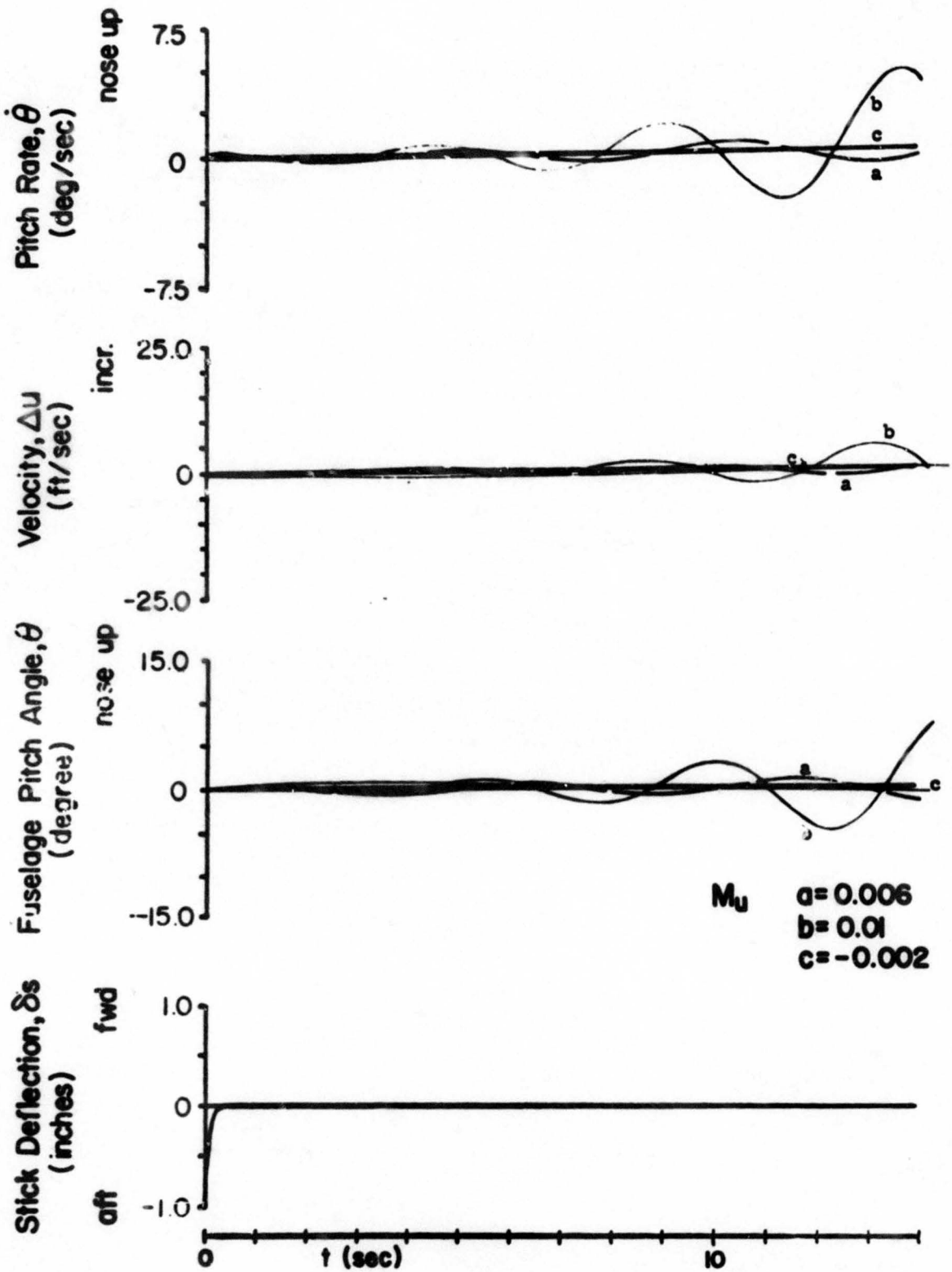


FIGURE 32. SUPERPOSED ANALOG RESPONSES FOR INDIVIDUALLY VARIED DERIVATIVES; $i_w = 50^\circ$, $V_0 = 75$ FT/SEC (A) VARYING M_u

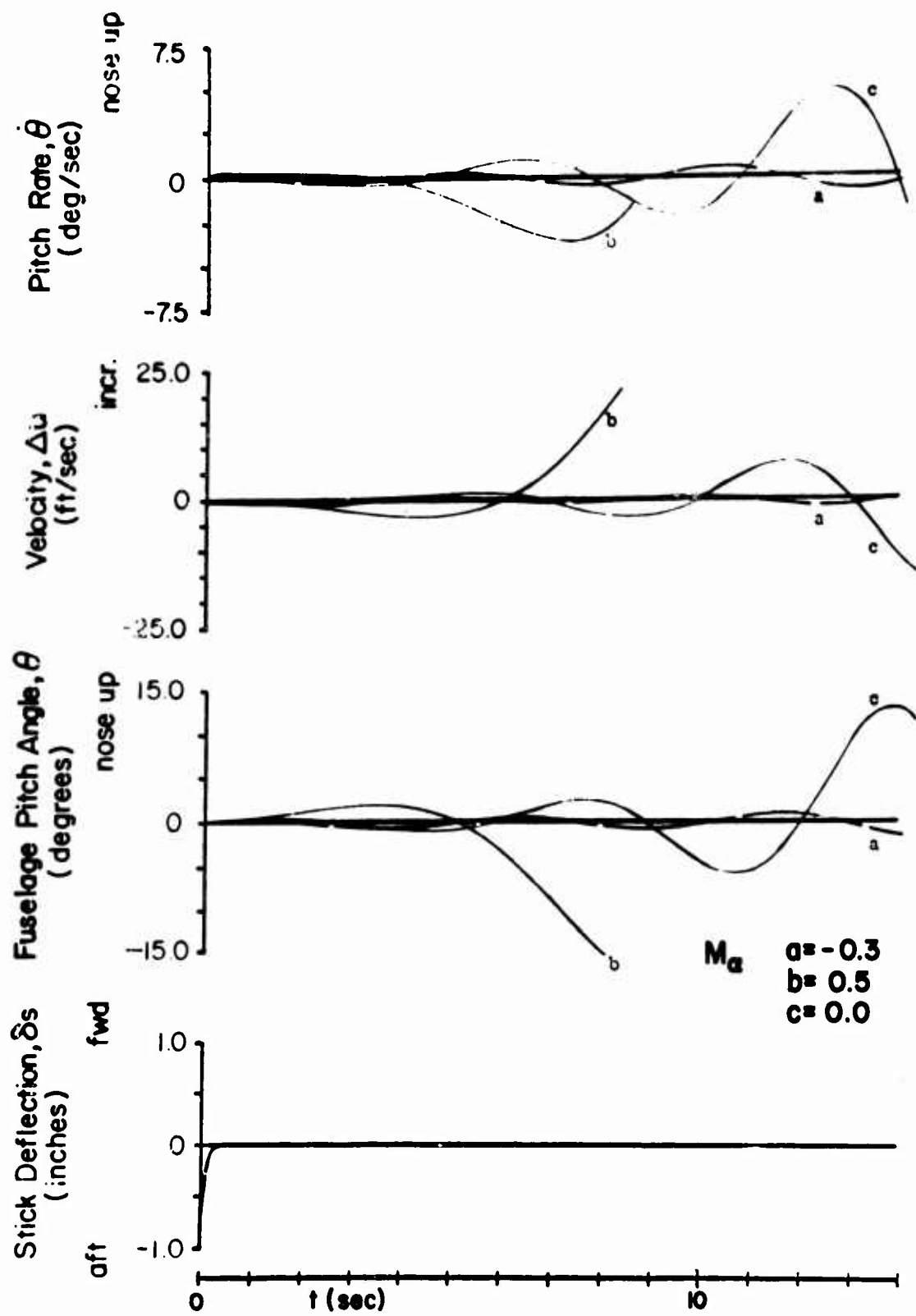


FIGURE 32 (B). VARYING M_a

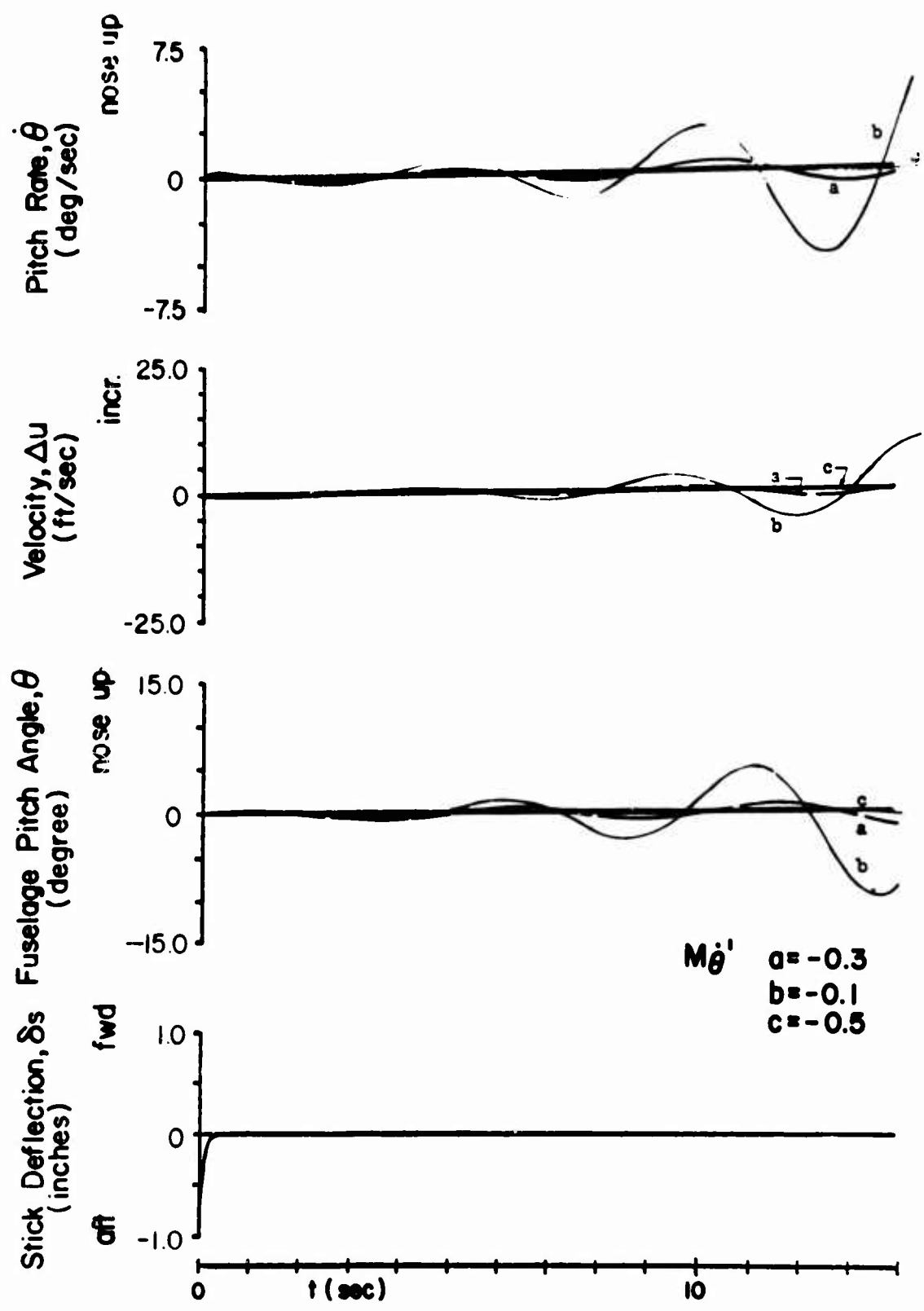


FIGURE 32 (C). VARYING $M\dot{\theta}'$

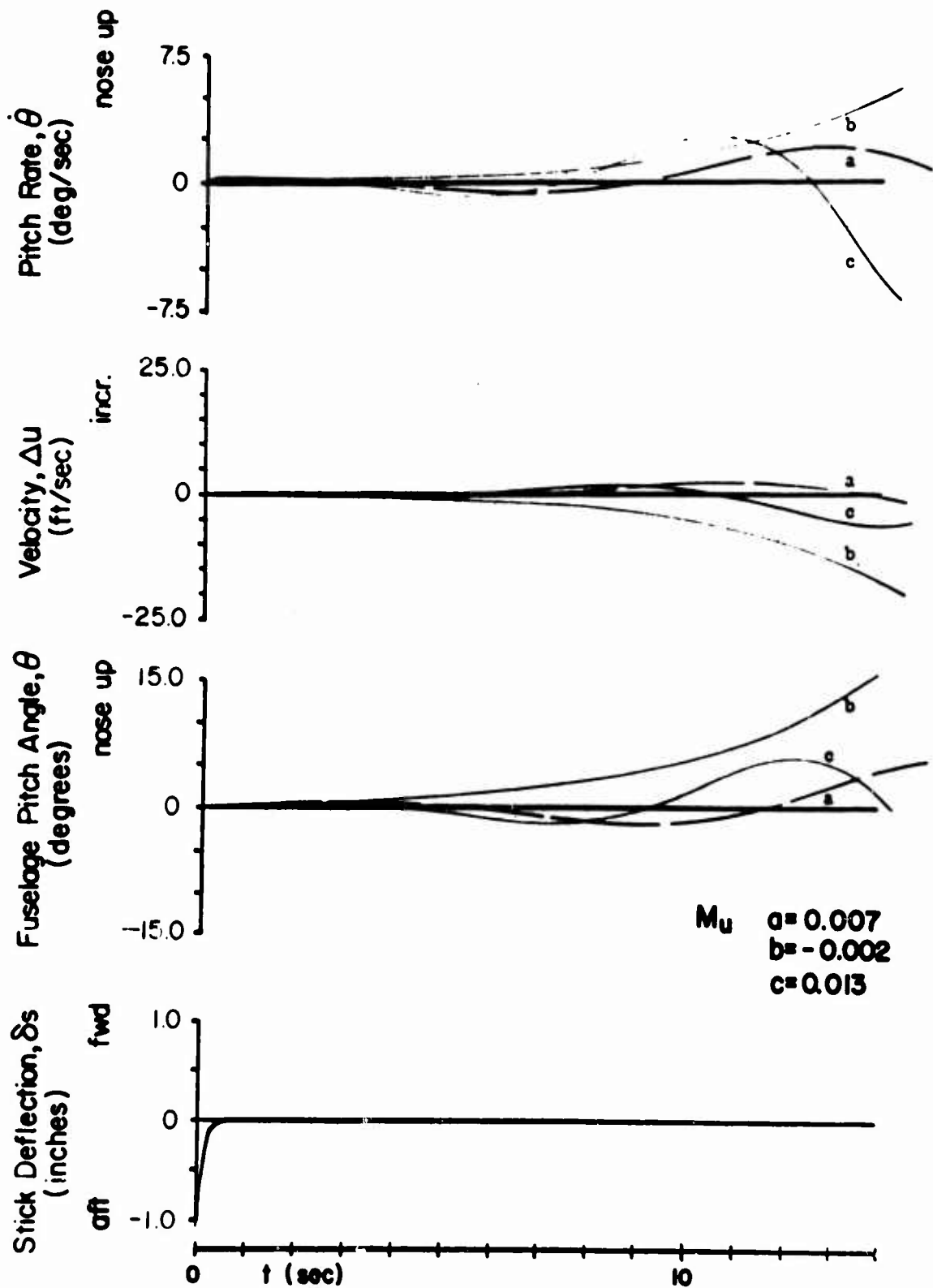


FIGURE 33. SUPERPOSED ANALOG RESPONSES FOR INDIVIDUALLY VARIED DERIVATIVES; $i_w = 55^\circ$, $V_0 = 65$ FT/SEC (A) VARYING M_u

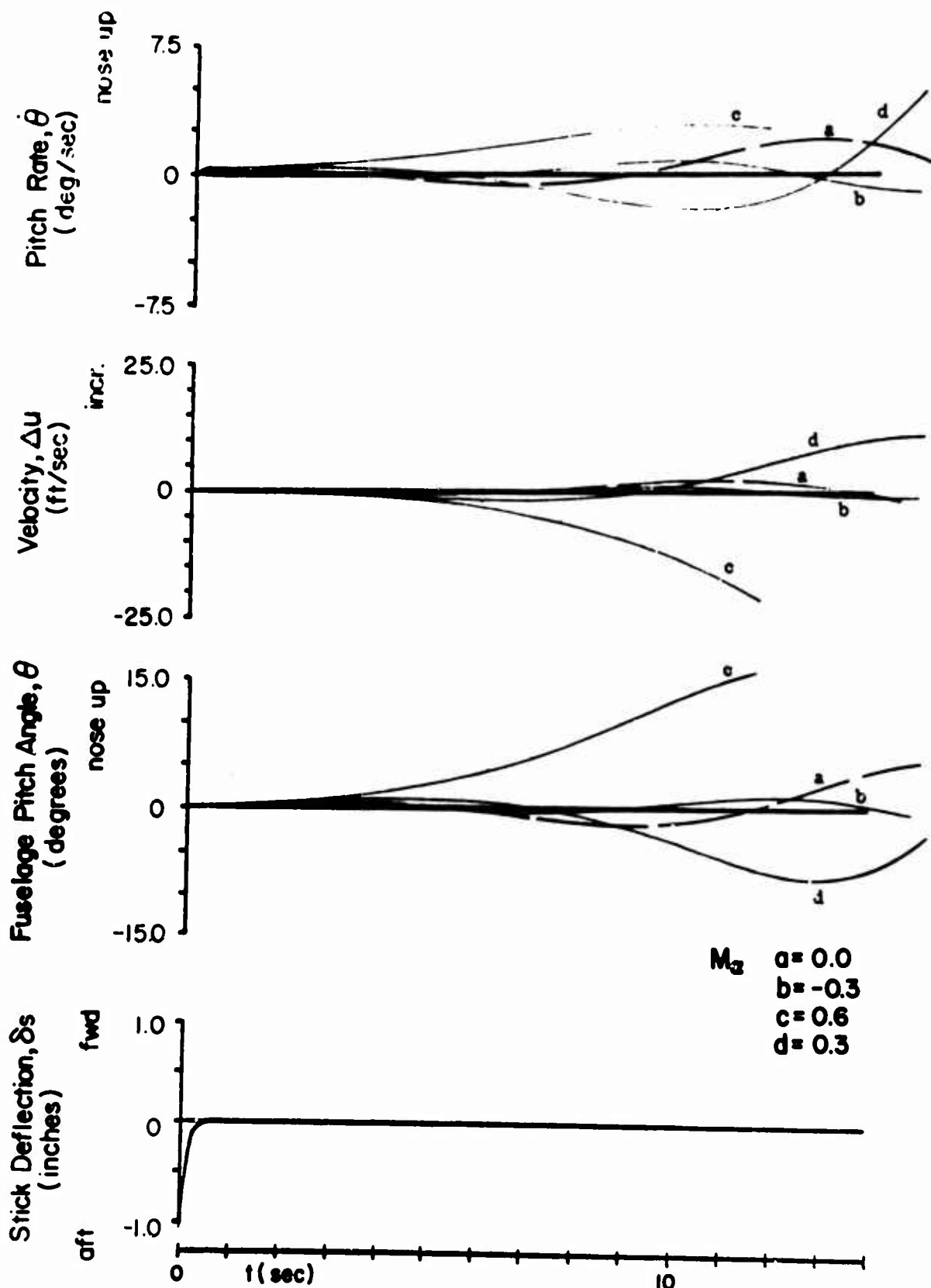


FIGURE 33 (B). VARYING M_a

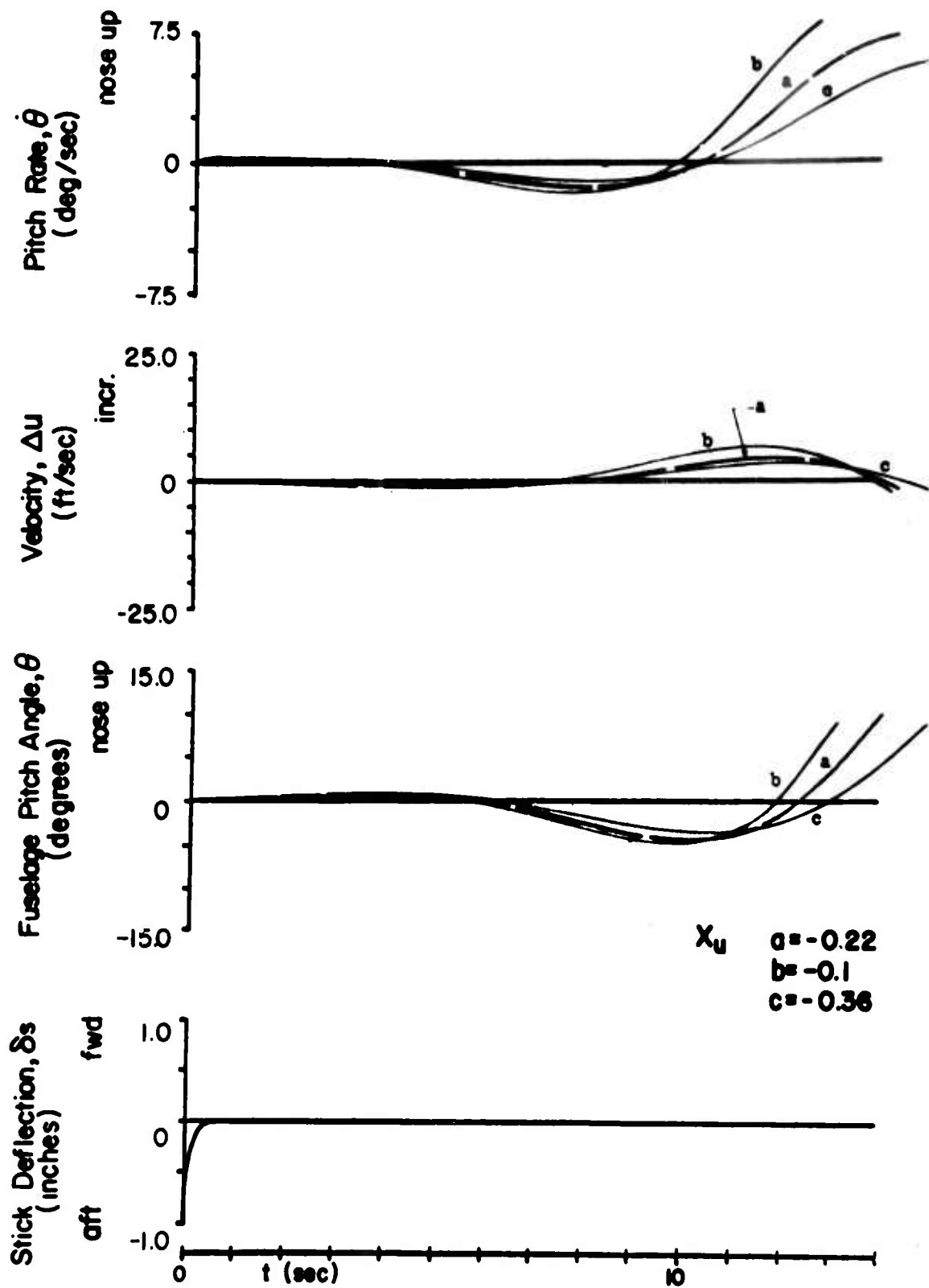


FIGURE 34. SUPERPOSED ANALOG RESPONSES FOR INDIVIDUALLY VARIED DERIVATIVES; $i_w = 60^\circ$, $V_0 = 55$ FT/SEC (A) VARYING X_U

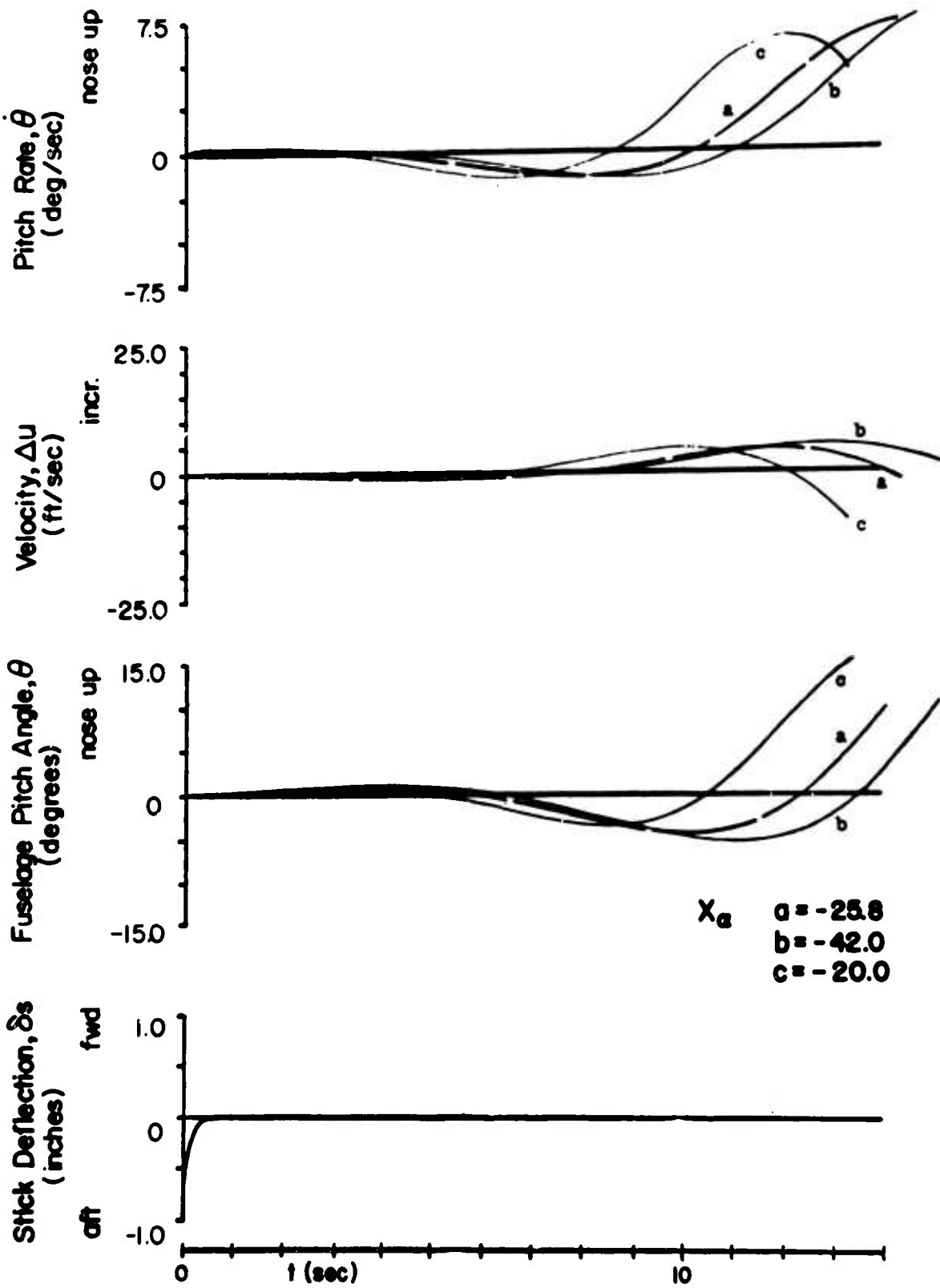


FIGURE 34 (B). VARYING X_α

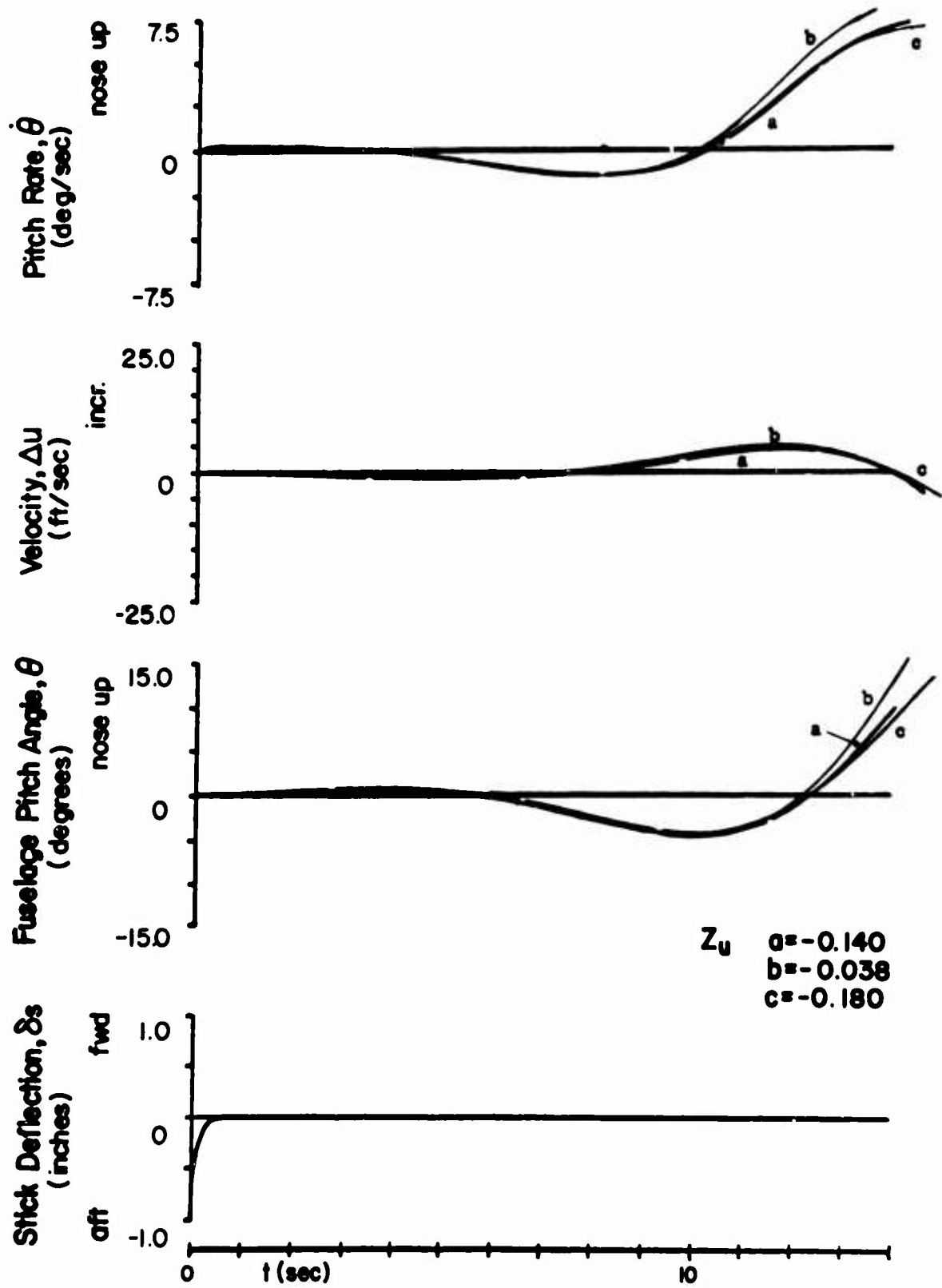


FIGURE 34 (C). VARYING Z_u

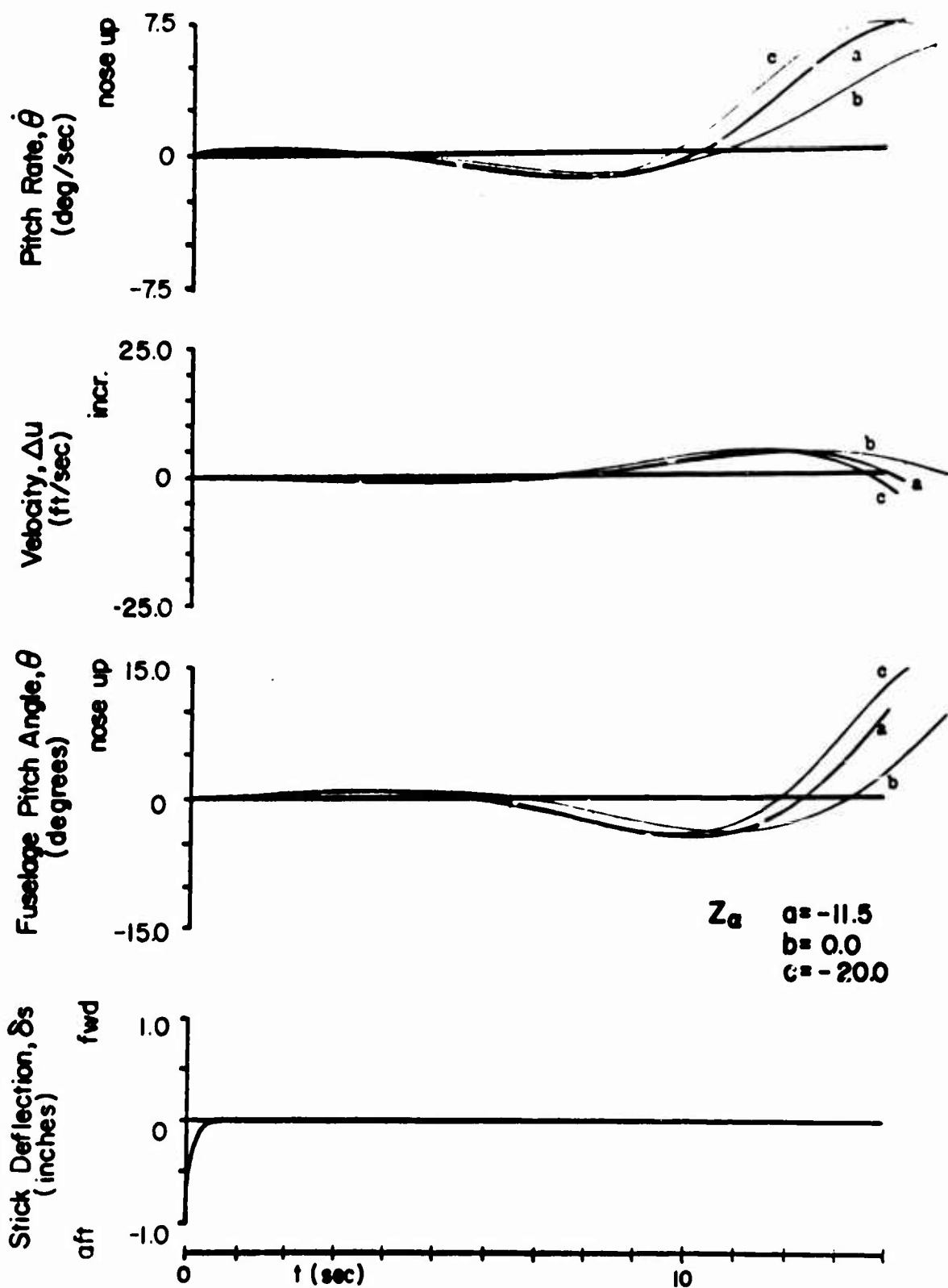


FIGURE 34 (D). VARYING Z_α

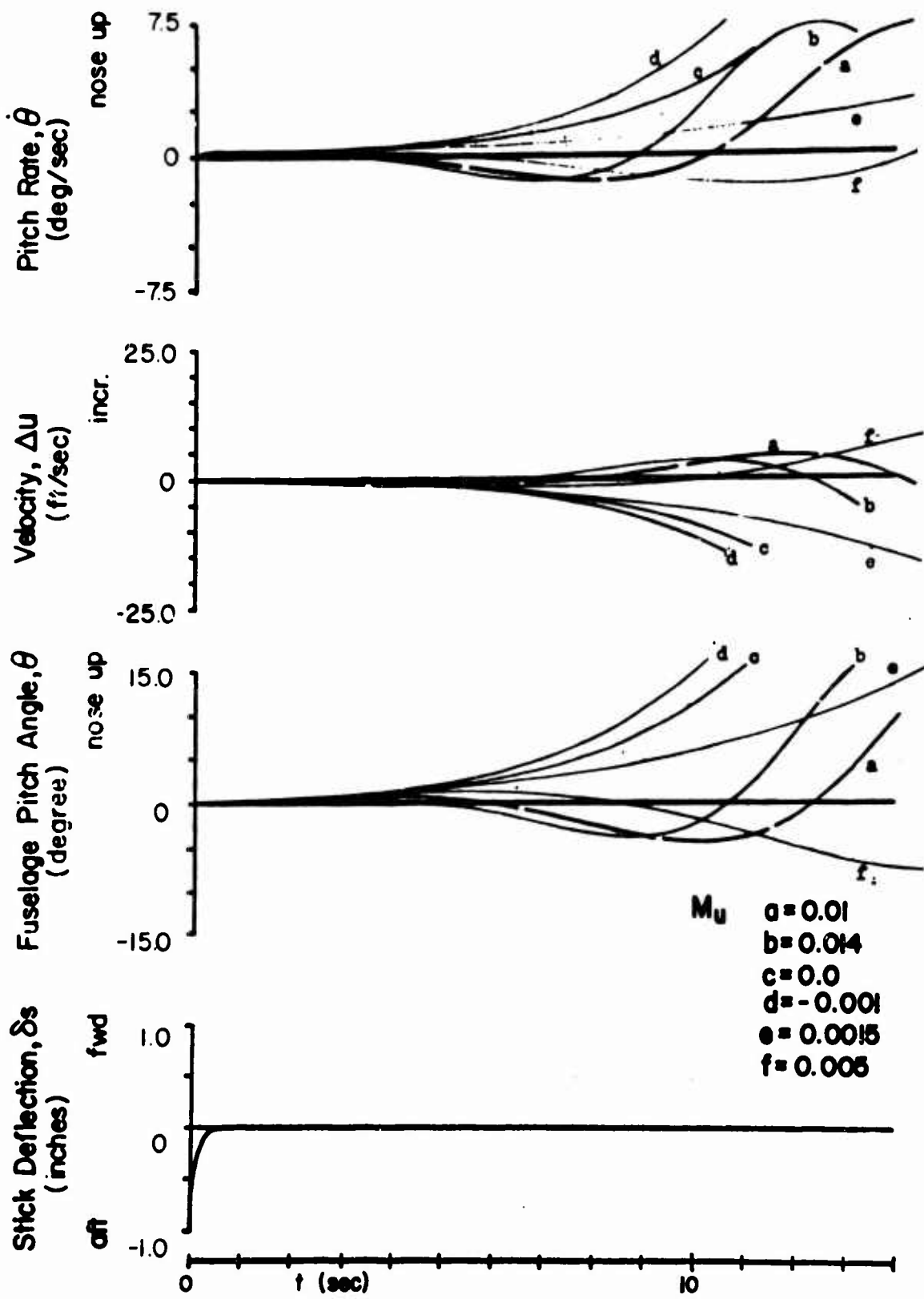


FIGURE 34 (E). VARYING M_u

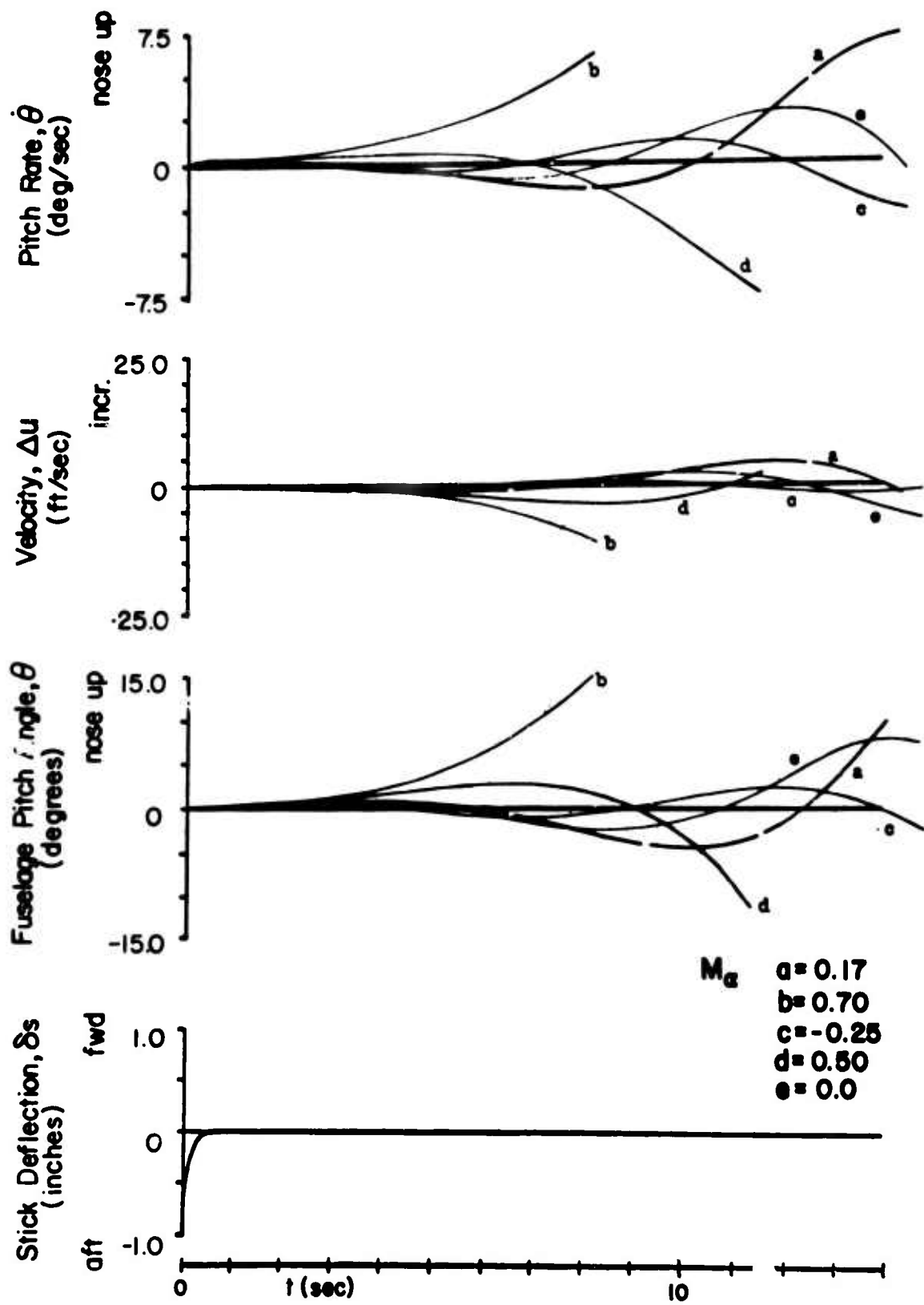


FIGURE 34 (F). VARYING M_a

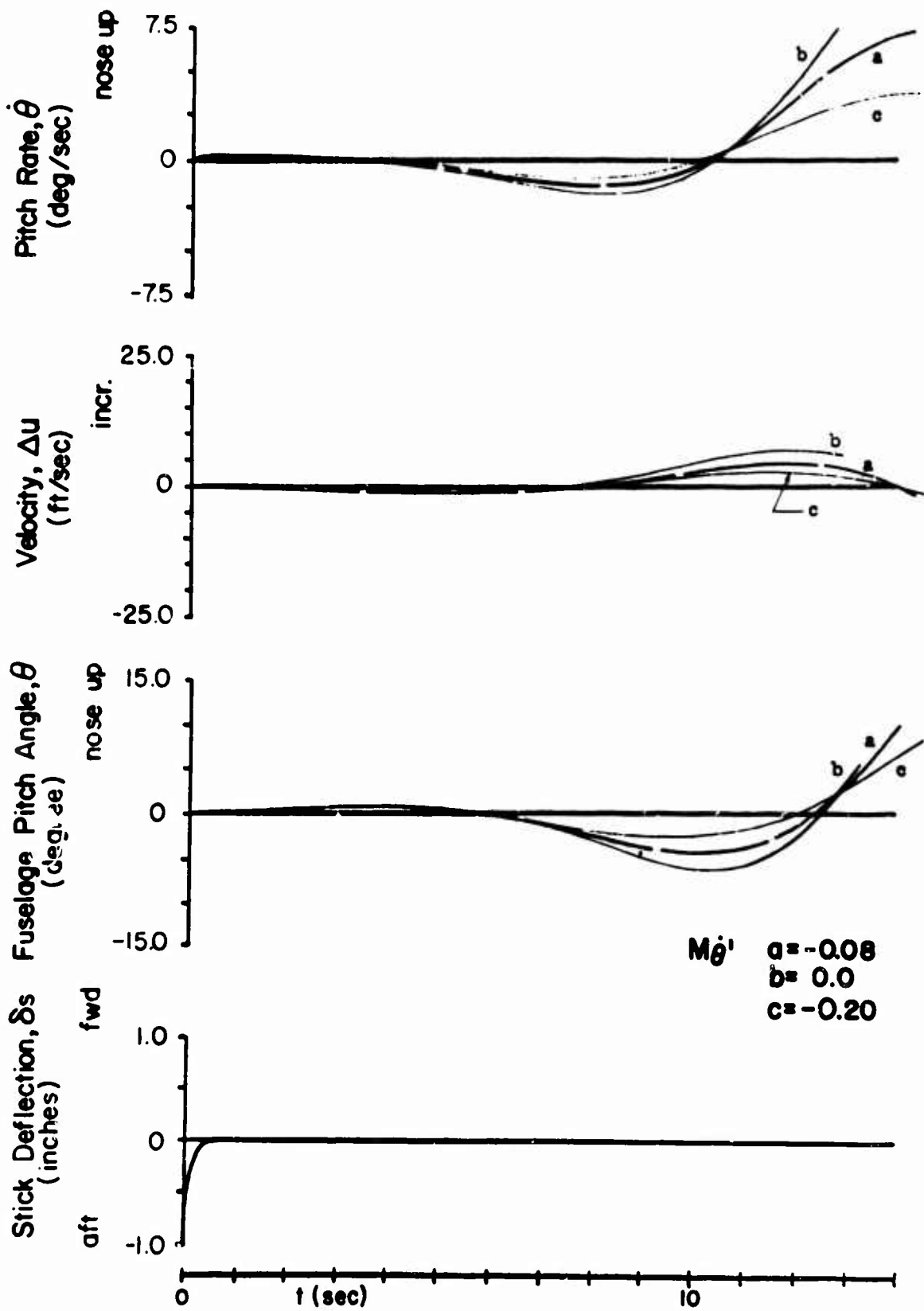


FIGURE 34 (G). VARYING $M_{\dot{\theta}'}$

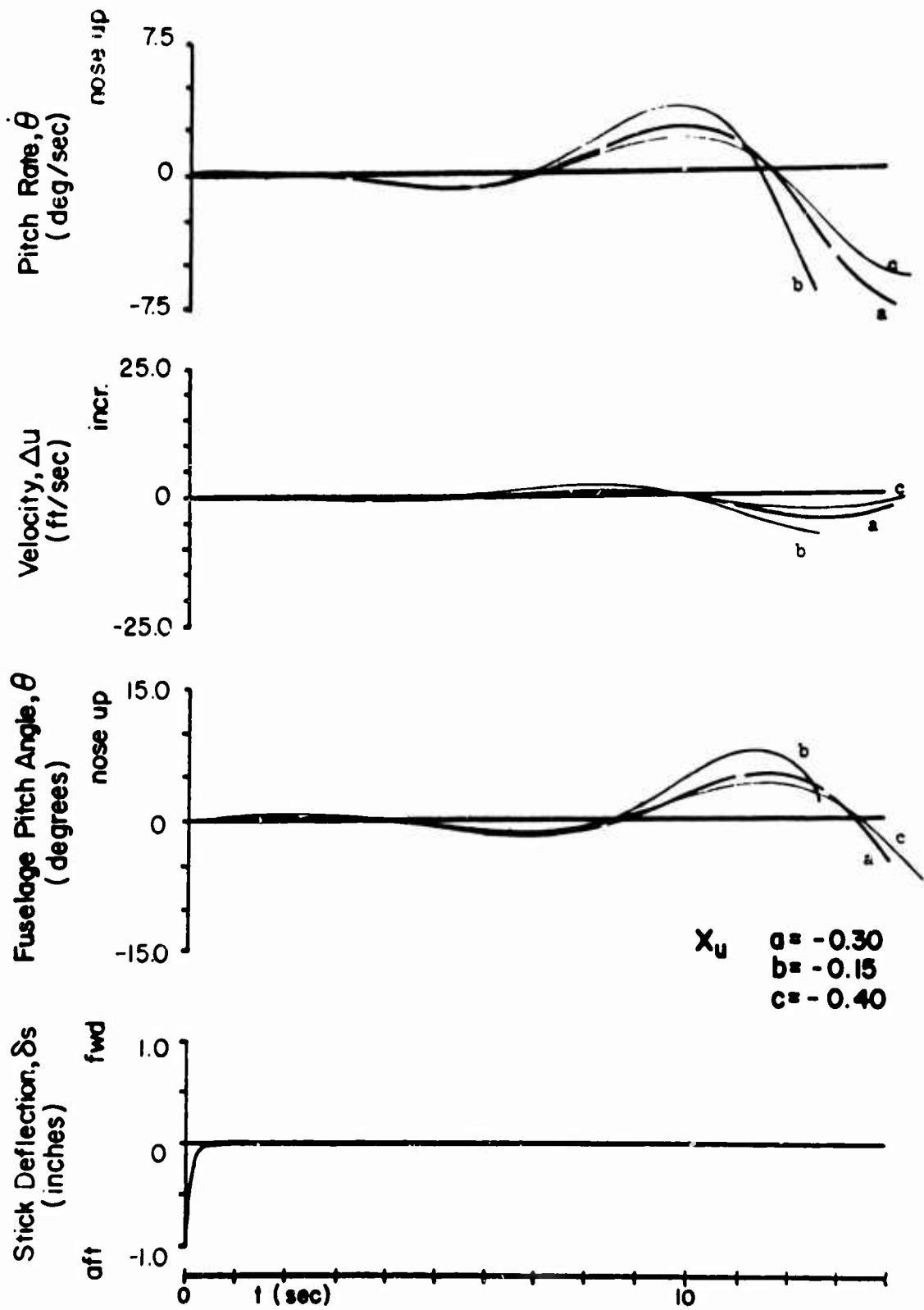


FIGURE 35. SUPERPOSED ANALOG RESPONSES FOR INDIVIDUALLY VARIED DERIVATIVES; $i_w = 90^\circ$, $V_0 = 0$ (A). VARYING X_U

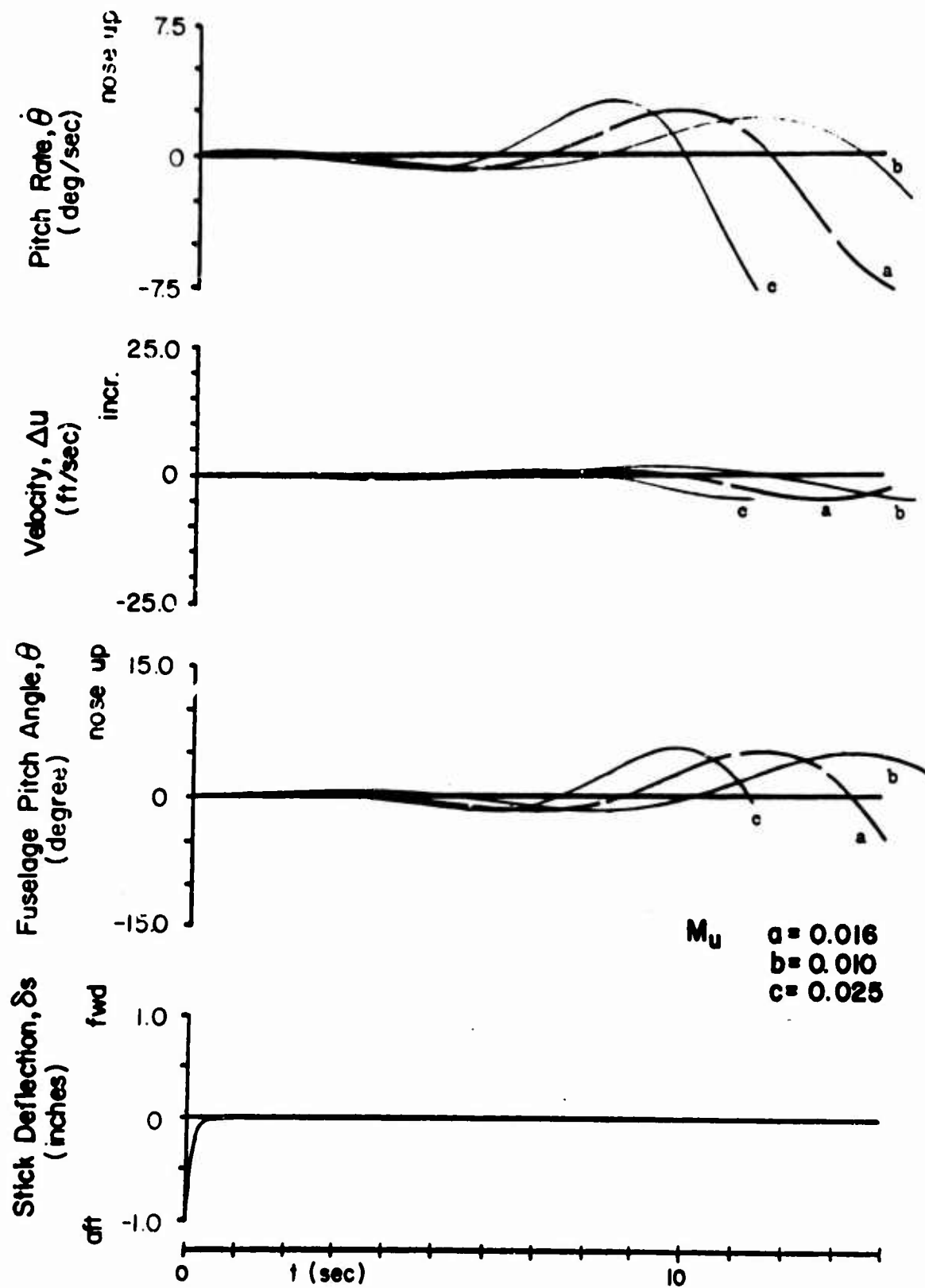


FIGURE 35 (B). VARYING M_u

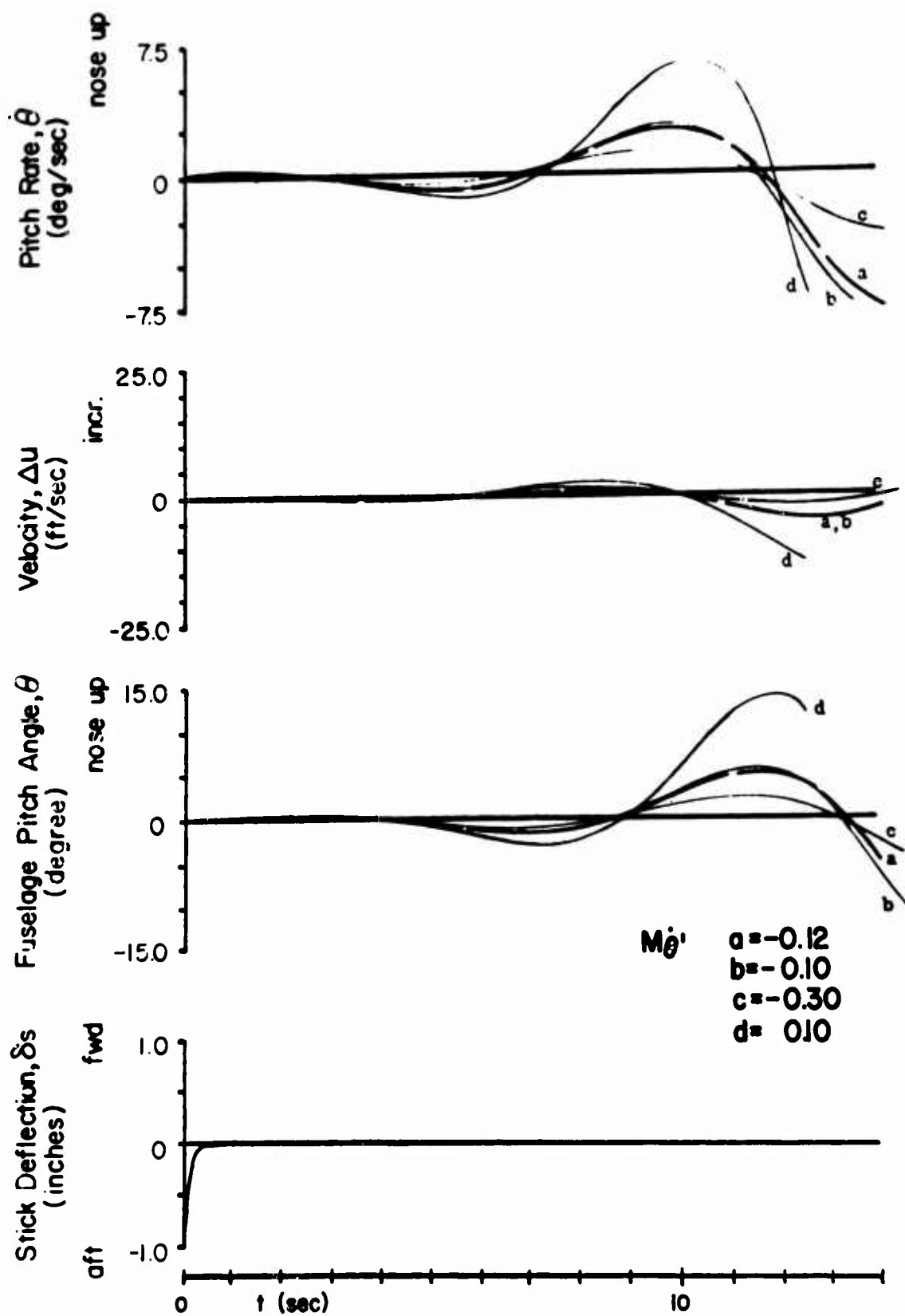


FIGURE 35 (C). VARYING $M\dot{\theta}'$

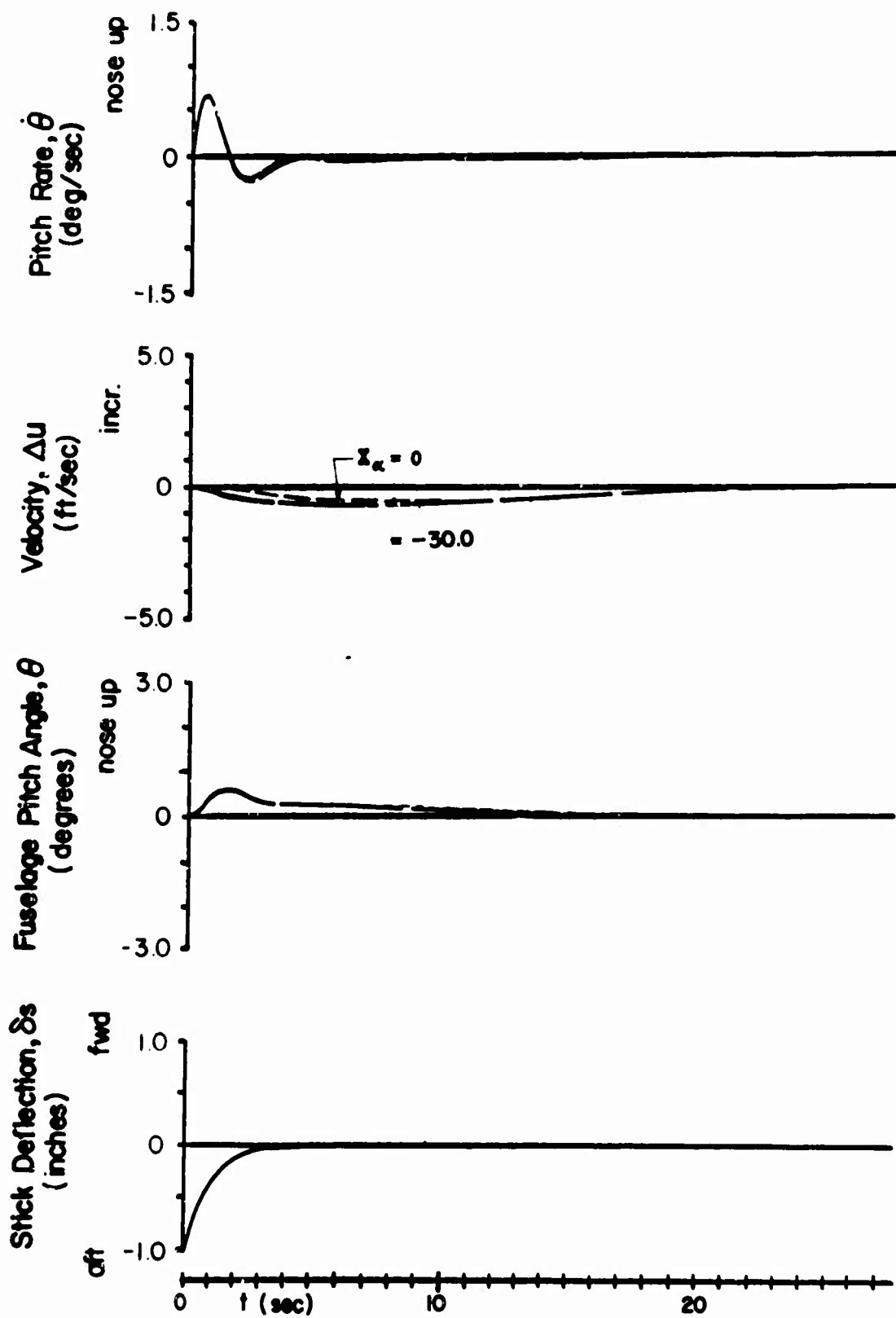


FIGURE 36. ANALOG RESPONSES WITH INDIVIDUAL DERIVATIVES EXHIBITING BOTH AVERAGE AND ZERO VALUES ; $i_w = 20^\circ$, $V_o = 160$ FT/SEC (A) $X_{\alpha} = 0$

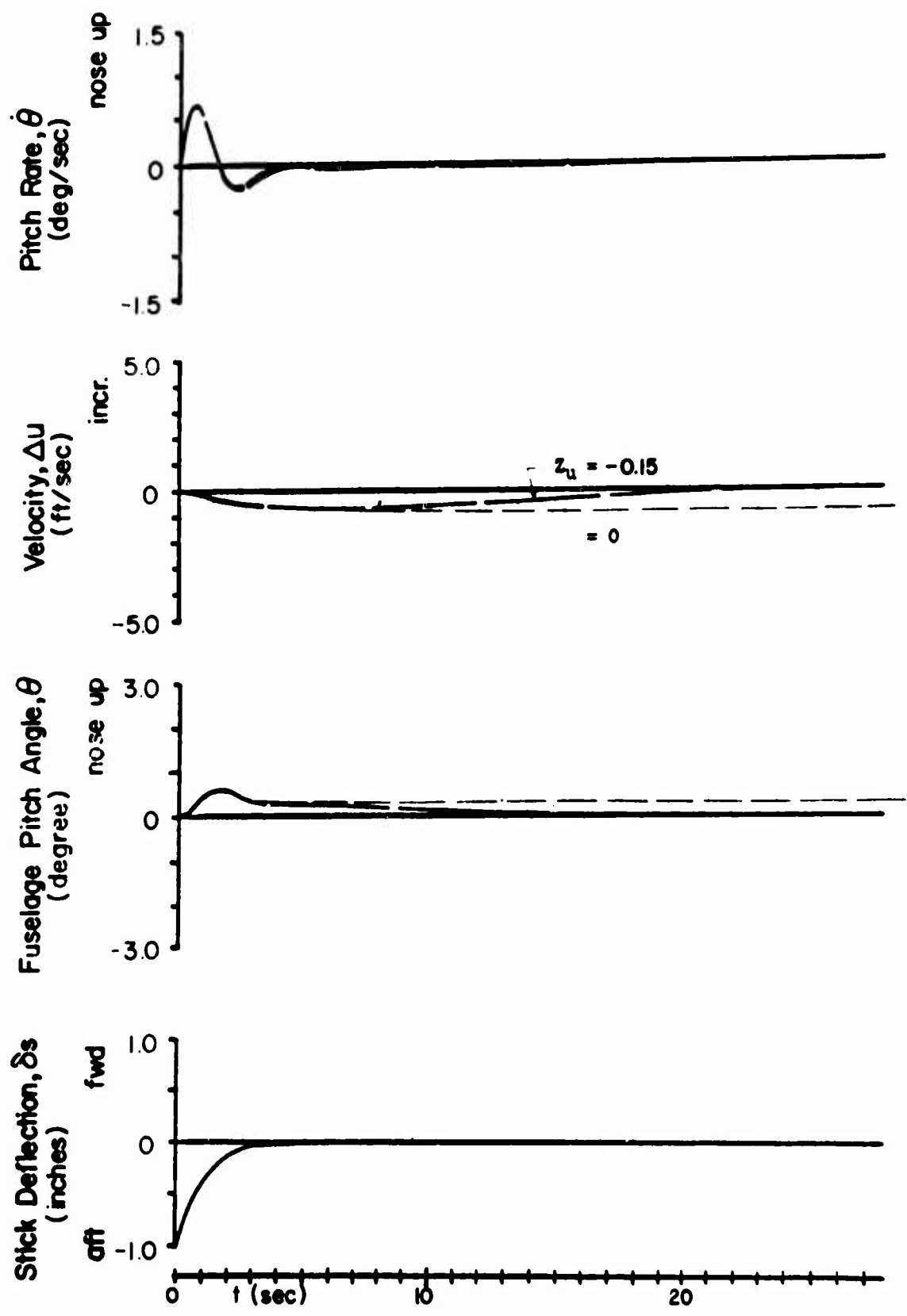


FIGURE 36 (B). $Z_u = 0$

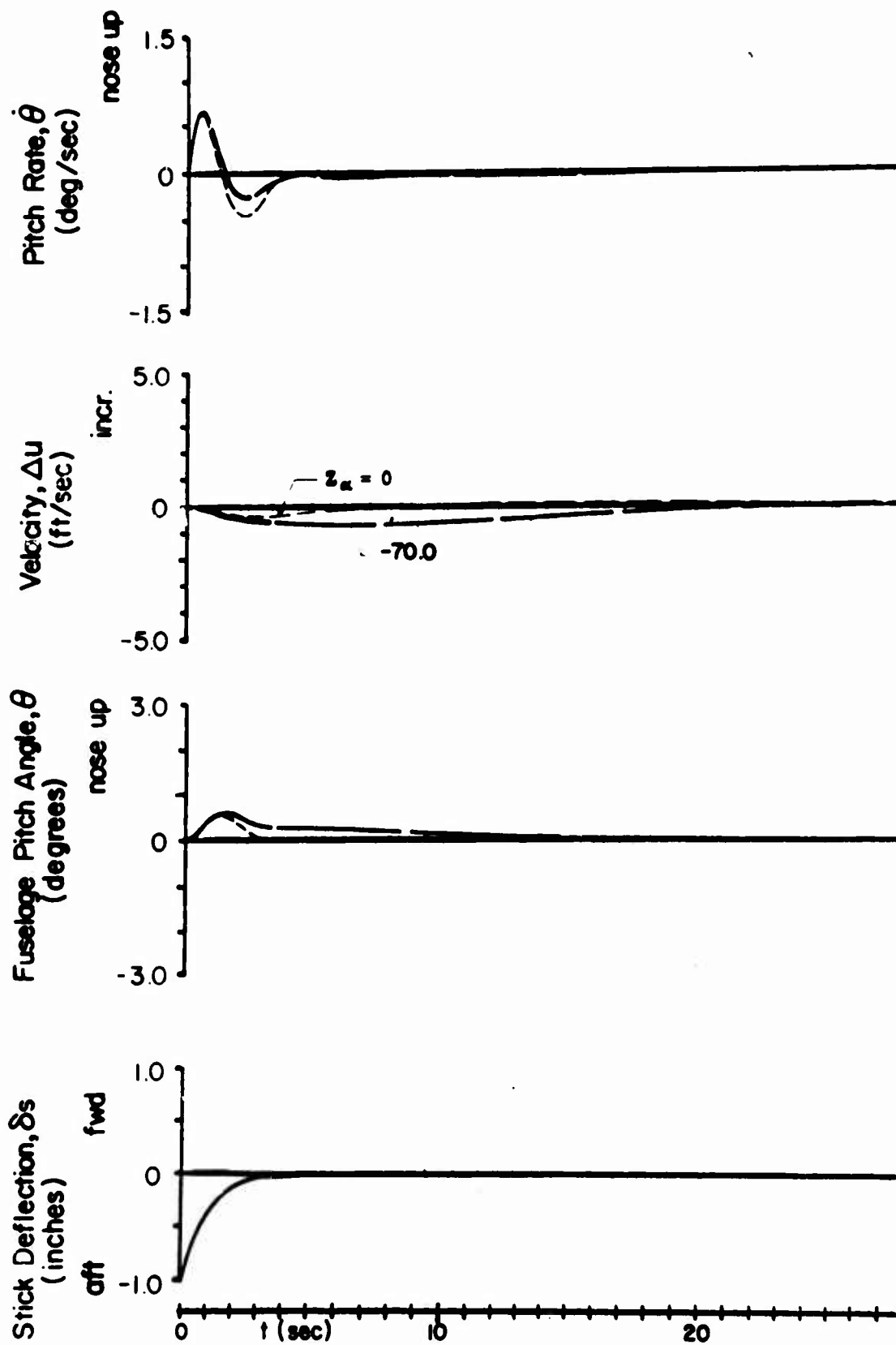


FIGURE 36 (C). $Z_q = 0$

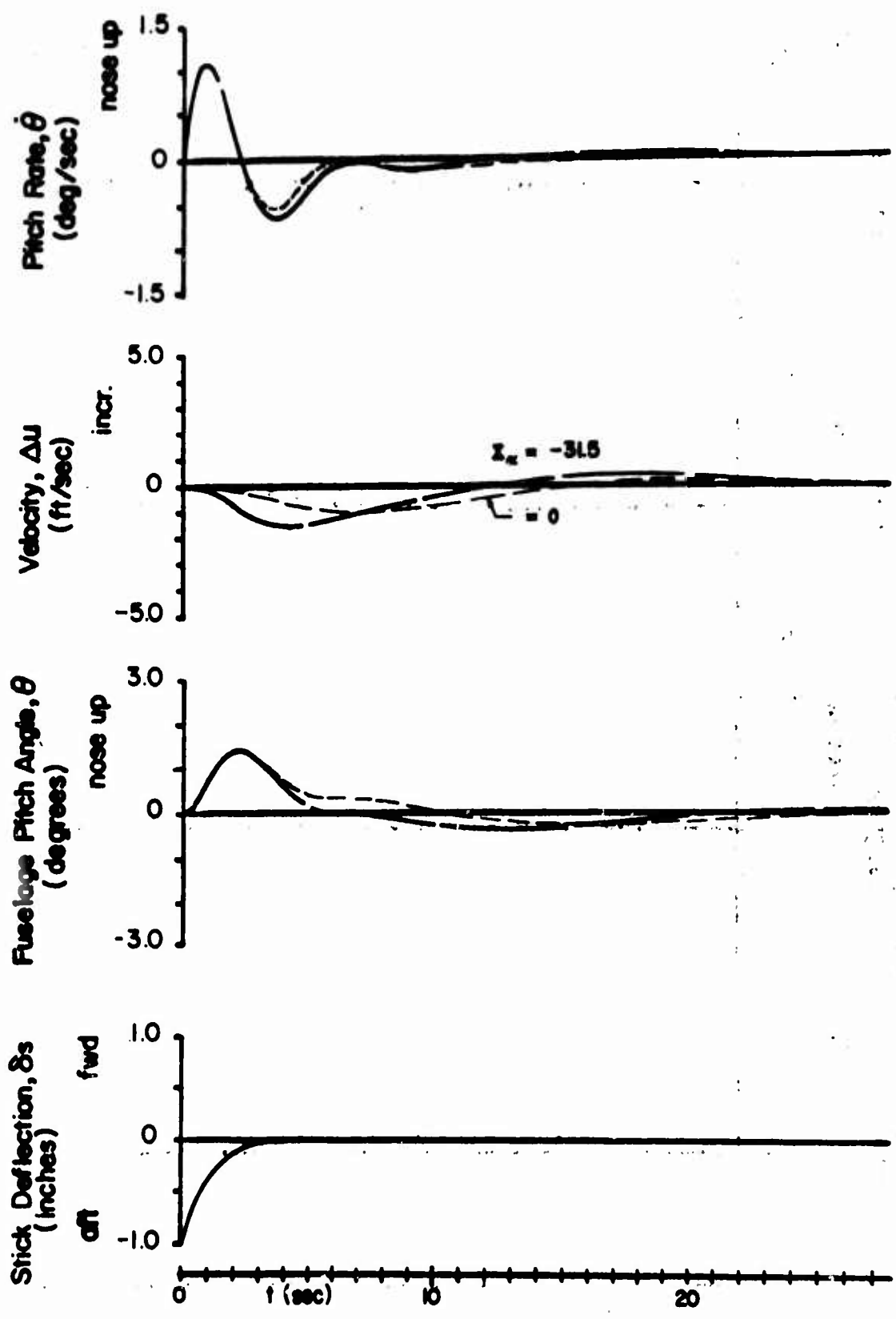


FIGURE 37. ANALOG RESPONSES FOR AVERAGE AND ZERO VALUES OF X_a ; $i_w = 40^\circ$, $V_0 = 100$ FT/SEC

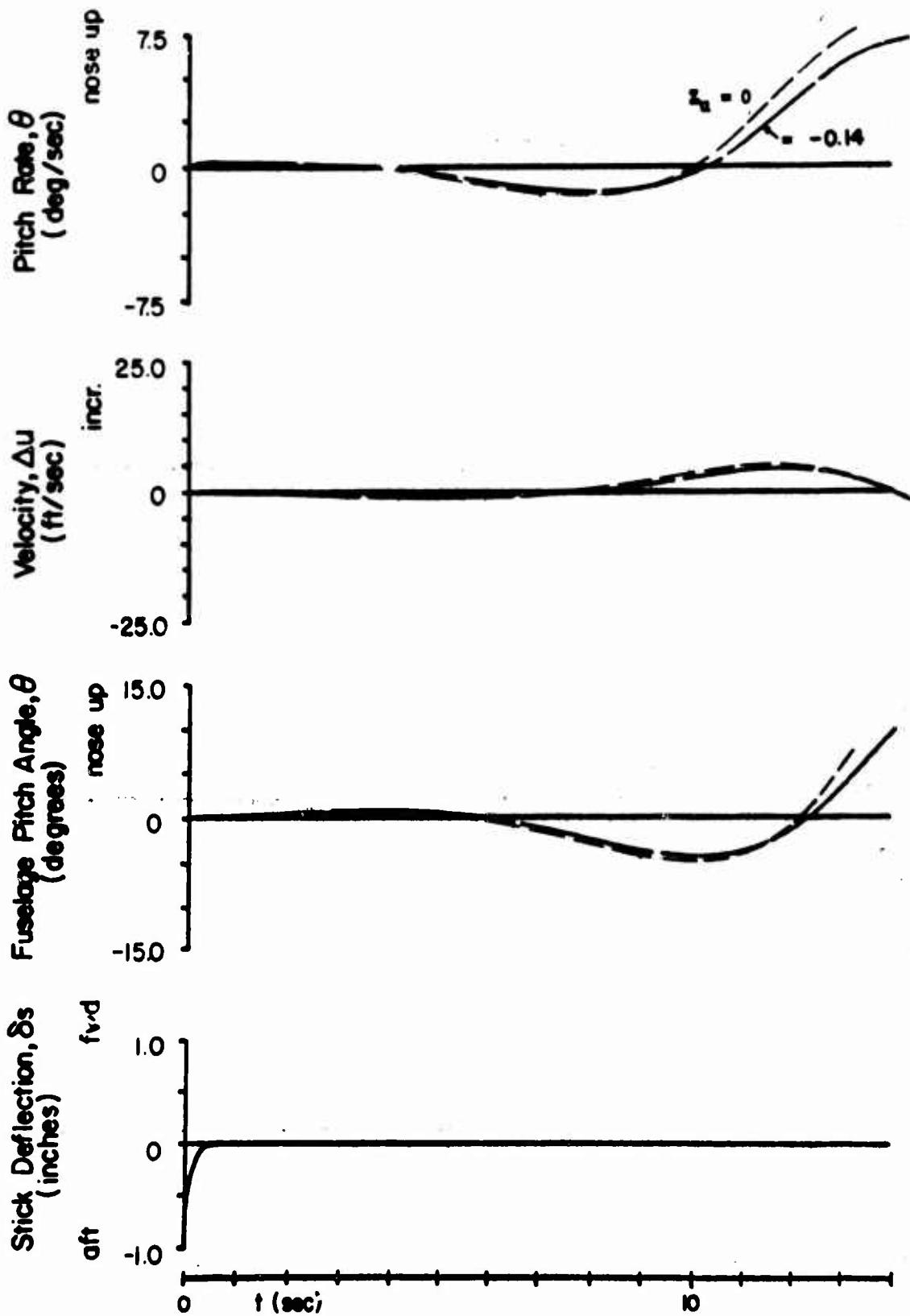


FIGURE 38. ANALOG RESPONSES FOR AVERAGE AND ZERO VALUES OF Z_u ; $i_w = 60^\circ$, $V_0 = 55$ FT/SEC

REFERENCES

1. Newsom, W. A., Jr., and Tosti, L. P., "Force-Test Investigation of the Stability and Control Characteristics of a 1/4-Scale Model of a Tilt-Wing VTOL Aircraft", Memo 11-3-58L, NASA, Washington, D. C., January 1959.
2. Tosti, Louis P., "Longitudinal Stability and Control of a Tilt-Wing VTOL Aircraft Model With Rigid and Flapping Propeller Blades", TN D-1365, NASA, Washington, D. C., July 1962.
3. Pegg, Robert J., "Summary of Flight-Test Results of the VZ-2 Tilt-Wing Aircraft", TN D-989, NASA, Washington, D. C., February 1962.
4. Mitchell, Robert G., "Full-Scale Wind Tunnel Test of the VZ-2 VTOL Airplane With Particular Reference to the Wing Stall Phenomena", TN D-2013, NASA, Washington, D. C., December 1963.
5. Seckel, E., Traybar, J. J., and Miller, G. E., "Longitudinal Handling Qualities for Hovering", Princeton University, Department of Aeronautical Engineering, Report No. 594, Princeton, N. J., December 1961.
6. Newsom, W. A., Jr., and Kirby, R. H., "Flight Investigation of Stability and Control Characteristics of a 1/9-Scale Model of a Four-Propeller Tilt-Wing V/STOL Transport", TN D-2443, NASA, Washington, D. C., September 1964.
7. Traybar, Joseph J., "Princeton Dynamic Model Track Tests of a Sikorsky VTOL Aircraft Design", Princeton University, Department of Aerospace and Mechanical Sciences, Report No. 712, Princeton, N. J., December 1964.
8. Putman, W. F., "Results of Experiments on a Tilt-Wing VTOL Aircraft Using the Princeton University Forward Flight Facility", Princeton University, Department of Aeronautical Engineering, Report No. 542, Princeton, N. J., May 1961.
9. Seckel, Edward, Stability and Control of Airplanes and Helicopters, Academic Press, New York, 1964.
10. Goldberg, J., "Stability and Control of Tandem Helicopters", Princeton University, Department of Aeronautical Engineering, Report No. 362, Princeton, N. J., September 1956.
11. Curtiss, H. C., Jr., "Some Basic Considerations Regarding the Longitudinal Dynamics of Aircraft and Helicopters", Princeton University, Department of Aeronautical Engineering, Report No. 562, Princeton, N. J., July 1961.

12. White, R. M., "A Low Speed Wind Tunnel Test of a .11 Scale Powered XC-142 VTOL Model Investigating Longitudinal and Lateral-Directional Stability and Control in Forward Transition", Chance Vought Corp., Report No. 2-59730/3R831, Dallas, Texas, March 1963.
13. Bennett, R. M., and Curtiss, H. C., Jr., "An Experimental Investigation of Helicopter Stability Characteristics Near Hovering Flight Using a Dynamically Similar Model", Princeton University, Department of Aeronautical Engineering, Report No. 517, Princeton, N. J., July 1960.
14. Curtiss, H. C., Jr., and Putman, W. F., "Results of Experimental Correlation of Model and Full-Scale Helicopter and VTOL Longitudinal Dynamics", Princeton University, Department of Aeronautical Engineering, Report No. 543, Princeton, N. J., April 1961.
15. Curtiss, H. C., Jr., Putman, W. F., and Lebacqz, J. V., "An Experimental Investigation of the Longitudinal Dynamic Stability Characteristics of a Four-Propeller Tilt-Wing VTOL Model", U. S. Army Aviation Materiel Laboratories, USAAVLABS Technical Report 66-80, Fort Eustis, Virginia, 1966.
16. Curtiss, H. C., Jr., Traybar, J. J., and Putman, W. F., "The Princeton Dynamic Model Track", Princeton University, Department of Aerospace and Mechanical Sciences, Report No. 738, Princeton, N. J., May 1965.
17. Curtiss, H. C., Jr., "An Analytical Study of the Dynamics of Aircraft in Unsteady Flight", U. S. Army Aviation Materiel Laboratories, USAAVLABS Technical Report 65-48, Fort Eustis, Virginia, October 1965.
18. Guile, R. J., Jr., and Underwood, E. H., "Model XC-142A Aircraft Flight Test Bi-Weekly Summary", LTV Vought Aeronautics Division, Report No. 23, Dallas, Texas, September 1965.

Unclassified

Security Classification

DOCUMENT CONTROL DATA - R&D		
<i>(Security classification of title, body of abstract and indexing annotation must be entered when the overall report is classified)</i>		
1. ORIGINATING ACTIVITY (Corporate author) Department of Aerospace and Mechanical Sciences Princeton University		2a. REPORT SECURITY CLASSIFICATION Unclassified
		2b. GROUP
3. REPORT TITLE Comparison of Longitudinal Stability Characteristics of Three Tilt-Wing VTOL Aircraft Designs		
4. DESCRIPTIVE NOTES (Type of report and inclusive dates)		
5. AUTHOR(S) (Last name, first name, initial) Curnutt, R. A. and Curtiss, H. C. Jr.		
6. REPORT DATE January 1968	7a. TOTAL NO. OF PAGES 101	7b. NO. OF REFS 18
8a. CONTRACT OR GRANT NO. DA 44-177-AMC-8(T)	8b. ORIGINATOR'S REPORT NUMBER(S) USAAVLABS Technical Report 66-64	
b. PROJECT NO. 1P125901A14233	8c. OTHER REPORT NO(S) (Any other numbers that may be assigned this report) Princeton Univ. Aero. & Mech. Sci. Report No. 749	
d.		
10. AVAILABILITY/LIMITATION NOTICES This document has been approved for public release and sale; its distribution is unlimited.		
11. SUPPLEMENTARY NOTES	12. SPONSORING MILITARY ACTIVITY U.S. Army Aviation Materiel Laboratories Fort Eustis, Virginia	
13. ABSTRACT Experimental values of the longitudinal stability derivatives of three tilt-wing VTOL aircraft configurations as obtained from tests of several models are presented. Results from the NASA full-scale wind tunnel at Langley Field, the Princeton track, the IITV Aerospace Corporation wind tunnel and flight test are included. An analysis is included which utilizes root-locus and analog computer studies to compare the characteristic roots and transient response of the aircraft as the longitudinal derivatives are varied within the range exhibited by these data. Trim conditions at wing incidences from 20 to 90 degrees are considered. The three configurations included in the analysis were found to exhibit quite similar stability characteristics in the low-speed regime. Good correlation was found to exist between NASA wind tunnel data and Princeton Dynamic Model Track data for the VZ-2 aircraft. Consideration is given to the importance of various derivatives in determining the response characteristics. A large number of analog computer traces are included, showing variations in response characteristics caused by changes in individual derivatives.		

DD FORM 1473
1 JAN 64

89

Unclassified

Security Classification

Unclassified

Security Classification

14 KEY WORDS	LINK A		LINK B		LINK C	
	ROLE	WT	ROLE	WT	ROLE	WT
Stability, longitudinal						
Airplane, VTOL						
Airplane (VZ-2)						
Airplane (XC-142A)						
Trim						
Angle of Incidence (-0° to 90°)						

INSTRUCTIONS

1. **ORIGINATING ACTIVITY:** Enter the name and address of the contractor, subcontractor, grantee, Department of Defense activity or other organization (*corporate author*) issuing the report.
- 2a. **REPORT SECURITY CLASSIFICATION:** Enter the overall security classification of the report. Indicate whether "Restricted Data" is included. Marking is to be in accordance with appropriate security regulations.
- 2b. **GROUP:** Automatic downgrading is specified in DoD Directive 5200.10 and Armed Forces Industrial Manual. Enter the group number. Also, when applicable, show that optional markings have been used for Group 3 and Group 4 as authorized.
3. **REPORT TITLE:** Enter the complete report title in all capital letters. Titles in all cases should be unclassified. If a meaningful title cannot be selected without classification, show title classification in all capitals in parentheses immediately following the title.
4. **DESCRIPTIVE NOTES:** If appropriate, enter the type of report, e.g., interim, progress, summary, annual, or final. Give the inclusive dates when a specific reporting period is covered.
5. **AUTHOR(S):** Enter the name(s) of author(s) as shown on or in the report. Enter last name, first name, middle initial. If military, show rank and branch of service. The name of the principal author is an absolute minimum requirement.
6. **REPORT DATE:** Enter the date of the report as day, month, year, or month, year. If more than one date appears on the report, use date of publication.
- 7a. **TOTAL NUMBER OF PAGES:** The total page count should follow normal pagination procedures, i.e., enter the number of pages containing information.
- 7b. **NUMBER OF REFERENCES:** Enter the total number of references cited in the report.
- 8a. **CONTRACT OR GRANT NUMBER:** If appropriate, enter the applicable number of the contract or grant under which the report was written.
- 8b, 8c, & 8d. **PROJECT NUMBER:** Enter the appropriate military department identification, such as project number, subproject number, system numbers, task number, etc.
- 9a. **ORIGINATOR'S REPORT NUMBER(S):** Enter the official report number by which the document will be identified and controlled by the originating activity. This number must be unique to this report.
- 9b. **OTHER REPORT NUMBER(S):** If the report has been assigned any other report numbers (*either by the originator or by the sponsor*), also enter this number(s).
10. **AVAILABILITY/LIMITATION NOTICES:** Enter any limitations on further dissemination of the report, other than those

imposed by security classification, using standard statements such as:

- (1) "Qualified requesters may obtain copies of this report from DDC."
- (2) "Foreign announcement and dissemination of this report by DDC is not authorized."
- (3) "U. S. Government agencies may obtain copies of this report directly from DDC. Other qualified DDC users shall request through _____."
- (4) "U. S. military agencies may obtain copies of this report directly from DDC. Other qualified users shall request through _____."
- (5) "All distribution of this report is controlled. Qualified DDC users shall request through _____."

If the report has been furnished to the Office of Technical Services, Department of Commerce, for sale to the public, indicate this fact and enter the price, if known.

11. **SUPPLEMENTARY NOTES:** Use for additional explanatory notes.

12. **SPONSORING MILITARY ACTIVITY:** Enter the name of the departmental project office or laboratory sponsoring (*paying for*) the research and development. Include address.

13. **ABSTRACT:** Enter an abstract giving a brief and factual summary of the document indicative of the report, even though it may also appear elsewhere in the body of the technical report. If additional space is required, a continuation sheet shall be attached.

It is highly desirable that the abstract of classified reports be unclassified. Each paragraph of the abstract shall end with an indication of the military security classification of the information in the paragraph, represented as (TS), (S), (C), or (U).

There is no limitation on the length of the abstract. However, the suggested length is from 150 to 225 words.

14. **KEY WORDS:** Key words are technically meaningful terms or short phrases that characterize a report and may be used as index entries for cataloging the report. Key words must be selected so that no security classification is required. Identifiers, such as equipment model designation, trade name, military project code name, geographic location, may be used as key words but will be followed by an indication of technical context. The assignment of links, rules, and weights is optional.